ERNST-MORITZ-ARNDT-UNIVERSITÄT GREIFSWALD

INSTITUT FÜR BIOCHEMIE

ENGINEERING AND ANALYSIS OF THE ENANTIOSELECTIVITY OF ESTERASES

PhD THESIS

ELENA FERNÁNDEZ ÁLVARO

GREIFSWALD, 2010

Engineering and analysis of the enantioselectivity of esterases

Inauguraldissertation

zur Erlangung des akademischen Grades
doctor rerum naturalium (Dr. rer. nat.)
an der Mathematisch-Naturwissenschaftlichen Fakultät
der Ernst-Moritz-Arndt-Universität Greifswald

vorgelegt von
Elena Fernández Álvaro
geboren am 27.11.1983
in Madrid

Greifswald, im November 2010

Dekan: Prof. Dr. Klaus Fesser

1. Gutachter: Prof. Dr. Uwe T. Bornscheuer

2. Gutachter: Prof. Dr. Vlada Urlacher

Tag der Promotion: 18.03.2011

A mis padres

The important thing is not to stop questioning.

Albert Einstein

Index

List of abbreviations vii
Table of compounds ix

1. Introduction 1
1.1. Significance of chirality 4
1.2. Obtaining of enantiopure compounds 5
1.2.1. Transition metal catalysts 7
1.2.2. Organocatalysis 8
1.2.3. Biocatalysis 9
1.2.3.1. Enzymes 9
1.2.3.1.1. Enzyme catalysis 10
1.2.3.1.2. Esterases 12
1.3. Protein engineering 15
1.3.1. Rational design 16
1.3.2. Directed evolution 17
1.3.2.1. Methods of mutagenesis 17
1.3.2.1.1. Non-recombining methods 19
1.3.2.1.2. Recombining methods 20
1.3.3. Choosing the best protein engineering strategy 21
1.4. Assay systems 24
1.4.1. Screening methods 24
1.4.1.1. Chromogenic/fluorogenic methods 25
1.4.1.2. Alternative screening strategies 27
1.4.2. Selection methods 28
1.4.2.1. *In vitro* selection 28
1.4.2.2. *In vivo* selection 30
1.4.3. The use of flow cytometry and cell sorting in protein engineering 32
1.4.3.1. Cell surface display 33
1.4.3.2. Green fluorescence protein and its variants as activity reporters 34
1.4.3.3. Screening of intracellular enzymes 35
1.4.3.4. *In vitro* compartmentalisation and fluorescence-activated cell sorting 35

2. Aim of this thesis 37
2.1. In vivo selection and flow cytometry as a tool
for the identification of enantioselective esterases 39

2.2. Crystallization, structure elucidation and analysis of the esterase from *Pyrobaculum calidifontis* (PestE) 40

3. Results and discussion – Chapter I: *In vivo* selection and flow cytometry as a tool for the identification of enantioselective esterases 41

3.1. Selection of substrates 44
3.1.1. Choice of the positive impulse 44
3.1.1.1. Bacterial growth on **1a** 45
3.1.2. Synthesis of the pre-positive impulse 45
3.1.2.1. Deprotection of **1b** 46
3.1.2.2. Direct esterification with **2a** 46
3.1.2.2.1. Azeotropic esterification of **3-PBA** and **2a** 46
3.1.2.2.2. Esterification of acyl chloride with **2a** 47
3.1.3. Choice of the negative impulse 47
3.1.4. Synthesis of the pre-negative impulses 51
3.2. Control esterases and selection simulations 52
3.2.1. Negatve control esterase 52
3.2.1.1. PFEI-pGASTON vector 52
3.2.1.2. Analysis of the *in vivo* selection system components 55
3.2.1.2.1. Model catalyst 55
3.2.1.2.2. Selection medium 56
3.2.1.3. BS2-pET vector 57
3.2.2. Positive control esterase 59
3.2.2.1. Enzyme screening: enantioselectivity towards ethyl esters 59
3.2.2.2. Hits: enantioselectivity towards selection substrates 62
3.2.2.3. Positive controls: CL1 and PestE 65
3.3. Establishment of the *in vivo* selection system 66
3.3.1. Strain optimisation 66
3.3.2. Solubility optimisation 66
3.3.3. Cell counting: optimisation of pre-selection substrates concentration 67
3.3.3.1. Racemic substrates 67
3.3.3.2. Pure enantiomers 69
3.4. Establishment of the flow cytometric detection method 70
3.4.1. PI staining 71
3.4.2. GFP/PI 72
3.4.3. Double-dye system 75
3.5. Validation of the *in vivo* selection system 78

3.6. Analysis of PFEI mutant library 82
3.6.1. Characterisation of the interesting clones 84
3.7. Preliminary studies on selective *in vivo* evolution 88

4. Results and discussion – Chapter II: Crystallization, structure elucidation and analysis of PestE 93
4.1. PestE purification 95
4.2. PestE crystallization and structure elucidation 97
4.3. Structural basis for enantioselectivity towards 3-phenylbutanoates 100

5. Summary and conclusions 103

6. Materials and methods 109
6.1. Materials 111
6.1.1. Chemicals and consumables 111
6.1.2. Strains 111
6.1.3. Genes and plasmids 112
6.1.4. Primers 114
6.1.4.1. Sequencing primers 114
6.1.4.2. QuickChange™ primers 114
6.1.5. Enzymes 114
6.1.6. Media, additives and inducers 115
6.1.6.1. General media 115
6.1.6.2. *In vivo* selection media 116
6.1.6.3. Additives and inducers 117
6.1.7. Buffers and solutions 118
6.1.7.1. Cell washing, cell disruption and separation of inclusion bodies 118
6.1.7.2. Preparation of competent cells 119
6.1.7.2.1. Chemically competent cells 119
6.1.7.2.2. Electro-competent cells 119
6.1.7.3. Agarose gel electrophoresis 120
6.1.7.4. Protein purification 120
6.1.7.4.1. Heat precipitation 120
6.1.7.4.2. Anion exchange chromatography 120
6.1.7.4.3. Gel filtration 121
6.1.7.4.4. His-tag purification 121
6.1.7.5. SDS-Polyacrylamide gel electrophoresis 122
6.1.7.6. Coomassie blue staining of SDS-Polyacrylamide gels 123

6.1.7.7. Activity assays 124
6.1.7.7.1. Esterase activity staining for SDS polyacrylamide gel 124
6.1.7.7.2. Overlay assay for esterase activity 124
6.1.7.7.3. Overlay assay for amidase activity 124
6.1.7.7.4. *p*NPA assay 125
6.1.7.7.5. pH assay for esterase activity screening in MTPs 125
6.1.7.7.6. Enantioselectivity screening with *p*-nitrophenyl-3-phenylbutanoates 125
6.1.7.8. Biocatalysis 125
6.1.7.9. TLC detection 126
6.1.8. Equipment 126
6.1.9. Special computer programs 127
6.2. Methods 127
6.2.1. Microbiological methods 127
6.2.1.1. Conservation of *E. coli* strains and clones 127
6.2.1.2. Overnight culture 128
6.2.1.3. Protein expression 128
6.2.1.3.1. Expression of PFEI mutants in MTP-scale 128
6.2.1.3.2. Protein expression in flasks 128
6.2.1.4. Growth/toxicity assays 129
6.2.1.4.1. Growth/toxicity assays in MTP-scale 129
6.2.1.4.2. Growth/toxicity assays in flasks 130
6.2.1.5. *In vivo* selection 131
6.2.1.5.1. Pseudo-selection media in MTP-scale 131
6.2.1.5.2. Pseudo-selection media in cultivation tubes 131
6.2.1.5.3. Selection and anti-selection media 131
6.2.1.6. Flow cytometer analysis and cell sorting 132
6.2.1.6.1. Cell counting 132
6.2.1.6.2. Cell viability analysis and cell sorting 132
6.2.2. Molecular biology methods 133
6.2.2.1. Plasmid isolation 133
6.2.2.2. Polymerase Chain Reaction 133
6.2.2.2.1. Site directed mutagenesis (QuickChange^{TM}) 133
6.2.2.2.2. Colony PCR 134
6.2.2.3. Digestion 135
6.2.2.4. Agarose gel electrophoresis 136
6.2.2.5. Purification of DNA from agarose gels 136
6.2.2.6. Ligation 136
6.2.2.7. Preparation of competent cells 137

6.2.2.7.1. Chemically competent *E. coli* cells 137
6.2.2.7.2. Electro-competent *E. coli* cells 137
6.2.2.8. Transformation 137
6.2.2.8.1. Transformation of chemically competent *E. coli* cells 137
6.2.2.8.2. Transformation of electro-competent *E. coli* cells 138
6.2.3. Biochemical methods 138
6.2.3.1. SDS-PAGE 138
6.2.3.2. Coomassie staining 138
6.2.3.3. SDS esterase activity staining 139
6.2.3.4. Overlay activity assays 139
6.2.3.4.1. Overlay assay for esterase activity 139
6.2.3.4.2. Overlay assay for amidase activity 139
6.2.3.5. Protein purification 140
6.2.3.5.1. Heat precipitation 140
6.2.3.5.2. Anion exchange chromatography 140
6.2.3.5.3. Gel filtration 140
6.2.3.5.4. His-tag purification 140
6.2.3.6. Ultrafiltration 141
6.2.3.7. Determination of the protein content 141
6.2.3.8. Protein crystallization 141
6.2.3.8.1. Crystallization by sitting drop method 141
6.2.3.8.2. Crystallization by hanging drop method 141
6.2.3.9. *p*NPA assay 141
6.2.3.10. pH assay for activity screening 142
6.2.3.11. Enantioselectivity screening with *p*-nitrophenyl-3-phenylbutanoates 142
6.2.4. Biocatalysis 143
6.2.4.1. Biocatalysis in analytical scale 143
6.2.4.2. Biocatalysis in preparative scale 143
6.2.5. Chemical methods 144
6.2.5.1. Analytics 144
6.2.5.1.1. Chiral GC methods 144
6.2.5.1.2. Chiral HPLC methods 144
6.2.5.1.3. Preparation of methyl esters from carboxylic acids 145
6.2.5.2. Organic synthesis 145
6.2.5.2.1. Azeotropic esterification 145
6.2.5.2.2. Deprotection of **1b** 145
6.2.5.2.3. Esterification of acyl chloride 146

7. Literature 153

Aknowledgements 177

List of abbreviations

Å	angstrom
δ	chemical displacement
°C	centigrade
ΔG	free energy
ΔH	enthalpy
ΔS	entropy
ε	extinction coefficient
µg	microgram
µl	microliter
%	percentage
$^{\neq}$	transition state
abs	absorbance
AEC	anion exchange chromatography
Amp	ampicillin
bp	base pair
bs	broad singlet
BS2	*p*-nitrobenzyl esterase from *Bacillus subtilis*
BTB	bromothymol blue
c	conversion
CAL-B	lipase B from *Candida antarctica*
CE	capillary electrophoresis
CAE	capillary array electrophoresis
cm	centimeter
CMC	critical micelle concentration
conc	concentration
CVL	lipase from *Chromobacterium viscosum*
d	doublet, -CH=
Da	Dalton
DCM	dichloromethane
dd	doublet of doublets
DERA	D-2-desoxyribose-5-phosphate aldolase
DMSO	dimethylsulfoxide
DMF	dimethylformamide
DNA	desoxyribonucleic acid
dNTP	desoxyribonucleoside triphosphate
dt	doublet of triplets
E	enzyme, enantioselectivity
E_{app}	apparent enantioselectivity
E_{true}	true enantioselectivity
EB	ethidium bromide
E. coli	*Escherichia coli*
E. C.	Enzyme commission
ee	enantiomeric excess
EF	enrichment factor
e. g.	example given
equiv.	equivalents
FACS	fluorescence-activated cell sorting
FDA	US food and drug administration
fl	femtoliter
FL1	green fluorescence
FL2	red fluorescence
FSC	forward scatter
g	gram or acceleration
GC	gas chromatography
GF	gel filtration
GFP	green fluorescent protein
GT	glycosyltransferases
h	hour
HPLC	high performance liquid chromatography
HRP	horseradish peroxadise
HTS	high-throughput screening
Hz	Hertz
IC	compensation index
IPTG	isopropyl-β-D-thiogalactopyranoside
IR	infrared
IPG	isopropyliden glycerol
IVC	*in vitro* compartmentalisation
J	coupling constant
kb	kilobase
k_{cat}	reaction rate constant
kDa	kilodalton
kg	kilogram
K_M	Michaelis-Menten constant
l	liter
LB	Luria-Bertani
Ln	natural logarithm
m	meter
M	molar or marker
mA	milliamperium
MIC	minimum inhibitory concentration
mg	milligram
min	minute
ml	milliliter
mm	millimeter
mM	millimolar
mmol	millimol
MNNG	N-methyl-N-nitrosoguanidine

mol	6.022 x 10^{23} particles
MPD	2-methyl-2,4-pentanediol
MTP	microtiter plates
M.W.	molecular weight
n.d.	not determined
nm	nanometer
NMR	nuclear magnetic resonance
OD_{600nm}	optical density at 600 nm
PAGE	polyacrylamide gel electrophoresis
PC	positive control
PCR	polymerase chain reaction
PEG	polyethylene glycol
PestE	esterase from *Pyrobaculum calidifontis*
PFEI	esterase I from *Pseudomonas fluorescens*
pH	*pondus hidrogenii*
PI	propidium iodide
pl	picoliter
PON1	paroxonase 1
ppm	parts per million
PPTS	pyridinium *p*-toluenesulfonate
PSL	lipase from *Pseudomonas stutzeri*
PTSA	*p*-toluenesulfonic acid
q	quartet, $-CH_3$
R	8.314472 J mol^{-1} K^{-1}
rpm	rotations per minute
RTEM	Type IIIa enzyme, specified by a gene carried on an R-factor
s	singlet, -C≡
SDS	sodium dodecyl sulfate
sec	seconds
SSC	side scatter
T	temperature
t	time, triplet, $-CH_2-$
TAE	Tris/acetate/EDTA
Taq	*Thermus aquaticus*
TEA	triethylamine
TEMED	N,N,N′,N′-tetramethylendiamine
Tet	tetracycline
TFA	trifluoroacetic acid
THF	tetrahydrofuran
TLC	thin layer chromatography
TMS	tetramethylsilan
Tris	Tris-(hydroxymethyl)-aminomethane
U	unit (µmol/min)
UV	ultraviolet
V	volt
v	reaction speed
V_{max}	maximum reaction speed
wt	wild type

Table of compounds

Compound	Identification	Compound	Identification
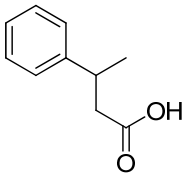	**3-PBA**	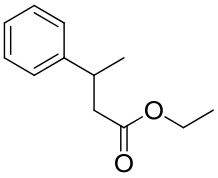	**Et-3-PB**
		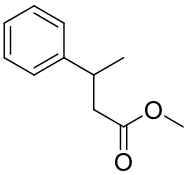	**Me-3-PB**
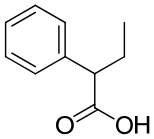	**2-PBA**	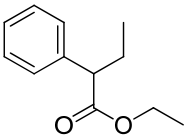	**Et-2-PB**
		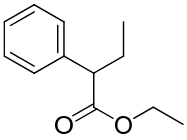	**Me-2-PB**
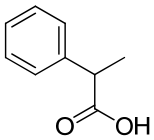	**2-PPA**	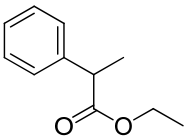	**Et-2-PP**
		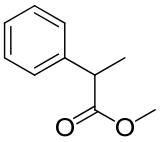	**Me-2-PP**
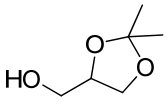	**1a**	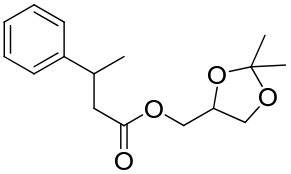	**1b**
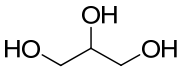	**2a**	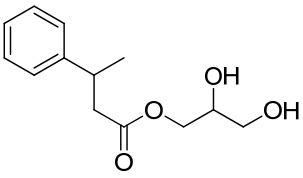	**2b**

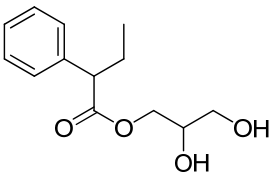

2c

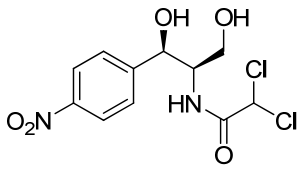

3a

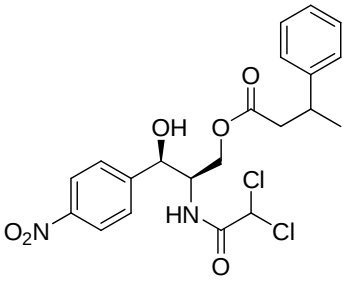

3b

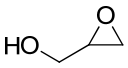

4a

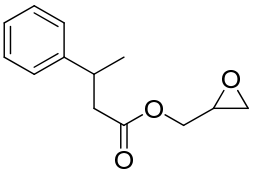

4b

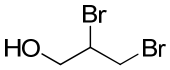

5a

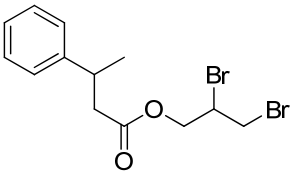

5b

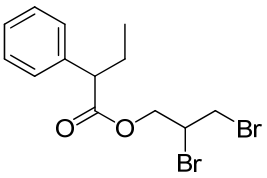

5c

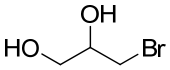

6a

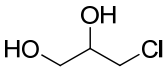

7a

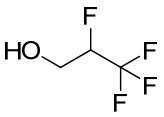

8a

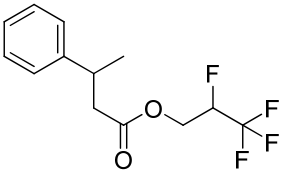

8b

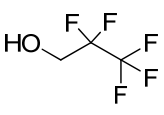

9a

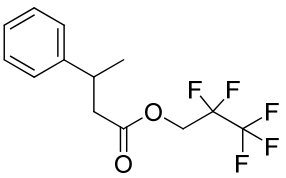

9b

1. INTRODUCTION

1. INTRODUCTION

Chirality is the mathematical approach to the term of "handedness", as human hands are probably the most universally recognized example of it. Indeed, the term *chirality* originates from the Greek word for hand: Χειρ (cheir). In chemistry, a chiral molecule lacks an internal plane of symmetry and has a non-superimposable mirror image. This is generally caused by the presence of an asymmetric atom in its structure; however, chirality is not only referred to atoms but also applies to all kind of elements. Thus, in addition to central chirality, there is helical, axial and planar chirality.

In the beginning of the 19th century, Jean Baptiste Biot observed for the first time that some quartz crystals rotated the plane of polarized light in one direction while other crystals rotated it to the same extent in the opposite direction. He observed this phenomenon in some liquids (e.g. turpentine) as well as in solids dissolved in water (e.g. sugar, tartaric acid). In 1848, Louis Pasteur concluded that this effect was a molecular property: the optical activity caused by the chirality of molecules. He studied the fact that tartaric acid (Figure 1-1) derived from living organisms rotates the plane of polarized light passing through it, while the same molecule synthesized chemically does not have such effect. Examining tartrate crystals, Pasteur discovered that these had two asymmetric forms, which were mirror images of one another. These forms corresponded to both diastereoisomers of tartaric acid because, as in many other cases,[1] the distinct isomers crystallize separately.

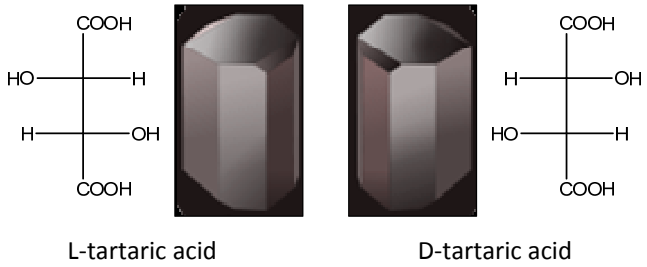

Figure 1-1. Chemical structure and crystal of the different conformations of tartaric acid.

Later in 1874, Van′t Hoff and Le Bel discovered independently the stereoisomerism, based in the previous molecular models of the tetrahedral carbon made by August Kekulé. The theory of stereoisomerism affirms the tetrahedral structure of the carbon atom and

was decisive for rationalisation of the whole organic chemistry. Thus, it is considered one of the greatest scientific events of the XIX century.

1.1. Significance of chirality

Many biologically active molecules like amino acids, sugars, and nucleotides are chiral, and these compounds have the same chirality in almost all biological systems (amino acids are L and sugars are D). This homo-chirality of life has been subject of debate for a long time. There are two theories on this phenomenon: one claims that the existence of homo-chirality in nature was purely random, and the other one that it is the result of a selective process which took place in the first origin of amino acids.[2]

In living organisms, biochemical processes are modulated by ligand-receptor interactions. This is the basis of modern pharmacology as drugs interfere in biological routes and modify them in a variety of ways. Receptors are proteins, composed of amino acids and thus chiral. The geometry of a bioactive agent is decisive for its interaction with the pertinent receptor and in consequence for the activity.[3] There are numerous examples of this: (*R*)-(-)-carvone (Scheme 1-1) smells like spearmint and (*S*)-(+)-carvone like caraway. This is because olfactory receptors are chiral as well and behave different in presence of different enantiomers.

In pharmacology, the different effect of enantiomers can lead to serious consequences when the racemic form is administrated. One of the most known medical incidents in modern times is the one related to thalidomide (Scheme 1-1). This drug (Contergan®) was sold all over the world between 1957 and 1961. Due to its sedative-hypnotic effect it was marketed as "the drug of choice" for pregnant women with morning sickness. Until its withdrawal from market it caused birth defects to 10000 to 20000 children, where most of them died before their 1st birthday. The effect of thalidomide was further investigated, and it came up that the (*R*)-enantiomer was responsible for the teratogenic effect while the (*S*)-enantiomer caused the sedative effect. However, administration of the enantiopure (*S*)-form to avoid the undesired side-effects is not possible because *in vivo* racemisation takes place.[4] This incident led to much stricter test requirements for drugs and pesticides before introducing them on the market.

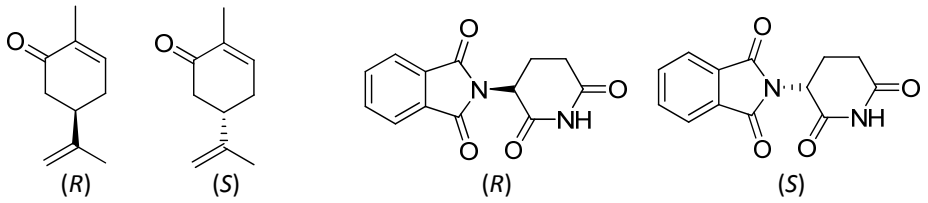

Scheme 1-1. Chemical structure of the different enantiomers of carvone and thalidomide.

Commonly, the most active isomer of a bioactive molecule is called "eutomer" while the isomer possessing less or even undesired activities is called "distomer".[5] The activity ratio of eutomer and distomer, called eudimistic ratio, is a measure of the enantioselectivity of the receptor.

A proof of the enantioselectivity of biochemical processes is that natural products are usually obtained in enantiopure forms (e.g. tartaric acid, taxol etc.). On the contrary, organic synthesis usually results in racemic products composed of 50% of each enantiomer. E. J. Ariëns suggested in 1984 that the distomer of bioactive compounds such as drugs and pesticides should be regarded as an impurity[6] as it does not contribute to the desired effect but causes side-effects and environmental pollution. Thus, racemic mixtures would present at least 50% impurities. Although racemates are still used for economic reasons, the situation is changing due to increasing legislation pressure. In 1992, the US Food and Drug Administration (FDA) adopted a policy which established that racemates can be developed but their approval will be based on separate testing of the individual enantiomers.[7] Simultaneously, the mechanisms for approval of pure enantiomers have been accelerated (the chiral switch).[8] As a consequence, pharmaceutical industry has moved to the development of pure enantiomers if their production is feasible.

1.2. Obtaining of enantiopure compounds

Obtaining enantiopure compounds is not always trivial due to the identical physico-chemical properties of both enantiomers. A few substances (e.g. lactic acid) can be obtained from natural resources (the chiral pool) in sufficient amounts and with an acceptable grade of purity. Fermentative processes constitute another strategy. If the yield

of the substances of interest is low, it can be increased by modification of metabolic routes.

The separation of enantiomers from racemic mixtures is the most extended procedure to obtain enantiopure compounds. Mechanical separation by crystallization[9] is the most straightforward strategy; however, it succeeds in less than 10% of the organic compounds.[10] Chromatographic separation is another alternative which can be applied on analytical scale but its scale-up is rather unsuitable because of the low capacity and high solvent consumption of these methods. An elegant alternative is the kinetic resolution[11] of a racemic mixture using a chiral catalyst which converts one enantiomer faster than the other one. The maximal theoretical yield of 50% in these processes can be increased to 100% by *in situ* racemisation of the slow reacting enantiomer in dynamic kinetic resolutions.[12] In this case, substrate racemisation can be performed by different ways: protonation/deprotonation, addition/elimination, nucleophilic substitution, oxidation/reduction, etc. Asymmetric syntheses[13] allow obtaining enantiopure products at 100% yield, but work only for *meso*[13] or pro-chiral compounds.[14,15] A *meso* compound is a non-optically active member of a set of stereoisomers that is not chiral despite containing two or more stereocenters. Pro-chiral compounds have two enantiotopic groups, which are pro-*R* or pro-*S*. These groups are constitutionally identical, and replacement of one of them by a different group makes the molecule chiral.

Asymmetric syntheses and kinetic resolutions of racemic mixtures (Scheme 1-2) are the most promising strategies to follow. In contrast to fermentations and extractions from natural sources, those approaches guarantee access to non-natural enantiopure substrates. The reaction catalysts used in these asymmetric syntheses and kinetic resolutions mostly posses the chiral information that is transferred to the substrate. In addition to enantioselectivity, further properties of the catalyst like activity, stability and ability to be recycled are crucial for their use. The currently available catalysts are discussed below.

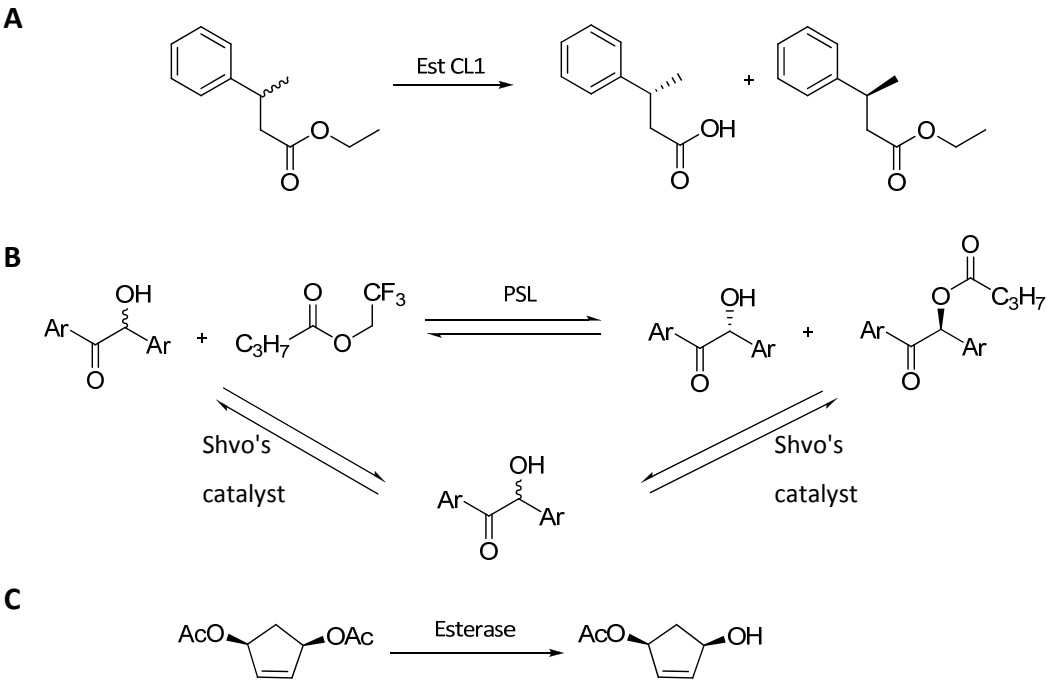

Scheme 1-2. Examples of: kinetic resolution[11] (A), dynamic kinetic resolution[12] (B) and asymmetric hydrolysis of a prochiral substrate[13] (C). PSL: lipase from *Pseudomonas stutzeri.*

1.2.1. Transition metal catalysis

Chiral complexes with transition metals have been used for asymmetric catalysis since the 60's.[16] One of the most famous examples is the rhodium (I) complex of the chiral diphosphin BINAP (Scheme 1-3) which is used by Takasago International Corporation in the production of (-)-Menthol since 1984.[17]

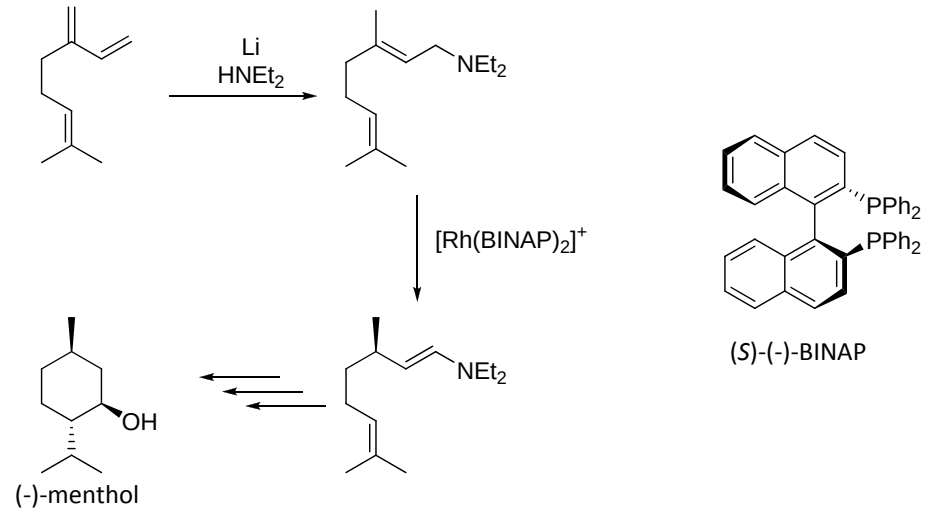

Scheme 1-3. Takasago process for the synthesis of (-)-menthol from myrcene.

Although catalysis with transition metals has proved to be useful to obtain enantiopure compounds,[18,19] each chelate-ligand has to be optimized separately for a given reaction, which involves huge economical and practical efforts. The use of high-throughput screening methods analogous to the methods used in biocatalysis has been attempted[20] without significant progress.

Another drawback of this kind of catalysis is the high environmental impact as recovery and recycling procedures of these catalysts have not been broadly established. Furthermore, metal catalysts are designed to work under harsh reaction conditions[21] and the use of transition metal complexes in the production of substances for human or animal consume is not recommended as they may leave traces of heavy metals.

1.2.2. Organocatalysis

This strategy uses low-molecular weight organic compounds, which do not contain a metal atom, to accelerate chemical reactions. Although organic molecules have been used as catalysts in organic chemistry from the very beginnings, their application in asymmetric synthesis emerged only some decades ago, and special attention has been paid to it since 2000. Nowadays, organocatalysis is considered as the bridge between the two major forms of catalysis: metal complex-mediated and enzymatic catalysis.[22]

The majority of organocatalytic reactions are amine-based reactions.[23] The first example of asymmetric enamine catalysis was the Hajos-Parrish-Eder-Sauer-Wiechert reaction,[24,25] an intramolecular aldol reaction catalyzed by proline to yield steroid CD ring fragments (Scheme 1-4), which was developed in the early 70′s by Schering AG and Hoffmann La Roche. Despite its use in natural products and steroid synthesis, the mechanism of the reaction was poorly understood and its use was rather limited. Thus, little effort was dedicated to this field and the next proline-catalyzed enantioselective intermolecular aldol reactions were discovered 30 years later.[26,27]

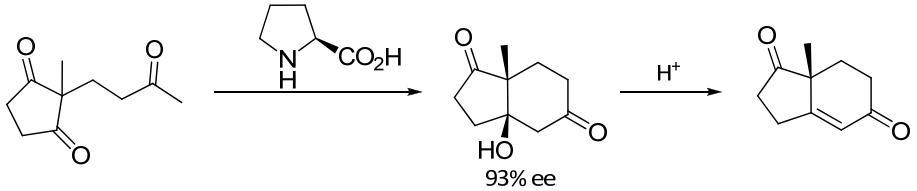

Scheme 1-4. The Hajos-Parrish-Eder-Sauer-Wiechert reaction.

Organocatalysis has experienced a renaissance due to advances in biocatalysis. In many cases the design of organocatalysts is inspired by the mechanisms of enzyme catalysis.[28] However, despite considerable efforts to explore and extent the scope of asymmetric organocatalytic reactions in the recent years, their use in medicinal and process chemistry is still rather low.

1.2.3. Biocatalysis

Biocatalysis consists on the use of biological systems to catalyze the transformation of non-natural man-made organic compounds. It was already employed in the ancient Mesopotamia, China and Japan in the production of food and alcoholic drinks and nowadays, its use has been expanded to the production of a broad range of products in food manufacture, fine chemicals and pharmaceuticals.[29] Advances in genetic engineering, recombinant expression techniques and process engineering permit even further growth.[30] Enzymes (and whole cells) are the predominant biocatalysts used, but advances in the study of catalytic nucleic acids and antibodies open new pathways and possibilities for new reactions and processes.

1.2.3.1. Enzymes

Due to their three-dimensional structure, enzymes display often high regio-, enantio-, and stereoselectivity. For decades it was thought that the selectivities obtained with enzymes would never be achievable with metal catalysis. Enzyme catalysis proceeds generally at mild conditions avoiding extreme temperatures or high pressures which can cause problems like isomerisation, racemisation, epimerisation or rearrangement of the reaction components.[31] Enzymes can be immobilized and reused for many catalytic cycles. Some can be overexpressed in organisms like *E. coli* or *Pichia pastoris* reducing process costs and becoming more accessible for industrial applications. Nowadays, one-step reactions and hydrolytic enzymes still dominate the biocatalytic market, but as know-how in this field is increasing, new possibilities for applications emerge constantly (Table 1-1). To overcome the need of cofactor recycling whole cell systems have been implemented and these are used for industrial applications as well.

Apart from their high selectivity, an additional potential of enzymes is that they can effectively perform reactions that challenge organic chemistry, like stereoselective carbon-carbon bond formation[32] (aldol condensation).

Table 1-1. Selected examples of the use of biocatalysis in the synthesis of chiral pharmaceutical intermediates.

Drug	Effect	Biocatalytical processes used in the synthesis	References
Saxagliptin (Onglyza™)	Antidiabetic drug	Reductive amination of 2-(3-hydroxy-1-adamantyl)-2-oxoethanoic acid	Hanson et al.[33]
		Ammonolysis of (5*S*)-4,5-dihydro-1H-pyrrole-1,5-dicarboxylic acid,1,-(1,1-dimethyl)-5-ethyl ester	Gill et al.[34]
Atazanavir (Reyataz)	HIV protease inhibitor	Preparation of (1*S*, 2*R*)-[3-chloro-2-hydroxy-1-(phenylmethyl) propyl]-carbamic acid, 1,1-dimethyl-ethyl ester	Patel et al.[35]
		Synthesis of (*S*)-tertiary-leucine	Patel et al.[31]
Carbovir™ (c-d4G)	Antiretroviral	Deamination of *cis*-4-[2,6-diamino-9H-purin-9-yl]-2-cyclopentenemethanol	Mahmoudian and Dawson[36]
		Hydroxylation of 2-cyclopentylbenzoxazole	Münzer at al.[37]
Paclitaxel (Taxol®)	Anticancer drug	Bioconversion to facilitate extraction	Hanson et al.[38] Nanduri et al.[39]
		Synthesis of C13 side chain	Patel et al. [40] Feske et al.[41]

1.2.3.1.1. Enzyme catalysis

As in all catalytic processes, enzymes accelerate reactions by lowering the energy barrier between substrate and product, the activation energy. The catalytic efficiency of an enzyme towards a given substrate is measured by determination of the kinetic parameters K_M, k_{cat} and V_{max}, and is defined as k_{cat}/K_M. The Michaelis constant, K_M is defined as the substrate concentration at which the reaction rate is $½V_{max}$ and is inversely proportional to the affinity of the enzyme for the substrate (Figure 1-2). The term k_{cat} is the number of substrate molecules handled by one active site per second.

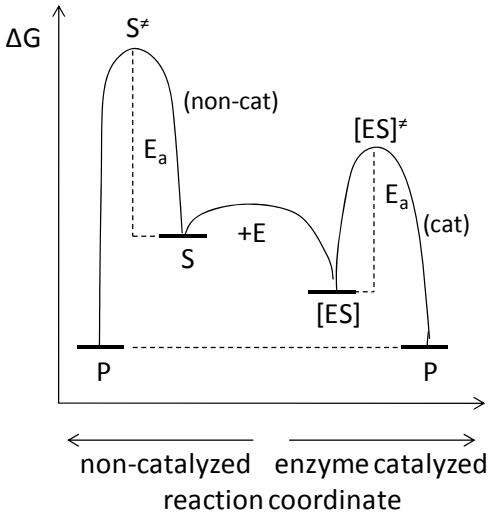

$$E + S \underset{}{\overset{K}{\rightleftharpoons}} [ES] \overset{k_{cat}}{\rightleftharpoons} E+P$$

$$K = \frac{[ES]}{[E] \cdot [S]} = \frac{1}{K_M}$$

$$v \sim k_{cat} \cdot [ES] \sim \frac{k_{cat}}{K_M}$$

Figure 1-2. Energy diagram of catalyzed versus non-catalyzed reaction.
E = enzyme, S = substrate, [ES] = enzyme-substrate complex, P = product, K = equilibrium constant for [ES] formation, k_{cat} = reaction rate constant for [ES] → E+P, E_a = activation energy, $^{\neq}$ = transition state, K_M = Michaelis-Menten constant, v = reaction velocity.

Enzyme enantioselectivities originate from the difference of free energy in the transition state complexes ($\Delta G^{\neq}$) between each enantiomer and the enzyme, which are diastereomeric complexes. This difference in free energy ($\Delta\Delta G^{\neq}$) is a direct measure for the selectivity of the reaction, which in turn depends on the ratio of the reaction rates for each enantiomer (v_R and v_S). $\Delta\Delta G^{\neq}$ is composed of an enthalpy ($\Delta\Delta H^{\neq}$) and an entropy ($\Delta\Delta S^{\neq}$) term, thus enantioselectivity is the result of differences between the enantiomers both in activation enthalpy and activation entropy[42,43] (Equation 1-1).

$$\Delta\Delta G^{\neq} = -RT \ln \frac{v_R}{v_S}; \quad \Delta\Delta G^{\neq} = \Delta\Delta H^{\neq} - T \cdot \Delta\Delta S^{\neq}; \quad \ln E = -\frac{\Delta_{R-S}\Delta H^{\neq}}{R} \cdot \frac{1}{T} + \frac{\Delta_{R-S}\Delta S^{\neq}}{R}$$

Equation 1-1. Determination of enantioselectivity in function of activation enthalpy and entropy between enantiomers.

In enantioselective catalysis, the enantioselectivity of an enzyme towards a given substrate is given by the enantiomeric purity (enantiomeric excess, ee%) of the substrate or the reaction product. As these values vary with the reaction course, they are not constant parameters.[44] Enantioselectivity can be measured more accurately using the E-value, which is a proportion of specific constants of the enzyme (k_{cat}/K_M) for both enantiomers of a substrate and thus, in theory, independent of the reaction conversion.[45]

In the last decades, different strategies have been developed for the determination of the E-value. The first method is the one developed by Chen et al.[46] (Equation 1-2) which assumes irreversible reactions where only one substrate and one product exist, without product inhibition and with competition of both enantiomers for the binding site. Later, variations of Chen′s method were created attempting to reduce the error rates[47] or to ease calculations.[48] Computer programs have been also created to include the existence of product inhibition or reversible reactions in the determination of both K and E.[49] In all cases, low to moderate E-values are determined more accurately than high E-values because the enantiomeric ratio is a logarithmic function of the enantiomeric purity.

$$E = \frac{\ln\left[1 - c\left(1 + ee_p\right)\right]}{\ln\left[1 - c\left(1 - ee_p\right)\right]};\ E = \frac{\ln\left[(1-c)(1+ee_s)\right]}{\ln\left[(1-c)(1-ee_s)\right]};\ E = \frac{\ln\left[\frac{1-ee_s}{1+(ee_s/ee_p)}\right]}{\ln\left[\frac{1+ee_s}{1+(ee_s/ee_p)}\right]}$$

Equation 1-2. Determination of enantioselectivity in function of enantiomeric excesses and reaction conversion. Equations developed by Chen et al.[46]

1.2.3.1.2. Esterases

As esterases are the subject of this thesis, a short overview of this enzyme subclass will be given below.

Esterases (carboxyl hydrolases EC 3.1.1.1) catalyze the hydrolysis of C-O bonds in carboxylic esters. In contrast to lipases (EC 3.1.1.3), esterases have preference for hydrophilic short chain substrates; however, there are many exceptions to this rule making the line between esterases and lipases blurred. Esterases are generally more unstable in organic solvents than lipases, and their substrate specificity is higher, which makes them often considered less useful for industrial purposes. However, there are many examples of esterases of great utility for the industry like acetyl-choline esterase and pig liver esterase.[45]

Esterases (and lipases) are α,β hydrolases as all of them present this canonical fold which consists of a core of mostly eight parallel (or anti-parallel) strands of a β-sheet surrounded on both sides by α-helices (Figure 1-3). They belong to the group of serine hydrolases as the catalytic machinery is formed by the triad: Ser, His, Asp (Glu in some cases, like in the *p*-nitrobenzyl esterase from *Bacillus subtilis*, BS2[50]); together with residues which contribute to the stabilization of the oxyanion formed in the tetrahedral intermediate: the

"oxyanion hole". Typically, one of the residues of this oxyanion hole is the Gly next to the catalytic Ser. There is also a conserved GXSXG motif around the active serine which allows the formation of the tight γ-turn where the Ser is located.

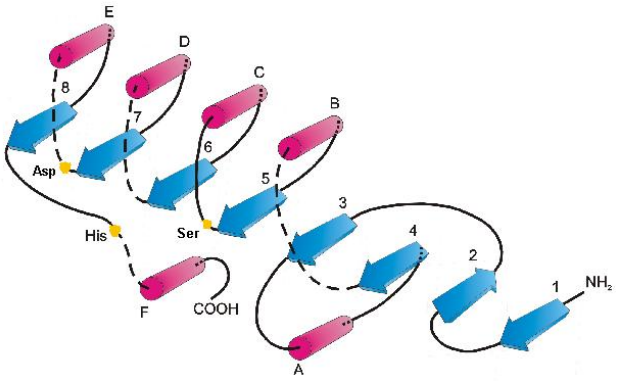

Figure 1-3. Typical α,β-hydrolase fold.[51]

The catalytic mechanism for ester hydrolysis mediated by esterases is similar to that described for serine proteases[52] (Scheme 1-5). Hydrogen bonds between the three amino acids of the catalytic triad increase the nucleophilicity of the Ser, which attacks the electrophilic carbon of the carbonyl group in an ester bond. The formation of this acyl enzyme represents the first tetrahedral intermediate (TI1). Next, alcohol is released remaining the acyl part of the ester bonded to the enzyme. With the participation of a molecule of water the acyl enzyme complex is broken and the carboxylic acid is released, this step involves the second tetrahedral intermediate (TI2). After release of the carboxylic acid the enzyme can start a new catalytic cycle. If an alcohol makes the nucleophilic attack of TI2 instead of water, an ester will be released and a transesterification takes place instead of hydrolysis.

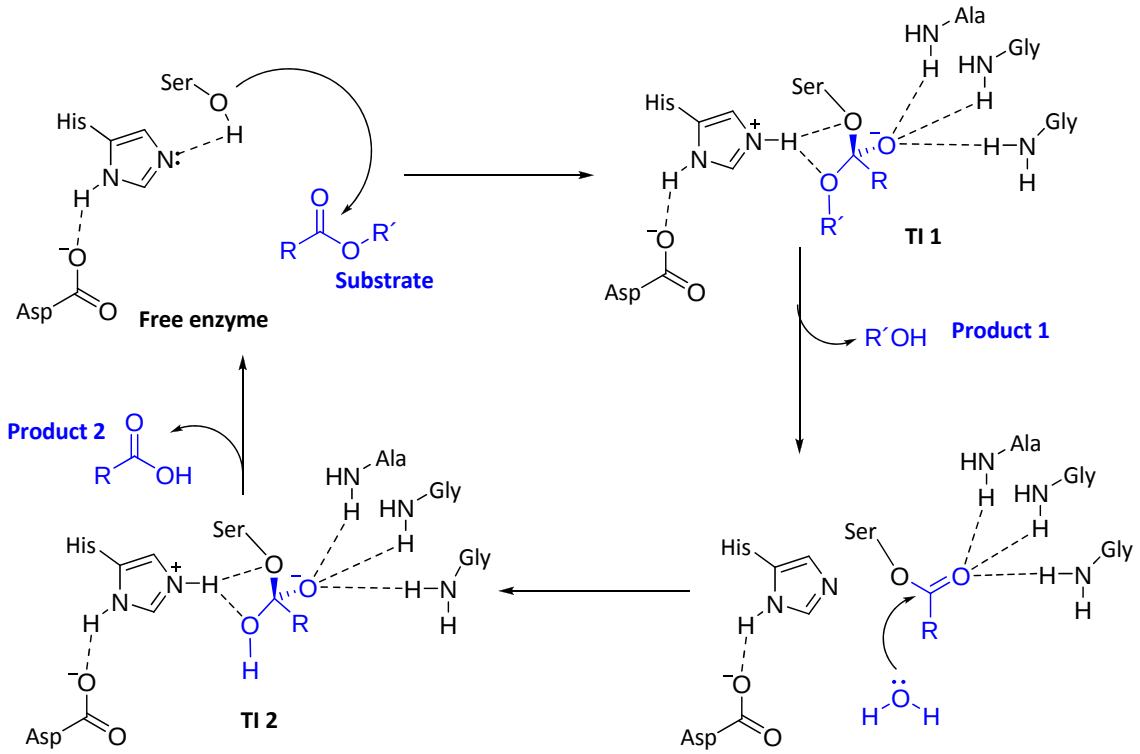

Scheme 1-5. Schematic representation of the hydrolytic mechanism of serine hydrolases. Ser, His and Asp form the catalytic triad; and Ala, Gly and Gly form the oxyanion hole.

Esterases and lipases occur in plants, animals and microorganisms. The biological role of lipases is mostly digestive whereas the physiological role of esterases is more various: digestion, hydrolysis of neurotransmitters, degradation of hemicelluloses, detoxification, etc.

Another difference between esterases and lipases is their reaction kinetic (Figure 1-4). Esterases strictly follow Michaelis-Menten kinetics, while most lipases have a lid that blocks the active site, and thus exhibit low activity in the basal state. When the substrate concentration is high enough to form micelles (the critical micelle concentration, CMC) the phenomenon called "interfacial activation" occurs. This results in the opening of the lid, orientation of all the catalytic residues and dramatic increase of the catalytic efficiency. The mechanism of the interfacial activation is not completely understood as there are lipases with small lids which do not show interfacial activation (e.g. *Candida antarctica* lipase B, CAL-B, *Chromobacterium viscosum* lipase, CVL, etc) and other lipases only show it in the presence of some substrates (e.g. lipase from *Staphylococcus hyicus*).[45]

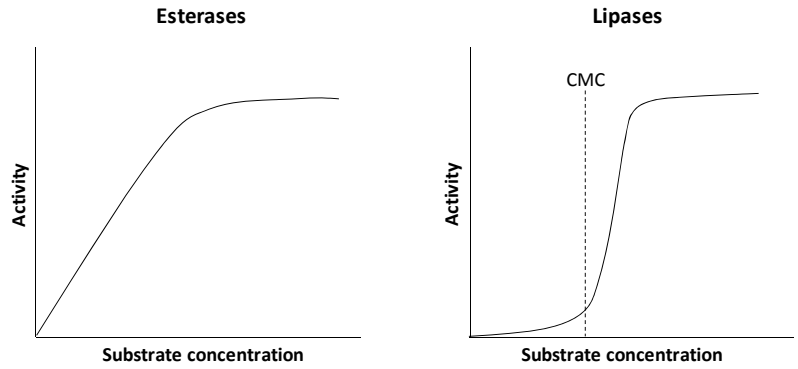

Figure 1-4. Schematic representation of the reaction kinetic in esterases and lipases.

The esterase/lipase superfamily is the most used enzyme class in industrial biotransformations, mainly because their cofactor independence facilitates the process up-scaling, and because their broad substrate spectrum is often combined with high stereoselectivity.

1.3. Protein engineering

As biocatalysis has proved to be a tool with great potential, much effort in its further applications and development is invested. To extend the possibilities of this field, two main strategies are followed nowadays: the discovery of novel and the optimisation of the ones already known biocatalysts.

For the discovery of new biocatalysts, the traditional methodology involves screening samples from various ecosystems to isolate unknown microorganisms with interesting catalytic activities. In the last decades, access to non-cultivable microorganisms became possible with the development of the metagenome approach – amplification and recombinant expression of the whole genetic material of an environmental sample – and the sequence-based enzyme discovery, possible thanks to the creation of genomic databases.

Most applications of enzymes do not focus on their natural catalyzed reaction, but rather use non-natural substrates. Moreover, the reaction system (i.e. solvent, molarity, pH, temperature) can differ substantially from the environment in which the enzymes have evolved. Thus, likely, activity, stability, substrate specificity, and enantioselectivity need to be improved. Besides reaction engineering (optimisation of the reaction system to find adequate conditions), protein engineering has emerged as an alternative thanks to

advances in molecular biology and bioinformatics, which make possible to effectively modify enzymes by changing its amino acid sequence. In the last decades not only protein modification has been performed of both, catalytic and non-catalytic scaffolds, but also *de novo* synthesis of proteins has been described.[53]

The two main strategies of protein engineering are rational protein design and directed evolution. Recently, combinations of these approaches have proved to be very effective.

1.3.1. Rational design

Rational design is based on the prediction of amino acid changes which will modify properties of a protein. Starting from the structure, the effects of these modifications are simulated *in silico* by molecular modelling and promising variants are generated by site-directed mutagenesis. To make this possible, information about the protein structure (or at least a homology model) and the catalytic mechanism are necessary. Conserved amino acids can also be identified by sequence or structure alignment.[54] These *in silico* studies not only require information about the target protein, but also a qualified experimenter who can interpret the data.

In rational design, only a small mutant library has to be created and thus, the analytical tools to identify the best variants are easier to manage. However, this strategy is restricted by the complexity of proteins and the impact of mutations on some properties, like thermostability, is difficult to predict rationally.

There are many examples of success in rational modification of enzyme activity. Based on steric principles, the substrate specificity of $P450_{cam}$ was extended from camphor to polycyclic aromatic hydrocarbons by mutation of two residues in the substrate-access channel.[55] Mouratov et al.[56] generated a dicarboxylic amino acid β-lyase, an enzyme not found in nature, from a tyrosine phenol-lyase by rational design. Jochens et al.[54] converted an esterase into an epoxide hydrolase by rational exchange of one of the protein loops.

Modification of the enantioselectivity of enzymes by pure rational design is more difficult to predict and thus, there are less examples of it. However, some successes have been reported like the inversion of enantioselectivity of esterase BS2 by two point mutations by Bartsch et al.,[57] or the alteration of the enantioselectivity of lipases by Scheib et al.[58]

After decades of supremacy of directed evolution techniques, protein engineering is now moving towards rational design, as the mechanisms of enzyme catalysis and protein engineering become better understood. However, mutations introduced/detected by *in silico* studies tend to be closer to the active site -*"closer is better"*- because only relevant substrate-protein interactions can be interpreted. Thus, distal residues, which often play important roles in enzyme activity and selectivity, might be ignored leading to failure in protein improvement.

1.3.2. Directed evolution

Directed evolution, also called *in vitro* or molecular evolution, emerged in the 90's and is based on generation of genetic diversity (by substitution, deletion or insertion of nucleotides) and identification of the best mutants from the pool of genes. The best candidates identified in the first generation are usually further optimized in subsequent cycles. Thus, it is a cyclic process that is continuously repeated until the result is satisfactory.

Prerequisites for this strategy are the availability of the gene(s) encoding enzyme(s) of interest, a suitable (usually microbial) expression system, an effective method to create mutant libraries, and a suitable screening or selection system.[59] In contrast to the rational approach, no structural data of the enzyme and no knowledge of the relationship between amino acid sequence, structure, and mechanism of catalysis are required. Indeed, directed evolution can be used as a tool for investigating structure-function relationships.

The two critical steps of directed evolution are the generation of diversity in order to create the desired mutant, and the development of a high-throughput screening methodology that allows identification of the improved mutant.

1.3.2.1. *Methods of mutagenesis*

Lutz and Patrick[60] enumerated the features that an ideal mutagenesis method should have: 1) unbiased mutational spectrum, 2) controllable mutation frequency, 3) consecutive nucleotide substitutions or codon-based substitutions, 4) enable subset mutagenesis (e.g. introducing mainly positively or negatively charged amino acids, bypassing stop codons, etc), 5) independence of gene length, 6) technically simple and reproducible and 7) economical.

Table 1-2. Overview of some of the current available methods of mutagenesis.

Non- recombinant methods	**Reference**
error-prone PCR (epPCR)	Leung et al.[61]
error-prone rolling circle amplification (epRCA)	Fujii et al.[62]
cassette mutagenesis	Borrego et al.[63]
mutator strains	Greener et al.[64]
strand overlap extension (SOE)	Ho et al.[65]
gene site saturation mutagenesis (GSSM)	Gray et al.[66]
random insertions and deletion mutagenesis (RID)	Murakami et al.[67]
MAX randomization	Hughes et al.[68]
MegaWHOP	Miyazaki et al.[69]
codon shuffling	Chopra et al.[70]
codon-based random deletion (COBARDE)	Osuna et al.[71]
random elongation mutagenesis (REM)	Matsuura et al.[72]
sequence saturation mutagenesis (SeSaM)	Wong et al.[73]
circular permutation (CP)	Qian et al.[74]
Homology based recombinant methods	**Reference**
DNA shuffling	Stemmer et al.[75,76]
family shuffling	Crameri et al.[77]
staggered extension process (StEP)	Zhao et al.[78]
random chimeragenesis on transient templates (RACHITT)	Coco et al.[79]
degenerate oligonucleotide shuffling (DOGS)	Gribbs et al.[80]
mutagenic unidirectional reassembly (MURA)	Song et al.[81]
degenerate homoduplex recombination (DHR)	Coco et al.[82]
synthetic shuffling	Ness et al.[83]
assembly of designed oligonucleotides (ADO)	Zha et al.[84]
recombined extension of truncated templates (RETT)	Lee et al.[85]
multiplex-PCR-based recombination (MUPREC)	Eggert et al.[86]
Non-homology based recombinant methods	**Reference**
incremental truncation for the creation of hybrid enzymes (ITCHY)	Ostermeier et al.[87]
SCRATCHY	Lutz et al.[88]
sequence homology independent protein recombination (SHIPREC)	Sieber et al[89]
structure-based combinatorial protein engineering (SCOPE)	O′Maille et al.[90]
sequence-independent site-directed mutagenesis (SISDC)	Hiraga et al.[91]
non-homologous random recombination (NRR)	Bittker et al.[92]

Due to the degeneracy of the genetic code, high mutation frequencies are not sufficient to obtain all possible amino acid exchanges. To saturate one amino acid position all three

nucleotides which form the codon have to be exchanged. Thus, in theory, an ideal mutagenesis method statistically replaces any amino acid of the protein with one of the other 19, without affecting the protein expression. In practice, those methods which generate the most diverse and unbiased libraries are also the most complicated ones.

1.3.2.1.1. Non-recombining methods

In non-recombining methods, also called asexual evolution strategies, the target protein is mutated without including any sequences from other genes.

The generation of mutations to modify properties of strains whose genome is not known is generally performed by UV radiation or addition of chemical mutagens (deaminating or alkylating agents). These disturb the replication of DNA and decrease its usually very high fidelity. Another easy-to-perform approach consists in the use of mutator strains[93,94] (e.g. *Epicurian coli* XL1-Red[64] from Stratagene), which lack one or more DNA repair mechanisms increasing the mutation frequency in genomic DNA, vector and gene of interest during DNA replication. Mutator plasmids,[95] which produce mutator proteins (e.g. mutD5, from *E. coli* CSH116) after induction, can be used as well. Control over the mutation frequency in these approaches is achieved through the cultivation time. The problem with all these strategies is that mutagenesis is indiscriminate and highly biased, and mutations occur in chromosomal DNA as well, leading to unstable cells.

As a more practical and faster method, epPCR[61] has become the most universal method to generate random mutations in a given DNA fragment. By non-optimal reaction conditions during PCR, like substitution of part of the cofactor Mg^{2+} by Mn^{2+} and alteration of the nucleotide ratio, the error rate of the *Taq* polymerase can be increased from 0.001-0.02% to more than 1%.[96,97] Further protocols have been developed to increase the frequency of mutations,[98] and commercial kits (Clontech and Stratagene) are available as well for this purpose.

Drawbacks of epPCR are the non-homogeneous mutational spectrum (error bias, codon bias and amplification bias) in the exchange of nucleotides, and an often observed low ligation efficiency of PCR fragment and vector.[99] To overcome these problems, improved polymerases have been developed (Taq-Pol I615K,[100] Mutazyme® I and II from Stratagene[101] and *Pfu*-Pol (exo^-) D473G[102]) as well as several modified PCR protocols (Table 1-2).

Circular permutation (CP) is a singular non-recombining strategy to generate protein diversity that consists in the relocation of the N- and C-termini of a protein to increase chain flexibility and active site accessibility. CAL-B variants with altered catalytic function were generated following this strategy.[74] Later, Peisajovich et al.[103] performed in the laboratory the natural equivalent of circular permutation: gene duplication and in-frame fusion followed by degradation from the 5′ and 3′ ends to generate new N- and C-termini. They used a DNA-methyltransferase as model enzyme and obtained active variants. Moreover, they predicted the existence of a new class of these enzymes based on their results that indeed was found through sequence database search.

1.3.2.1.2. Recombining methods

These methods of sexual evolution are based on the combination of DNA sequences to generate diversity. The aim is the accumulation of advantageous mutations and the removal of deleterious mutations in a similar way to the sexual recombination existing in nature. The pool of homologous parent genes can originate from enzyme variants generated by asexual evolution or rational design, or from related natural sequences. Recombination can make much larger jumps in sequence space than random mutation.[104]

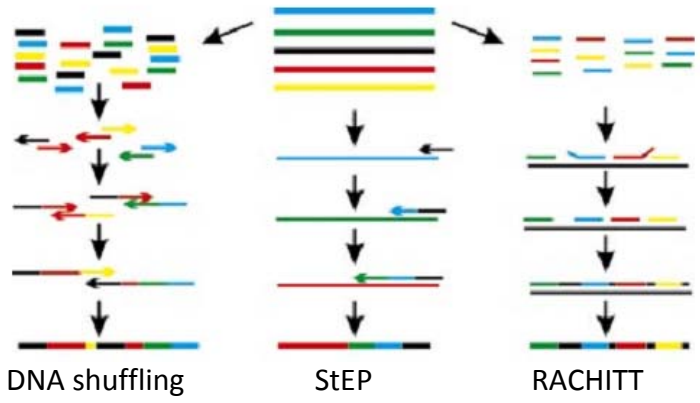

Figure 1-5. Diagram explaining three different recombination methods.

The first random recombination method described is the DNA shuffling, developed by Stemmer in 1994.[75,76] This method is based on recombination of DNA fragments generated by DNAseI digestion. Although it has proved to be a useful strategy,[105] it works only for recombination of homologous genes, and these are not always available; the DNAseI digestion is difficult to control; the ligation efficiency during PCR may be low

and crossovers will occur preferentially where the template sequences are most similar, yielding parental genes.

Many optimisations and variations of DNA shuffling have arisen since then (Table 1-2). Family shuffling[77] shuffles inter-species and accelerates the evolution process compared to intra-species shuffling. The staggered extension process (StEP)[78] is based on a modified PCR protocol where DNA fragments are not physically generated but added to the growing end of a strand. The random chimeragenesis on transient templates (RACHITT)[106] was designed to produce chimeras with a much larger number of crossovers. In synthetic shuffling[83] and assembly of designed oligonucleotides (ADO),[84] crossover events are directed and controlled by recombining synthetic oligonucleotides, which are designed based on the sequences of full length genes.

A variety of methods for the recombination of non-homologous sequences have been developed as well. The first protocol was developed by Benkovic′s group[87] and is called ITCHY (incremental truncation for the creation of hybrid enzymes). As it has proved to be difficult to control, an easier optimisation, thio-ITCHY,[107] was developed by the same group. The structure based combinatorial protein engineering (SCOPE),[90] and sequence independent site-directed chimeragenesis (SISDC)[91] designed in Arnold′s group and combined with the computational algorithm SCHEMA[108] are techniques that require structural information of the protein for the design of the crossover points. These methods already belong to semi-rational protein design strategies.

1.3.3. Choosing the best protein engineering strategy

In the last decades many different strategies for protein engineering have emerged, and finding the best choice for each individual case is not always easy. Strategies have been designed to simplify the process of chossing the most suitable method. Worth mentioning are the random mutagenesis strategy flowchart (RaMuS) and the keep it simple and smart (KISS)[109] tool. Arnold pointed out that in addition to the mutation strategy, another key factor for the success of protein engineering experiments is the choice of a suitable protein as starting point[104] in order to minimize the number of properties to be improved.

Kazlauskas and Bornscheuer[110] said that good evolution strategies should provide two advances simultaneously: first, the goal must be reached with the less effort; second, the success must be accompanied by a hypothesis of its molecular basis.

Recent examples in enzyme engineering have used a combination of the random methods of directed evolution together with elements of rational enzyme modification to overcome limitations of both strategies (Figure 1-6). In this way, smaller and "smarter" libraries, which are more likely to yield positive results, are created. This semi-rational approach is based in directing the generation of diversity to selected domains of the protein, identified mostly by *in silico* studies. The techniques are based on the incorporation of synthetic DNA sequences (degenerate or "doped" oligonucleotides) within the coding sequence. Targeted mutagenesis strategies allow the creation of neighbouring mutations, of multiple simultaneous mutations and of mutations requiring multiple nucleotide substitutions.[111]

Novo Nordisk combined directed evolution and rational design and created a mutant fungal peroxidase with 174 fold higher thermal stability and 100 fold higher oxidative stability than the wild type.[112] Following a similar approach, Park et al. [113] converted glyoxalase II, which hydrolyzes the thioester bond of (*S*)-D-lactoylglutathione, into a metallo-β-lactamase, catalyzing a similar reaction but in a completely different substrate (cefotaxime). The two naturally occurring enzymes that hydrolyze theses substrates share the overall fold and ancestry, but exhibit low sequence identity.

After the structure of the *Pseudomonas fluorescens* esterase I (PFEI) had been elucidated,[114] four positions were identified by Kazlauskas′ and Hult′s group to have an impact on enantioselectivity.[115] Thus, enzyme variants were identified with an increased E-value towards 3-bromo-2-methylpropionate. Jochens et al.[116] saturated these positions as well and succeeded increasing the enantioselectivity of the esterase towards ethyl-3-phenylbutanoate.

In iterative saturation mutagenesis (ISM)[117,118] proteins are analyzed to identify "hot spots" for the modification of an activity of interest. These sites are then subjected to saturation mutagenesis separately and the best variants of each position are further mutated until the goal is achieved. CASTing (combinatorial active-site saturation test) is a subcategory of ISM where positions are saturated simultaneously. It has proved to be effective in increasing enantioselectivity[119] and even inverting enantiopreference[57] of enzymes.

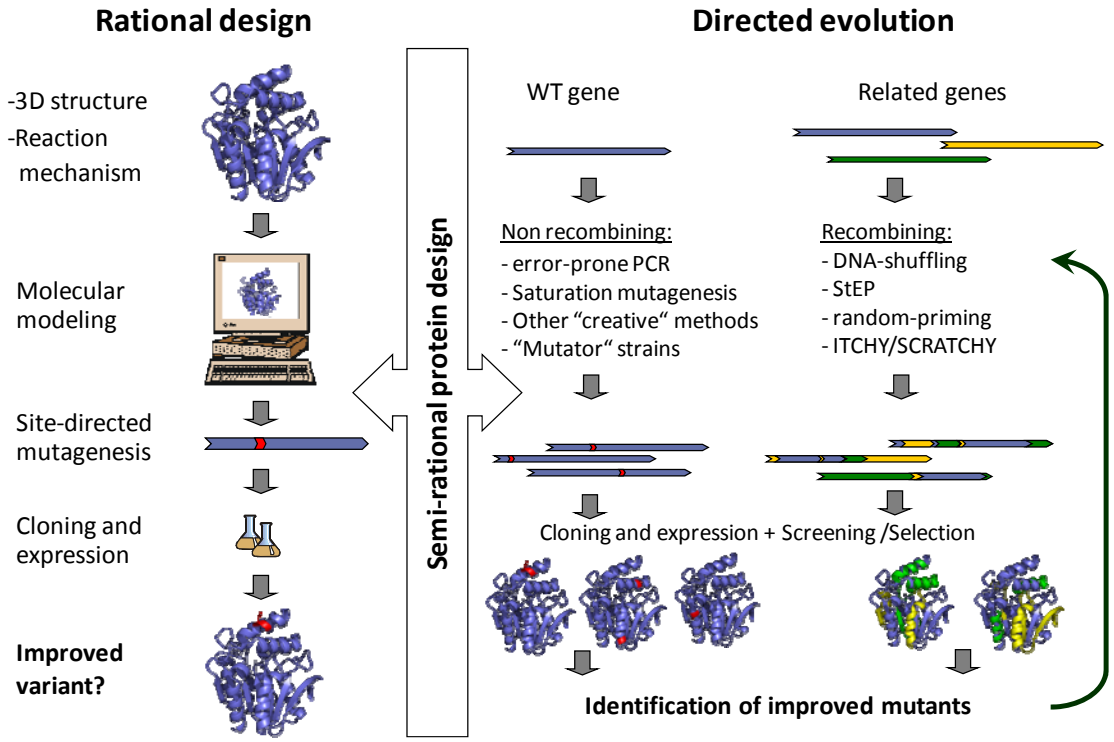

Figure 1-6. General schema of the different protein engineering approaches currently followed.

The neutral drift strategy supports the creation of small mutant libraries under selection to maintain the protein′s original function and structure. As a result a small amount of high polymorphic mutants are created which are functional and properly folded. Gupta and Tawfik screened less than 500 clones with "neutral" mutations from two paroxonase 1 (PON1) libraries (with high- and low-mutation rate) and found improved variants for five different substrates in both cases.[120]

The ProSAR approach[121] (Protein Sequence Activity Relationships) focuses the selective pressure on the mutations themselves rather than on the mutated gene. The ProSAR algorithm is an extension of the structure activity relationship (SAR)-based approaches for molecular optimisation. This study applied the concepts of quantitative structure-activity relationships (QSAR) to the problems of enzyme engineering and it consists of an iterative process of diversity generation and screening, followed by statistical analysis through linear regression on training sets derived from one or more combinatorial libraries per round. Using this methodology, Codexis evolved a bacterial halohydrin dehalogenase with improved productivity of a cyanation process ~ 4000 fold. This was achieved with variants containing at least 35 mutations.

Nowadays, it is clear that the structure of proteins can me modified in the laboratory in order to evolve activity and other properties. What remains to be seen, is whether it is possible to create enzymes as good as nature does.

1.4. Assay systems

Directed evolution and combinatorial optimisation strategies require a good assay for the identification of the mutant with the desired property from the diversity pool.

Molecular biology techniques have reached such a level that the creation of mutant libraries is rather uncomplicated. This is in contrast to analysis of those mutants which has become the major challenge. The typical library size is usually many orders of magnitude larger than the number of protein variants that can be screened. The same restriction applies to genomic libraries from natural sources, the diversity of which is almost unlimited. Thus, enzyme evolution is generally limited by the availability of a suitable high-throughput screening or selection system.[122]

Enzyme assays aim to make easily detectable the target reaction and its rate.[123] The substrate used in the assay should be identical or as close as possible to the target substrate, as the first rule of directed evolution is: *you get what you screen for.*[124] The protein found to be active or selective towards the screening substrate, will probably not have the same activity or selectivity towards the real substrate. In addition, the assay should be sensitive over the desired dynamic range and the procedure should be applicable in a high-throughput format. Therefore, assays often need to be tailored for every enzyme or reaction.

In principle, two strategies can be followed: screening or selection.

1.4.1. Screening methods

Screening is performed on individual clones and requires some spatial organization of the screened variants on agar plates, microtiter plates, arrays, chips, etc.[125]

Most screening methods rely on the use of fluorogenic or chromogenic substrates or sensors. Recently, flow cytometry coupled to cell sorting, has emerged as an important high-throughput mean of detection which allows to work in liquid media as the clones are individually analyzed in the stream of the flow cytometer (see 1.4.3).

1.4.1.1. Chromogenic/fluorogenic methods

These methods are usually employed because they are easy to handle. They are performed in a 96- or 384-well microtiter plate-based format in combination with high-throughput robot assistance (colony picker and/or pipetting robot) in the best case.

Umbelliferone,[126,127] and nitrophenol[128,129] derivatives are common substrates for screening. After hydrolysis of the esters occurs, umbelliferone is fluorescent and *p*-nitrophenolate has intense yellow colour. Thus, the reaction rate can be determined measuring fluorescence emission or UV/vis absorption and thus, activity can be determined or enantioselectivity can be estimated (using esters of single enantiomers). Detection of fluorescence signal is more sensitive and accurate than measurement of UV/vis absorption as emission signals have lower background.

When screening for enantioselectivity, the drawback of using pure enantiomers separately is that the factor of competition is lacking, and only determination of apparent enantioselectivities (E_{app}) is possible. This can lead to significant errors in enantioselectivity estimation, as differences of K_M towards each enantiomer do have substantial influence on enantioselectivity.[130] To overcome this issue, Kazlauskas' group developed an alternative screening method which they called Quick *E*.[131] Here, together with the pure enantiomers coupled to *p*-nitrophenol, an achiral reference compound coupled to resorufin was added (Scheme 1-6). This simulated the competitive condition between enantiomers of an enzymatic process and gave enantioselectivity values closer to the values obtained by end-point determination.[46] A variation of the Quick *E* method was later developed using *p*-nitrophenol as pH indicator in order to increase the substrate spectra.[132]

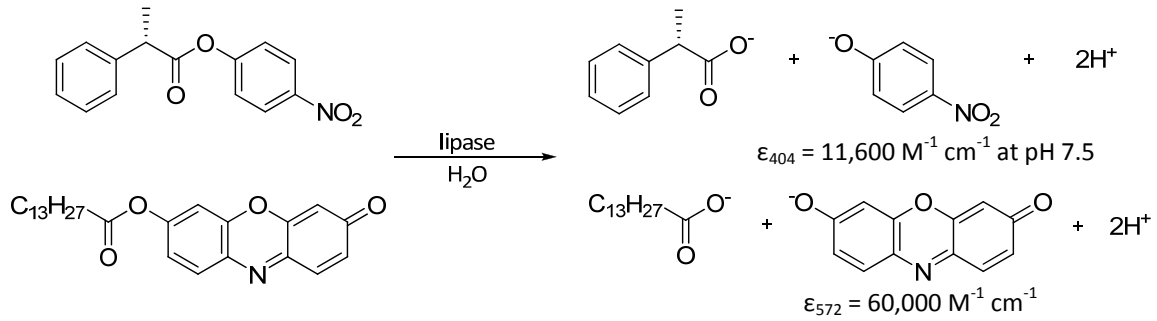

Scheme 1-6. Quick *E* test for enantioselectivity determination of lipases and esterases.[131]

An elegant variant to access to detection of enzymatic activity and enantioselectivity towards real substrates was developed by Baumann et al.[133] using a commercially available kit designed initially for the determination of acetic acid in food. The "acetic acid assay" is based on the release of acetic acid by hydrolysis of acetates, which is translated in an enzyme cascade to a proportional increase of NADH; and thus, measured spectrophotometrically or fluorometrically.

Compounds with 4-benzofurazane structure are fluorescent in different ways depending on the substituents at position 7. Thus, different derivatives (Scheme 1-7) have been employed to screen for transesterification reactions in organic media,[134] for amidase activity,[135] etc.

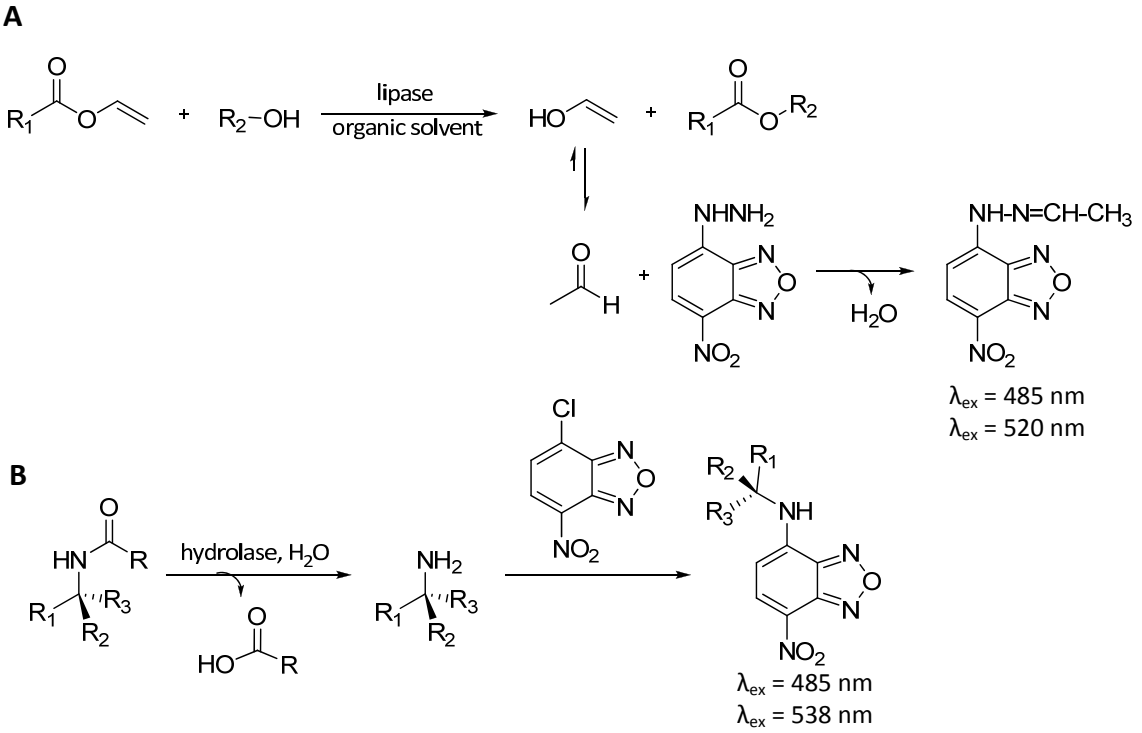

Scheme 1-7. Principle of 4-benzofurazane-based assays for transesterification in organic solvents (A) and for amidase activity (B).

The "adrenaline test"[136] is a useful assay developed by Reymond's group and is based on the principle of back-titration of sodium periodate with adrenaline. It has been used to detect epoxide hydrolases, lipases and esterases, and benzoin condensation of aldehydes to hydroxyketones. This method is in principle valid for any reaction that converts a periodate-resistant substrate to a periodate-sensitive product or vice-versa.

Many other chromophores and fluorophores have been reported for the assay of several enzymes: nitrilases,[137] epoxide hydrolases,[138-140] haloalkane dehalogenases,[141] aldolases,[142] acylases,[143] etc.

1.4.1.2. Alternative screening strategies

Some screening systems where detection of the reaction of interest is not based in colour formation or fluorescence emission will be discussed below.

Mass-spectrometric assays can be developed for screening of activity, stability, etc. Its application to enantioselectivity determination is more problematic because the (*R*)- and (*S*)-form of a chiral compound show identical mass spectra. The use of single enantiomers isotopically labelled can overcome this problem.[144] Thus, enantioselective nitrilases created by GSSM were detected using a pseudo-prochiral ^{15}N-labelled 3-hydroxyglutaronitrile.[145] Isotopically labelled pseudo-racemic substrates have also been analysed by high-throughput ^{1}H-NMR[146] and Fourier-transform infrared (FT-IR) spectroscopy.[147] Nevertheless, the requirement of expensive equipment, the need of isotopically labelled substrates and the low throughput make these strategies unaffordable for most researchers.

Chromatographic assays based on GC or HPLC are not commonly used for screening because although they are very exact, the throughput is too low. Reetz et al.[148] adapted gas chromatography to perform high-throughput screening of enantioselectivity. By coupling two GCs to one autosampler they could analyze up to 700 *ee* per day.

IR-thermographic assays are based on visualization of the different photon intensities of the detected infrared radiation. Moates et al.[149] were pioneers using this method for library screening in 1996. Since then, IR-thermography has been used to screen libraries of both metal catalysts[150,151] and enzymes.[152,153] Limitations of it are that only qualitative determination is possible and that thermoneutral reactions cannot be assayed.

Surface-enhanced resonance raman scattering (SERRS) allows a rapid and highly sensitive identification of both lipase activity and enantioselectivity at ultra-low levels measuring the deposition of released benzotriazole dye on dispersed silver nanoparticles.[154] Although this technique is very sensitive (pl range) and reproducible, the need of a specific apparatus to measure Raman intensity and the required adaptation to microtiter plate format are clear drawbacks.[155]

Capillary electrophoresis (CE) or its miniaturized derivatives like capillary array electrophoresis (CAE) or CE on microchips are possible screening techniques as well, because of features like small sample need, no solvent consumption, no high pressure pumps and valves, and high durability columns. CE is also effective in chiral separation of challenging substrates like amines.[156]

Competitive immunoassays using analyte-specific antibodies are classical analytical techniques for detection of small molecules. The method was adapted to screen for enantioselectivity in asymmetric synthesis (chiral product from achiral substrate) using enantiomer-specific antibodies.[157,158]

1.4.2. Selection methods

Selections have been traditionally based on enrichment of microorganisms, but advances in biotechnology currently allow the use of cell-free systems as well. Selection procedures act simultaneously over the entire pool of genes without need of individualization, the aim is that only variants of interest are selected for further analysis. Some selection strategies allow the analysis of 10^{10} variants at a time as they are generally less labour-intensive and, if well established and validated, more efficient than screening techniques.

Depending on whether living cells are used in the system or not, selection can be performed *in vitro* or *in vivo*.

1.4.2.1. In vitro selection

The main advantage of this type of selection is that it can be performed under harsher conditions. As it is not dependent on viable cells, non-physiological conditions such as elevated temperatures, extreme pH, or even organic media can be applied.

In order to link phenotype and genotype, different display techniques have been developed. These strategies have the advantage of providing the enzyme non-hindered accessibility to the substrate:

Phage display is specially useful to explore interactions between proteins, peptides, and small molecule ligands. Derivatives of M13 filamentous phages are most commonly used for display of proteins on the surface of *E. coli*. The successful display of many enzymes both periplasmic and intracellular, has been reported.[159-162]

Another strategy is bacterial cell surface display. In contrast to phage display, the size of the displayed protein is not a limiting factor in this strategy. Gram-positive bacteria (mainly *Bacillus* and *Staphylococcus* strains) are more suitable hosts for surface display than *E. coli* as they have only one cell membrane and their cell walls are thicker.[163]

In ribosome display, *in vitro* translation is performed in a cell-free system and the mRNA-ribosome-protein complexes formed constitute the association between genotype and phenotype.

mRNA display is an emerging selection route which has proofed to be effective for the selection of RNA modifying enzymes. Using this technique, Seelig and Szostak[164] created a new enzymatic activity from a non-catalytic scaffold. However, adaptation of mRNA display techniques to select for other protein activities is complicated.

Apart from display techniques, *in vitro* compartmentalisation (IVC)[165,166] has emerged as a new method to link phenotype and genotype. This technique consists of the simulation of cellular compartments by water-in-oil emulsions. The water phase is dispersed in the oil phase and forms microdroplets, artificial cells of ~ 5 fl. Each compartment contains in average a single gene and allows transcription, translation and expression of proteins to take place *in vitro* (Figure 1-7). As it is difficult that the product fluorophore remains associated with the gene and does not diffuse, most IVC screenings for enzymatic activity rely on physical linkage between the product and the gene. The most straightforward application of this strategy is the screening of DNA-modifying enzymes, in which case the substrate is the gene itself. Thus, IVC systems have been successfully used in evolution of DNA-methyltransferases,[167] restriction endonucleases,[168] polymerases,[169] and ribozyme Diels-Alderase.[170]

Stein et al.[171] developed a strategy based on cell-free protein expression in emulsion compartments where a link between protein and coding gene was established by a so called SNAP-tag. Thus, screening for activity and binding affinity of every protein could be performed.

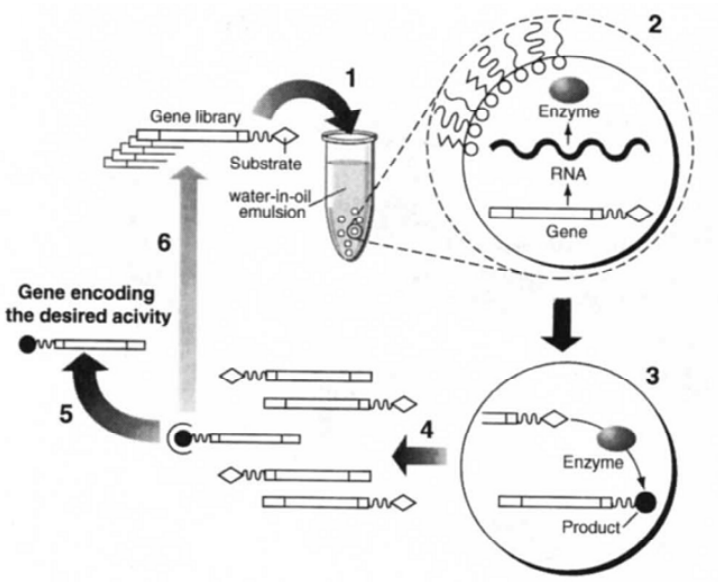

Figure 1-7. General strategy of enzyme screening using IVC.[172]

1.4.2.2. In vivo selection

This strategy is based on the theory of the *survival of the fittest* developed by Charles Darwin in 1859. All *in vivo* selection systems have in common the fact that the mutant library must be transformed into cells as a mean to associate genotype and phenotype. Limitations are the transformation efficiency, cells circumventing the selection pressure and the transport of the substrates through the cellular membrane.[122]

For effective selection, medium conditions are imposed in such a way that only those cells that express variants with the desired phenotype are viable. In positive selection, due to the enzyme activity a reaction occurs liberating a product which is an essential nutrient or which enables cell growth by neutralizing a given toxic effect; thus, reaction is coupled to survival or growth advantage. In negative selection, non-desired catalytic activities will release a toxin or growth disadvantage.

The general strategy for *in vivo* selection is the introduction of a metabolic requirement for the desired activity into the host cells: DeSantis et al.[173,174] engineered *E. coli SELECT*, auxotrophic for acetaldehyde, in order to select for mutants of *E. coli* D-2-desoxyribose-5-phosphate aldolase (DERA) with widened substrate specificity.

There are further strategies which do not require the use of special strains: racemases have been discovered in environmental samples using cultures with D-amino acids as sole carbon source.[175] The reaction product can be also linked with the transcription of a gene:

enzymatic activity can induce the activation/repression of the expression of an essential/toxic reporter gene.

Selection in prokaryotes is more commonly performed than in eukaryotes because of the lower complexity of the genomes, the higher transformation efficiency and the shorter division times.[176] It is recommended to use a well characterized organism as expression host, such as *Escherichia coli*.

There are many examples for the selection of new or increased activity. Bornscheuer et al.[94] evolved the *Pseudomonas fluorescens* esterase I and yielded activity towards a hydroxyl ester, a building block in the synthesis of epothilones, by implementing a selection system on agar plates supplemented with a glycerol ester of the target substrate. Crameri et al.[77] generated monolactamase activity in cephalosporinases by selection with the antibiotic.

Improved enantioselectivity is much more difficult to select for. An efficient selection system for enantioselectivity must select simultaneously for activity and enantioselectivity, otherwise all the non-active mutants (which are typically 50-80% of the library) will be selected as well. Reetz et al. were pioneers in this field demonstrating differences in growth inhibition of baker′s yeast expressing an enantioselective esterase in media supplemented with (*R*)- or (*S*)-fluoroacetate derivatives.[177] Later, Hwang et al. established a similar system based on pro-antibiotic substrates,[178] selection for chiral carboxylic acids and alcohols would be possible, varying the antibiotic coupled to the substrate. Very recently, real examples of *in vivo* selection for enantioselectivity in mutant libraries have been reported. Boersma et al.[179] established a system for selection of esterases expressed in the periplasmic space of *E. coli* using an aspartate auxotrophic strain. They synthetised an aspartate derivative for positive selection and a phosphonate ester for negative selection (Scheme 1-8). With this system they inverted the enantioselectivity of *Bacillus subtilis* lipase A towards isopropyliden glycerol from E = 1.8 (*S*-preference) to E = 8.5 (*R*-preference). In parallel, Reetz′s group managed it to apply their original fluoroacetate system for the evolution of CAL-B expressed in *Pichia pastoris*.[180] After system optimisation they achieved conditions in which the organism would grow in presence of acetic acid and would not grow when fluoroacetic acid would be released (Scheme 1-8). However, they achieved only moderate enantioselectivities (from E = 1.9 and *S*-preference, to E = 9 and *R*-preference) as well. If the reason for the

low selectivity improvement of these unique examples is a low quality of the libraries, or a sub-optimal selection system, remains unclear.

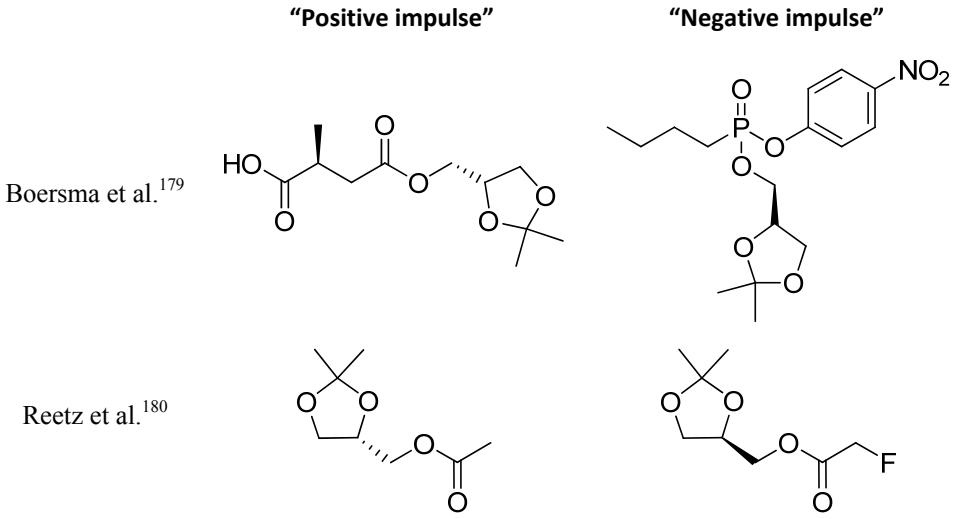
"Positive impulse"
"Negative impulse"
Boersma et al.[179]
Reetz et al.[180]
HO
O
O
O

challenging as the fluorophore product must remain linked to the enzyme coding gene and not diffuse away.

Flow cytometer screenings can be divided into four categories (listed below) according to the method used to link genotype and phenotype.

1.4.3.1. Cell surface display

By displaying enzymes on the cell surface, these can directly get in contact with their substrates without requirement of penetration into cell membranes. Georgiou's group was pioneer in this field with the establishment of a flow cytometer-based screening for the serine protease OmpT; the enzyme was chosen because it is naturally located in the outer membrane of *E. coli*. They increased the promiscuity of this enzyme[183] designing a FRET substrate, which was positively charged to interact non-covalently with the negatively charged *E. coli* surface. In a similar way, they also changed the enzyme selectivity using in addition to the selection substrate a counter-selection substrate.[184-186]

The genotype-phenotype coupling is more reliable when the product of the enzymatic reaction remains covalently bound to the surface of the cell decreasing the risk of labelling unrelated cells. Antipov et al. developed a system to enhance the enantioselectivity of horseradish peroxidase (HRP) displayed on yeast with a fluorescently labelled tyrosinol substrate.[187,188] HRP reacts with hydrogen peroxide and the phenolic part of tyrosinol to produce a quinine-like structure bearing a radical in C2. The radical couples then spontaneously with tyrosine residues of the membrane in vicinity to HRP. Becker and Kolmar suggested the use of this tyramide-mediated coupling approach to detect the activity of hydrolases by esterification of the phenolic hydroxyl group; this methodology was named enzyme screening by covalent attachment of products via enzyme display (ESCAPED),[189] and was successfully applied.[190] ESCAPED has been used recently to increase the enantioselectivity of EstA from *Pseudomonas aeruginosa* towards 2-methyldecanoic acid (2-MDA).[191] By linking each enantiomer to a different reacting group (2,4-dinitrophenyl (DNP) and biotin, Scheme 1-9), they were able to detect the enantioselectivity related to the level of red/green fluorescence emitted after specific group labelling (Alexa Fluor 488-labelled antiDNP antibody, and streptavidin-(*R*)-phycoerythrin, respectively).

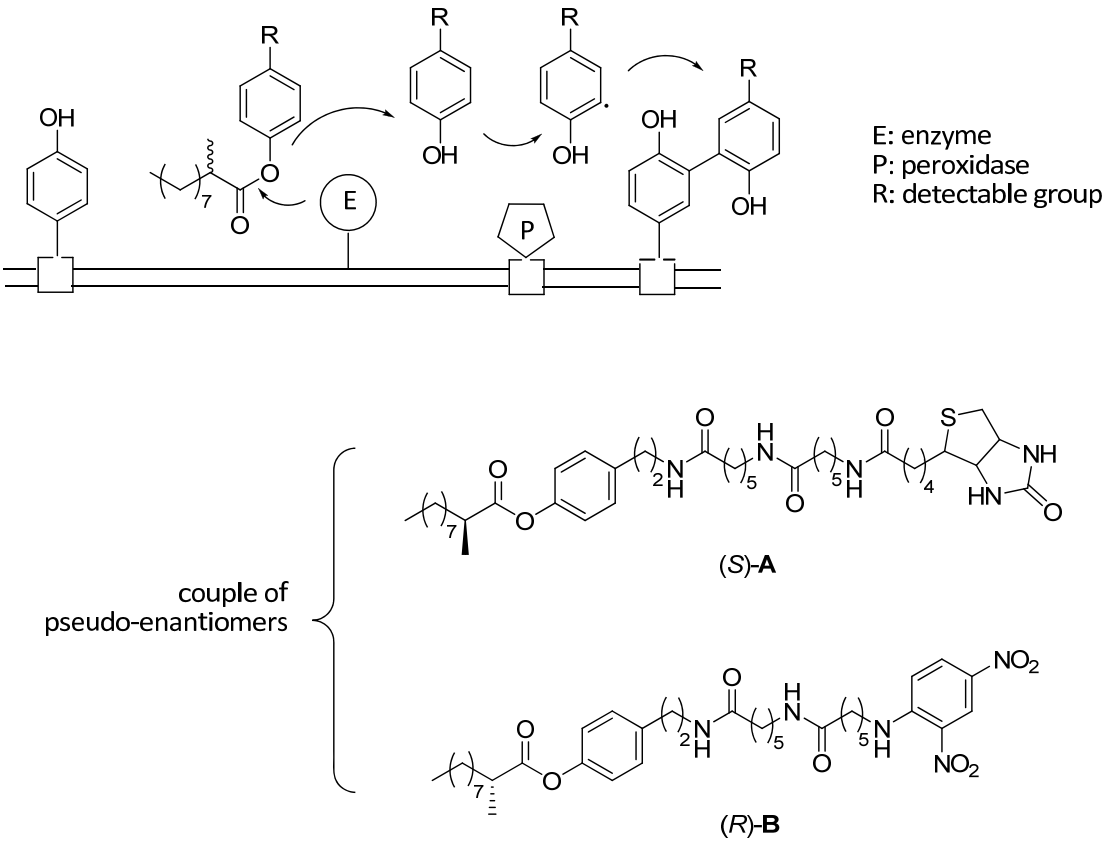

Scheme 1-9. General scheme of the ESCAPED method applied to increase the enantioselectivity of EstA.[191]

1.4.3.2. Green fluorescence protein and its variants as activity reporters

The green fluorescence protein (GFP)[192] and its variants are perfect candidates to be used in fluorescence analysis. These auto-fluorescent proteins can serve as targets of directed evolution themselves, but they can also be used to evolve the solubility of proteins[193,194] (Figure 1-8, A), or to remove completely inactive variants from directed evolution experiments, generating "cleaner" libraries.[120] The activity of the protein of interest can also be coupled to GFP expression (Figure 1-8, B). Following this strategy, the substrate specificity of a Cre recombinase[195] and an aminoacyl-tRNA synthetase[196] were altered. The development of a pH-sensitive GFP mutant[197] called pHluorin, allows the detection of almost any hydrolytic reaction via flow cytometric analysis with the advantage that the synthesis of pro-fluorescent substrates, which might be complicated, is not necessary anymore (Figure 1-8, C). pHluorin has different excitation ratios (fluorescence at 410 nm and 430 nm) depending on the pH and this makes hydrolysis detectable.

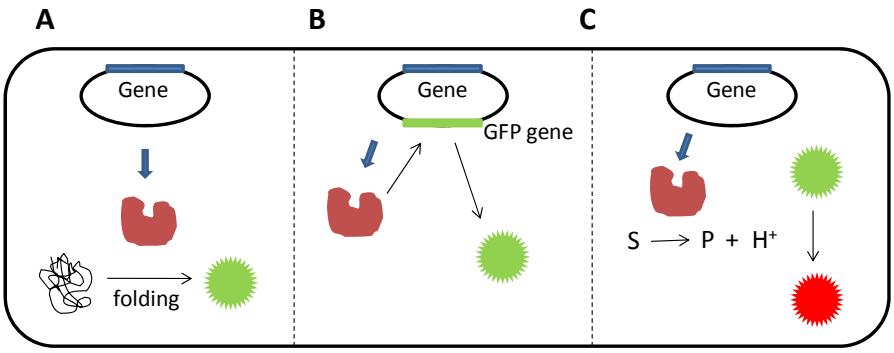

Figure 1-8. Schematic representation of some of the applications of GFP as activity reporter. A: reporter of protein solubility; B: reporter of protein activity; C: pHluorin, reporter of hydrolytic activity.

1.4.3.3. Screening of intracellular enzymes

The development of these flow cytometer screening systems is limited by the challenging design of a substrate that can penetrate the cell while the transformation product will be retained inside the cell. The incubation times can be optimized to minimize undesired substrate diffusion, but careful design of the process is necessary anyway. Despite the required laborious work, there are many examples of enzyme evolution using living cells as entrapment system: Aharoni et al.[198] developed a FACS-based high-throughput screening to detect the activity of glycosyltransferases (GT). Detection of GT activity is challenging, as no change in fluorescence/absorbance is associated with glycosidic bond formation. Thus, they synthesized the fluorescent substrate lactose-bodipy, which can enter and leave the cell while its sialylated product (sialyl lactoside) remains in the cell. Similar strategies have been used to evolve the activity of glutathione transferases,[199,200] ferrochelatases,[201] and ribozymes.[202]

1.4.3.4. In vitro compartmentalisation and fluorescence-activated cell sorting

The use of *in vitro* compartmentalisation (IVC) in association with fluorescence-activated cell sorting (IVC-FACS) exponentially increased the potential of both techniques, hence becoming an important tool in protein engineering experiments.

The gene, the encoded enzyme, and the enzyme products can be linked through microbeads. Griffiths and Tawfik used this system to evolve the activity of a

phosphotriesterase.[203] As the external oil phase of water-in-oil emulsions is not compatible with flow cytometry, in a further approach, double water-oil-water emulsions have been used to directly analyse intact emulsion droplets by flow cytometry. Thus, the attachment of the biocatalytic product to a microbead is not necessary anymore. The ancestral β-galactosidase EBG was evolved this way using a cell-free translation system and the commercial substrate di-β-D-galactopyranoside (FDG).[204] *In vitro* compartmentalisation of living cells is also possible. Aharoni et al. used double emulsions together with living cells to evolve the activity of serum paroxonase PON1.[205] The low enzymatic activity and the background hydrolysis of thiobutyrolactones made the activity of PON1 difficult to detect when *in vitro* expression in emulsion droplets was performed. The expression of PON1 on the surface of *E. coli* cells yielded higher protein levels and this allowed detection and selection of variants with 100 fold improvement in thiolactonase activity.

2. AIMS OF THIS THESIS

2. AIMS OF THIS THESIS

2.1. In vivo selection and flow cytometry as a tool for the identification of enantioselective esterases

The aim of this thesis was to develop an *in vivo* selection system for identification of enantioselective esterases using a flow cytometer with cell sorter to increase the throughput and sensitivity of the process. Esters of the chiral carboxylic acid 3-phenylbutyric acid (**3-PBA**) were chosen as model substrates for establishment and validation of the assay.

For development of the selection system, design and synthesis of adequate selection substrates was necessary. Optimisation of the selection medium to achieve solubility of the selection substrates in a system that allows cell viability was a requirement as well.

The search of suitable candidates for establishment and validation of the selection system had to be performed. Thus, esterases with different enantioselectivity towards the model substrate had to be identified and recombinant expressed in the host organism used for selection.

Once the assay had been implemented, a mutant library would be analyzed searching for variants with improved enantioselectivity towards 3-phenylbutanoates. The identified enantioselective variants would be analyzed and molecular hypothesis for the increase of enantioselectivity would be given.

After *in vivo* selection of an *in vitro* generated mutant library had been performed, simultaneous *in vivo* evolution and selection would be attepted. For this aim, identification of a suitable physicochemical mutagen, and optimisation of mutagen concentration to achieve good mutation rates compatible with the selection system was attempted.

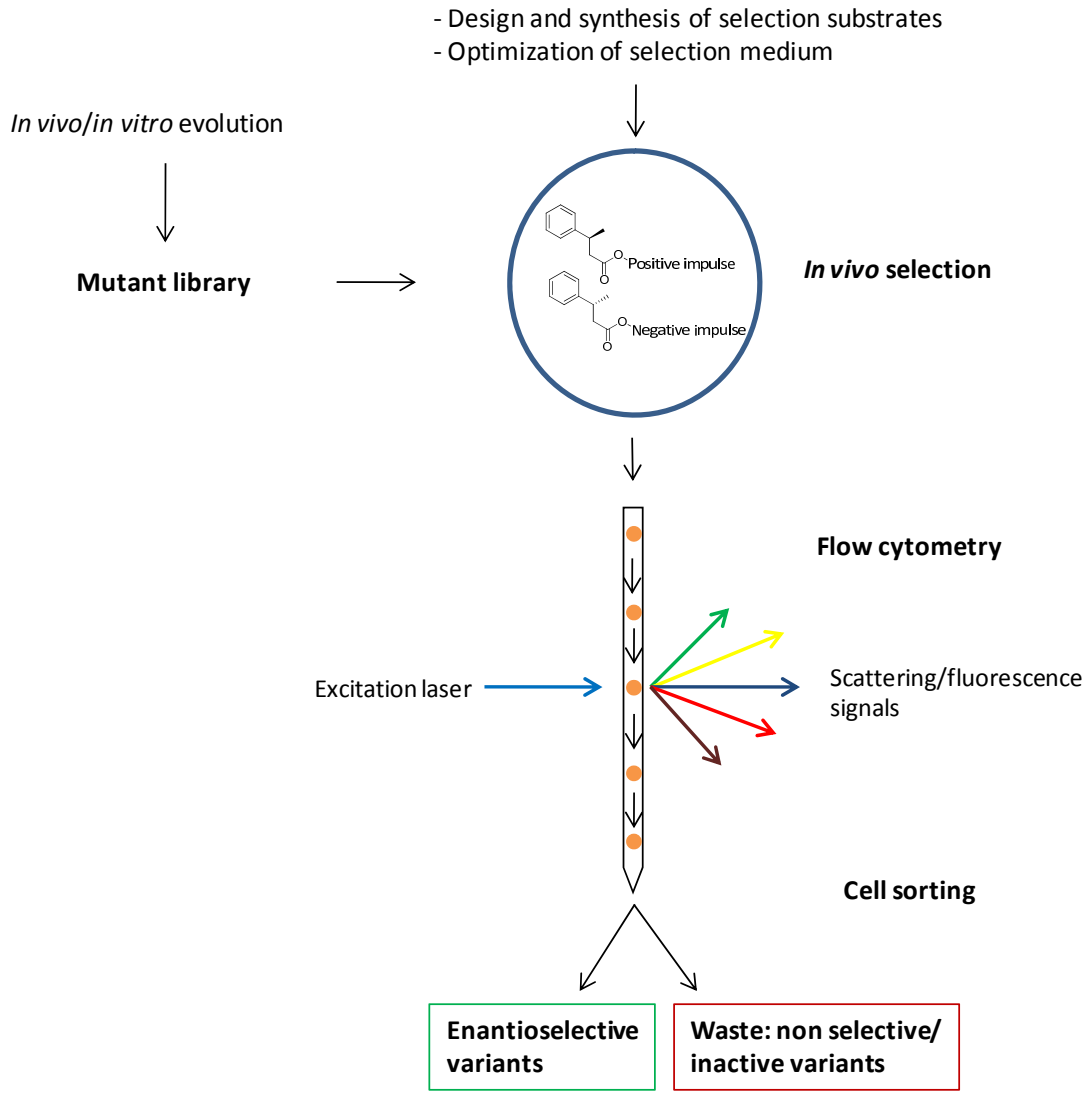

Figure 2-1. Scheme of the strategy followed in the implementation of an *in vivo* selection system coupled to flow cytometry for identification of enantioselective esterases.

2.2. Crystallization, structure elucidation and analysis of the esterase from Pyrobaculum calidifontis (PestE)

During this PhD thesis crystallization of the biocatalytically important esterase from the hyperthermophilic archaeon *Pyrobaculum calidifontis*[206] (PestE) was also attempted. For this aim, recombinant expression of PestE and obtaining of enough amount of the protein in high purity was necessary. After crystallization and resolution of the three-dimensional structure of the enzyme, hypothesis for biochemical properties like substrate selectivity and thermostability would be given.

3. RESULTS AND DISCUSSION – CHAPTER I:

IN VIVO SELECTION AND FLOW CYTOMETRY AS A TOOL FOR THE IDENTIFICATION OF ENANTIOSELECTIVE ESTERASES

3. *IN VIVO* SELECTION AND FLOW CYTOMETRY AS A TOOL FOR THE IDENTIFICATION OF ENANTIOSELECTIVE ESTERASES

The purpose of this project is the development of an *in vivo* selection system coupled to flow cytometry, in order to achieve straightforward identification of enantioselective esterases. Figure 3-1 describes the logical structure of the experiments carried out in this work.

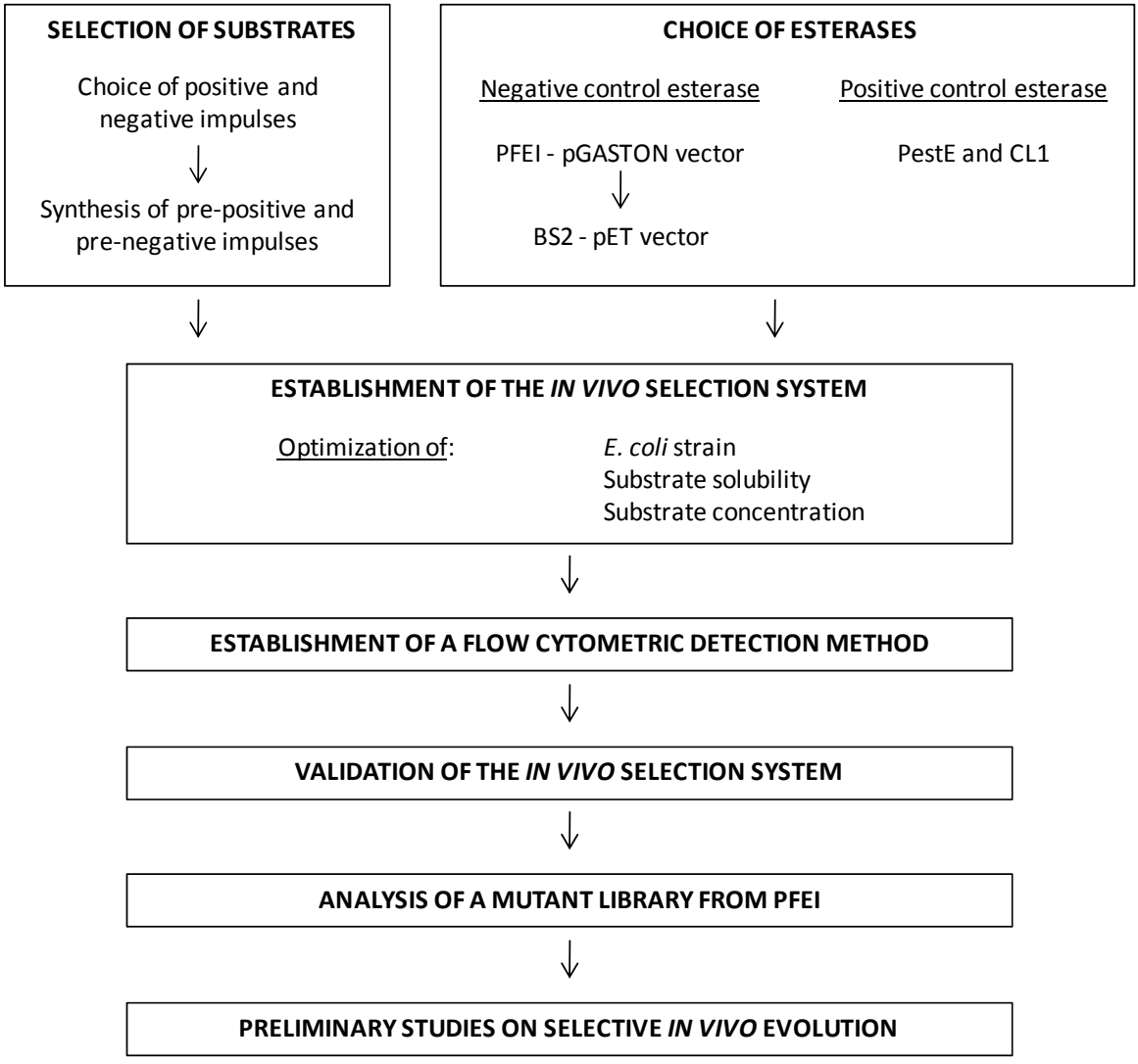

Figure 3-1. General scheme of the strategy followed to develop the *in vivo* selection strategy coupled to flow cytometry for identification of enantioselective esterases.

3.1. Selection of substrates

Aiming to apply the darwinian concept of *survival of the fittest*, selective pressure has to be applied. This pressure is represented by two impulses, positive and negative, which will enable cell survival or will cause cell death, depending on the nature of the expressed enzyme. In this way, cell viability can be coupled as a function of enzyme enantioselectivity. As model substrate, esters of a chiral carboxylic acid (3-phenylbutyric acid, **3-PBA**) were chosen. To generate positive and negative impulses, pseudo-enantiomeric esters of **3-PBA** with different alcohol moiety were designed and synthesized.

The bacterial host *Escherichia coli* was chosen as expression organism because it is simple and well characterised, a variety of esterases were recombinantly expressed so far in it, and its high transformation efficiency allows creation of large mutant libraries.

3.1.1. Choice of the positive impulse

A common strategy in positive selections is the fulfilling of a nutritional requirement in order to enable cell survival. Instead of using an auxotrophic strain, it was attempted to create a system where selection in any *E. coli* strain could be performed. Thus, a molecule containing a carbon source was considered as positive impulse. In previous studies[207] 1,2-isopropylideneglycerol (**1a**) was chosen as carbon source for coupling with carboxylic acids due to its ease of preparation. The choice of this molecule was based on the hypothesis that after ester hydrolysis occurs, a spontaneous cleavage of the acetal group would take place resulting in the formation of acetone and glycerol (**2a**, Scheme 3-1).

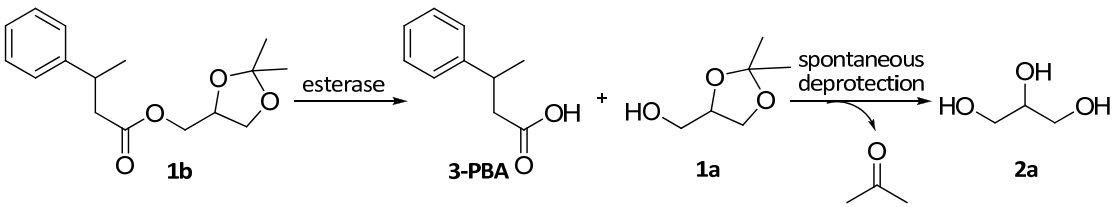

Scheme 3-1. General scheme for biocatalysis of the 1,2-isopropylideneglycerol ester **1b** resulting in final release of glycerol (**2a**).

3.1.1.1. Bacterial growth on 1a

Prior to selection experiments, *E. coli* DH5α cultures were grown in M9 minimal medium supplemented with **1a** as the only carbon source in various concentrations (5-300 mM). Bacterial growth was monitored and compared to cultures grown on glucose and glycerol (Figure 3-2). As no growth in the media supplemented with **1a** was observed, the substrate could not be used as positive impulse. Whether the absence of cell growth was due to non-ocurring cleavage of the acetal group of **1a**, due to problems of substrate diffusion into the cell, or due to toxicity of the acetone (by-product in acetal hydrolysis) was not further investigated.

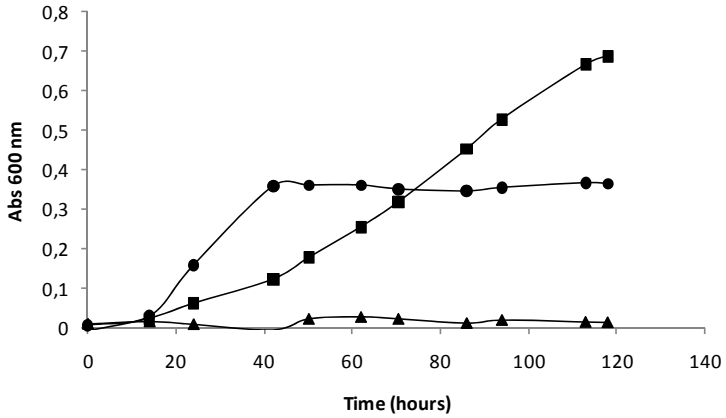

Figure 3-2. Growth curves with **1a**, **2a** or glucose as carbon source. Triangles: 30 mM **1a**; circles: 30 mM **2a;** squares: 30 mM glucose.

Glycerol was chosen as positive impulse because no secondary reaction is required for its availability as carbon source to cells. Compared to glucose, its structure is simpler and more similar to the ethyl group generally used for ester hydrolysis in kinetic resolutions, and similarity between substrates used in assays and real substrates is always desired. Hence, the next effort was put on the synthesis of the glycerol ester **2b**.

3.1.2. Synthesis of the pre-positive impulse

Two strategies have been considered for the synthesis of **2b**: deprotection of **1b**, and direct esterification with **2a**.

3.1.2.1. Deprotection of 1b

This strategy consists on a three step synthesis. First, **3-PBA** was derivatized to its acyl chloride followed by esterification with **1a**. As a final step, different chemical deprotection strategies for cleavage of the acetal group of **1b** were attempted (Scheme 3-2).

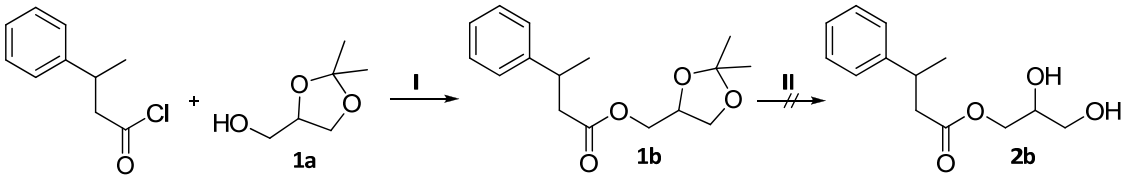

Scheme 3-2. General procedure for the synthesis of **2b** by the above described strategy. **I**: THF, 10 equiv. TEA, inert atmosphere. **II**: various deprotection techniques.

The synthesis of the acetonide of 2′,3′-dihydroxypropyl-3-phenylbutyrate (**1b**) was successful and the product was isolated in moderate yield. However, none of the tested conditions for acetal deprotection (Table 3-1) resulted in formation of the ester **2b**. Alternative synthetic routes towards **2b** were suggested instead of further deprotection attempts.

Table 3-1. Overview of the used strategies for acetal deprotection.

Deprotection technique	Result
75% TFA in water	Hydrolysis of the ester bond
1 equiv. PPTS in methanol	No reaction
5% mol PTSA in acetone	No reaction

3.1.2.2. Direct esterification with 2a

In order to overcome the difficulties of deprotection of **1b**, direct esterification with **2a** was carried out. In this case, two synthetic strategies were followed:

*3.1.2.2.1. Azeotropic esterification of **3-PBA** and **2a***

This strategy is based on direct esterification of the free acid (**3-PBA**) and the alcohol (**2a**, Scheme 3-3) at reflux temperature with in situ removal of the formed water (with a Dean-stark trap) in order to shift the reaction equilibrium.[208] After the reaction was completed,

the mixture was analyzed by thin layer chromatography (TLC) and the formation of multiple products in similar proportions (three non-identified spots and the substrate **3-PBA**) was observed. The strategy was refused due to the significant formation of by-products without their further characterization. It was predicted that due to the harsh reaction conditions (high temperature) no selective esterification with glycerol occurred resulting in formation of mono-, di-, and tri- glycerids.

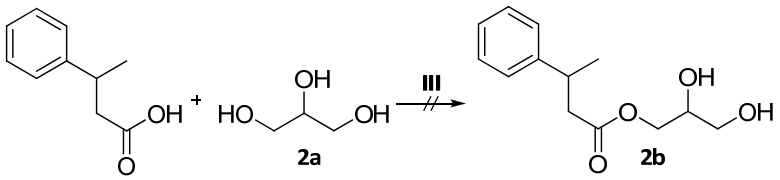

Scheme 3-3. General procedure for the synthesis of **2b** by azeotropic esterification. **III**: Toluene, catalytic amount of sulphuric acid, reflux, overnight.

*3.1.2.2.2. Esterification of acyl chloride with **2a***

Substrate **2b** was successfully synthesized by the direct esterification of **2a** with 3-phenylbutanoic acyl chloride. Based on the fact that primary alcohols are more reactive than secondary alcohols, a selective mono-esterification with glycerol was achieved by slow addition of the acyl chloride to a stirred mixture of the alcohol in tetrahydrofurane (THF). Glycerol must remain in excess to prevent poly-esterification, and excess is removed by extraction with basic water after reaction completion. Following this strategy **2b** was obtained in good yields.

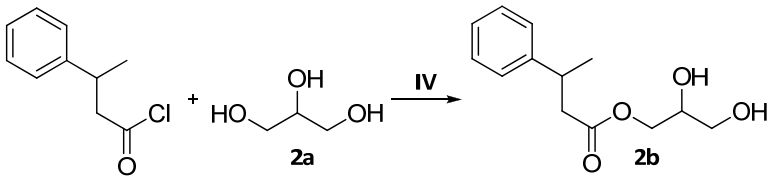

Scheme 3-4. General procedure for the synthesis of **2b** by esterification with acyl chloride. **IV**: THF, 10 equiv. TEA, nitrogen atmosphere.

3.1.3. Choice of the negative impulse

Regarding their clinical use as bactericide agents and previous work reporting their utilisation in enantioselectivity screening,[178] a pro-antibiotic substrate was designed as the

pre-negative impulse. Chloramphenicol (**3a**, Scheme 3-5) was the antibiotic selected, because it possesses one primary alcohol moiety in its structure, which makes the esterification with a carboxylic acid specific and simple.

According to the literature,[209] the minimum inhibitory concentration (MIC) of **3a** for *E. coli* in minimal medium supplemented with glycerol is 5 μg/ml (15 μM). The MIC of **3a** was experimentally determined for the *E. coli* strain of interest (*E. coli* DH5α) because *E. coli* strains have different characteristics, and variations in tolerance to antibiotics can exist. The MIC of the 3-phenylbutyric chloramphenicol ester (**3b**, Scheme 3-5) was also determined, because a prerequisite for negative selection is that toxicity occurs after enzymatic activity. Thus, low or no toxicity of the pre-selection esters is desired.

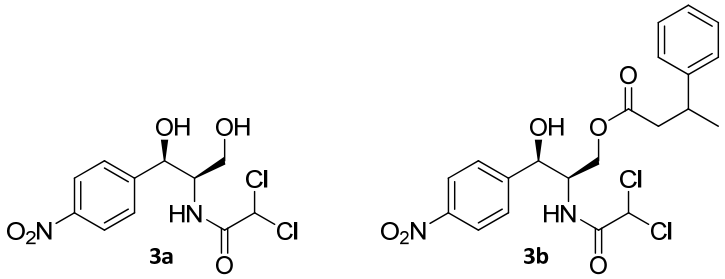

Scheme 3-5. Chemical structure of chloramphenicol (**3a**) and its ester of **3-PBA** (**3b**).

Growth assays with *E. coli* DH5α in M9 minimal medium supplemented with glycerol and different concentrations of **3a** (0-150 μM) or **3b** (0-1 mM) were performed and the MIC of both substances was determined: ≤ 9 μM (~ 3 μg/ml) for **3a** and ≤ 1 mM (~ 470 μg/ml) for **3b**. The antibiotic **3a** is 100 times more toxic than its ester **3b**. The toxicity interval between both molecules (negative impulse and pre-negative impulse) was considered adequate for an effective negative selection, as enzymatic activity would release the toxic compound.

After the first selection tests were performed (see 3.2.1), drawbacks in the use of chloramphenicol as negative impulse were revealed. The low structural similarity between alcohols **2a** and **3a**, and accordingly, between esters **2b** and **3b** (see Scheme 3-6) resulted in different hydrolytic activity of esterases towards **2b** and **3b** (estimation of reaction conversion by TLC, Figure 3-6 and Table 3-4).

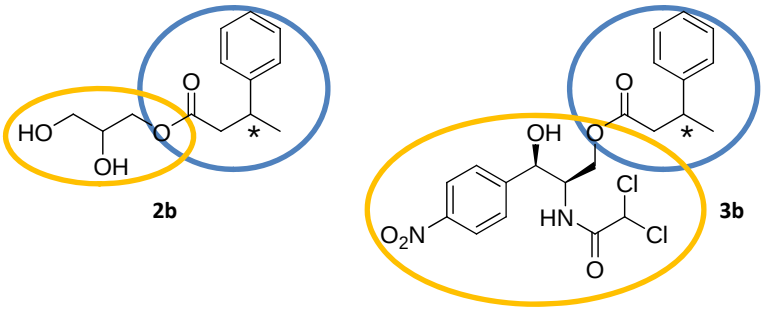

Scheme 3-6. Similarity between **2b** and **3b**. Acyl part highlighted in blue and alcohol moiety in yellow. The target chiral centre is indicated by an asterisk.

For the development of a selection assay for enantioselectivity in a high throughput manner, the selection molecules should ideally differ only in the target enantiomeric centre. In this case, the target enantiomeric centre is located in the acyl part (marked with an asterisk in Scheme 3-6) hence, similar alcohol moieties in the pseudo-enantiomeric selection substrates (pre-positive and pre-negative impulses) are desirable. Thus, alternative substances to chloramphenicol with higher structural similarity to glycerol were considered.

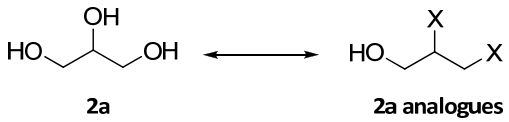

Scheme 3-7. General scheme of **2a** and its structural analogues.

Halogenated glycerol derivatives as well as an epoxide derivative of **2a** were investigated for their potential toxicity to *E. coli* (Scheme 3-8 and Table 3-2). Cultures of *E. coli* DH5α in M9 minimal medium supplemented with **2a** were set, and different concentrations of the potential toxins were added in order to determine the MIC by cell growth inhibition.

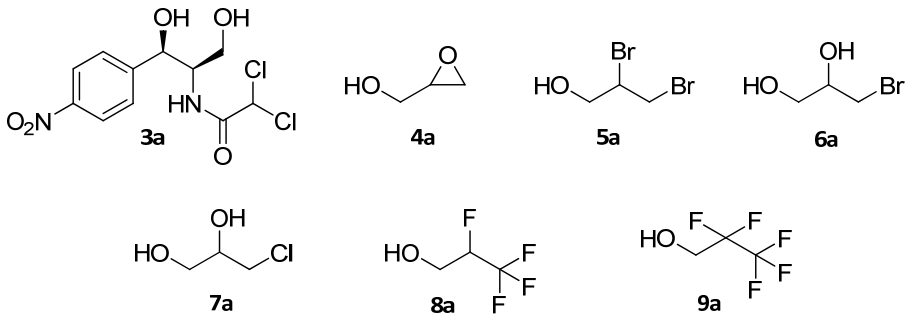

Scheme 3-8. Chemical structure of the substrates, which have been tested as toxins for *E. coli*.

Table 3-2. MIC of substrates **3a-9a** experimentally determined.

Substance	MIC (mM)
3a	≤ 0.009
4a	≤ 10
5a	≤ 10
6a	≤ 60
7a	≤ 250
8a	≤ 60
9a	≤ 40

Alcohols **6a** and **7a** were not further considered as substrates due to their low toxicity and low solubility in aqueous medium. Compounds **4a**, **5a**, **8a** and **9a** were further investigated and esters of **3-PBA** were synthesized (Scheme 3-10). The toxicity of esters **4b** and **5b** was determined upon growth of *E. coli* cultures (strains DH5α, BL21 (DE3) and JM109 (DE3)) in M9 minimal medium supplemented with glycerol and different concentrations of the substrates. Both substrates did not influence the growth at concentrations ≤ 20 mM, higher concentrations could not be assayed due to very low solubility of the substrates in aqueous media. As both substrates showed similar properties, **4b** was excluded because of the potential instability of the oxiran ring[210] which can hydrolyze leading to formation of the glycerol ester **2b** (Scheme 3-9).

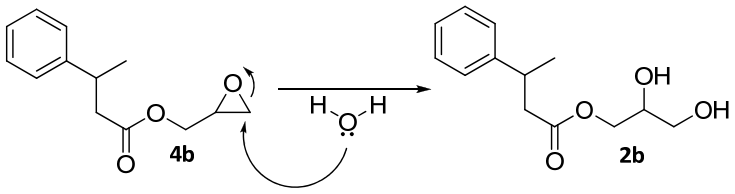

Scheme 3-9. Hydrolysis of pre-negative impulse **4b** to originate pre-positive impulse **2b**.

The fluorinated compounds **8a** and **9a** were good candidates despite their higher MIC than that of **4a** and **5a**, because their solubility in water was very good. Concentrations of **8a** and **9a** up to 80 mM could be dissolved in aqueous medium. Unfortunately, esters **8b** and **9b** showed similar MICs as the free alcohols (~ 60 mM in both cases), so these substances could not be further utilised due to the narrow toxicity interval between negative impulse and pre-negative impulse.

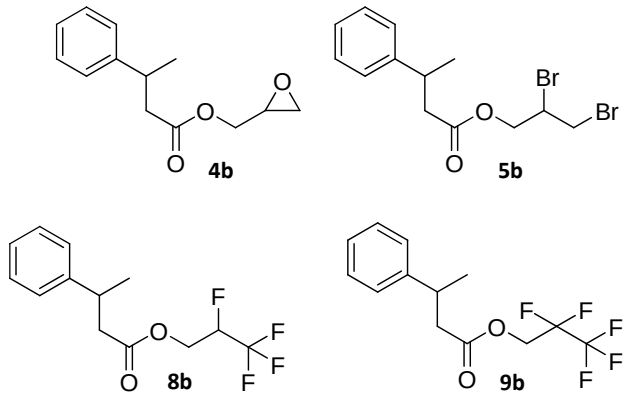

Scheme 3-10. Candidates for pre-negative impulse.

Due to the failure of all the other compounds for various reasons (toxicity, stability), **5a** was further studied. The toxic effect of **5a** and **5b** was determined by flow cytometric analysis to assure data correlation, and the results were comparable with those previously obtained by OD measurement (same MICs, see 3.3.3.). Flow cytometry allows analysis of emulsions as well as clear solutions; this enables to analyse the toxicity at higher concentrations of **5b**. The highest analysed concentration was 40 mM and it still did not affect cell growth. Higher concentrations of this ester could not be tested due to the low substrate solubility even after system optimisation (see 3.3.2.). Finally, **5a** was chosen as negative impulse because of its structural similarity to glycerol, the MIC of this substance is reasonably low, and there is a good toxicity interval between alcohol (negative impulse) and ester (pre-negative impulse).

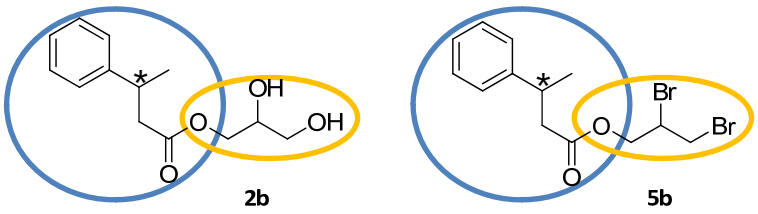

Scheme 3-11. Structural similarity between **2b** and **5b**. Acyl part highlighted in blue and alcohol moiety in yellow. The target chiral centre is indicated by an asterisk.

3.1.4. Synthesis of the pre-negative impulses

All pre-negative impulses were synthesized by direct esterification of 3-phenylbutyric acyl chloride with each of the alcohols, as previously described in 3.1.2.2.2. The procedure was optimized and moderate to good yields were obtained (Table 3-3).

Table 3-3. Overview of the yields obtained in the synthesis of pre-negative impulses **3b**-**9b**.

Substrate	Yield (%)
3b	25
4b	46
5b	70
8b	55
9b	73

3.2. Control esterases and selection simulations

Parallel to design and synthesis of the pre-selection substrates, search of control esterases to establish and validate the *in vivo* selection system was performed (Figure 3-1). Availability of a high enantioselective esterase and a non-enantioselective is desired, in order to use these as positive and negative control, respectively. Prerequisites for the control esterases are their recombinant expression in *E. coli* and ability to hydrolyze the pre-selection substrates.

Primarily, establishment of the selection system was performed by 'selection simulations', consisting of pseudo-selection media where only one impulse (positive or negative) was present, instead of presence of both impulses simultaneously. The effect of each impulse was determined separately studying cell growth and growth inhibition.

3.2.1. Negative control esterase

3.2.1.1. PFEI-pGASTON vector

The esterase I from *Pseudomonas fluorescens*, also named PFEI[211] (pdb: 1va4) had been chosen as model enzyme for this project in a previous work[207] as our working group has wide experience engineering this protein.[54,116,212-215] In addition, PFEI is not enantioselective towards 3-phenylbutanoates and former attempts of selectivity enhancement led to only minor successes (the highest enantioselectivity of a mutant was E = 6.6, the wild type has E = 3.3[93]).

Hence, 'selection simulations' were performed with PFEI as control esterase, cloned in a rhamnose-inducible expression vector (pGASTON) and expressed in *E. coli* DH5α. One

culture expressed active esterase and another culture expressed an inactive construct of PFEI, which was made by digestion of the PFEI gene with *Nco*I. The PFEI gene has two restriction sites for *Nco*I, at 284 and 654 bp. After restriction and ligation, a fragment of 342 bp resulted (Figure 3-3) which encoded for a protein without esterase activity. The absence of esterase activity was proofed by *p*NPA assay. The protein expressed was much smaller than the parental PFEI because, in addition to the fragment removed, a stop codon after 342 bp appeared due to codon frameshift.

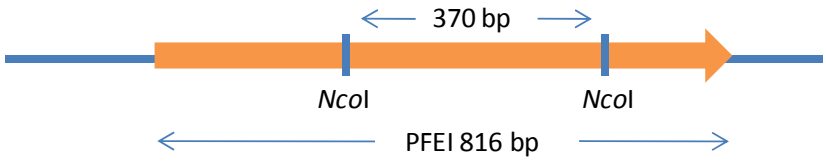

Figure 3-3. PFEI gene with indicated *Nco*I restriction sites.

Pseudo-selection media with different concentrations of **2b** (1-20 mM) or **3b** (200-700 µM) were utilised in order to optimise substrate concentration for the *in vivo* selection system. Concentrations of both, pre-positive and pre-negative impulses (**2b** and **3b**) were optimised separately and in parallel.

Unfortunately, the observed results were not those expected. In cultivations in M9 minimal medium supplemented with **2b** and 0.2% L-rhamnose (inducer for protein expression), bacterial growth was observed in cultures with and without esterase activity (Figure 3-4). This growth was comparable to the control culture supplemented with **2a** (glycerol). Thus, the activity of PFEI towards substrate **2b** and the effect of L-rhamnose on cell growth were further investigated (3.2.1.2.).

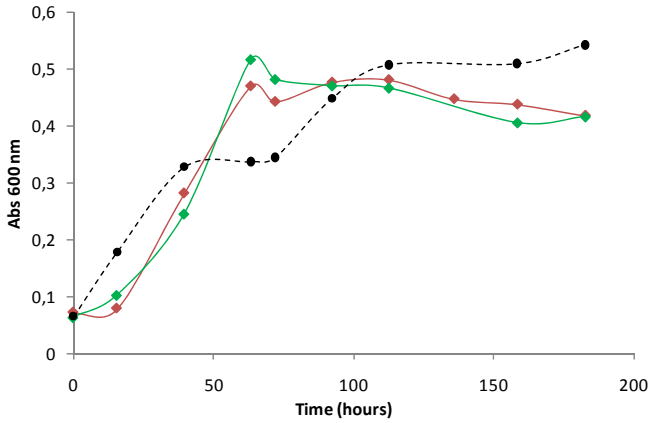

Figure 3-4. Growth curves in pseudo-selection medium supplemented with **2b**. Green diamonds: cultures expressing active PFEI. Red diamonds: cultures expressing inactive protein. Black circles: control culture, supplemented with **2a**.

In cultivations in M9 minimal medium supplemented with L-rhamnose, glycerol and different concentrations of **3b**, more encouraging results were obtained. Differences in cell growth in cultures expressing PFEI and inactive protein were observed; however, growth inhibition in cultures expressing PFEI was evidenced after 15 hours cultivation (Figure 3-5), which is longer time than desirable. This fact indicates that probably the hydrolysis of **3b** by PFEI is slow. In addition, the control culture (without addition of **3b**) showed better growth than the culture expressing inactive protein, which indicates toxicity of **3b**. Thus, decrease in **3b** concentration was necessary.

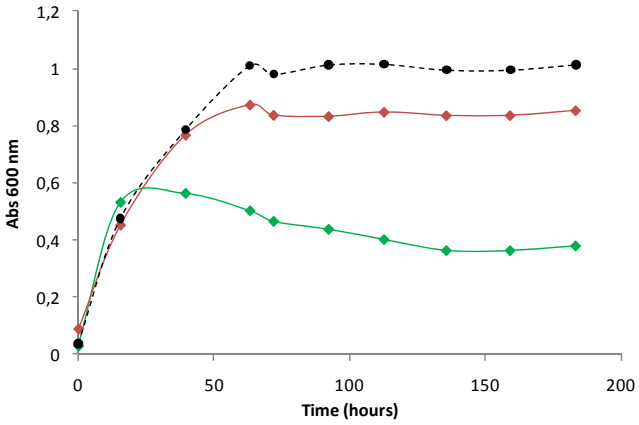

Figure 3-5. Growth curves in pseudo-selection medium supplemented with **3b**. Green diamonds: cultures expressing PFEI; red diamonds: cultures expressing inactive protein; black circles: control culture, without **3b**.

3.2.1.2. Analysis of the in vivo selection system components

The model catalyst and the components of selection medium were analyzed in order to find an explanation for the unexpected bacterial growth in the pseudo-selection media.

3.2.1.2.1. Model catalyst

The ability of PFEI to hydrolyze the pre-selection substrates was tested in biocatalysis monitoring conversion via TLC (Figure 3-6). Low hydrolytic activity towards substrate **3b** was detected, while no conversion of **2b** after 24 hours reaction time could be observed. This indicates that the activity of PFEI towards the selection substrates is too low; so, although it had been used in previous work on this project,[207] this esterase does not fulfil one of the prerequisites to be a control esterase and was thus excluded.

Esterases available in the laboratory, which were expressed in good levels in *E. coli*, were tested for activity towards **2b** and **3b**. Among the five tested esterases (BS2, SDE, PFEII, BsubE, BsteE), the *p*-nitrobenzyl esterase from *Bacillus subtilis*, BS2[50] (pdb: 1qe3) showed activity towards both selection substrates (Figure 3-6 and Table 3-4) and thus, it was chosen as new model catalyst.

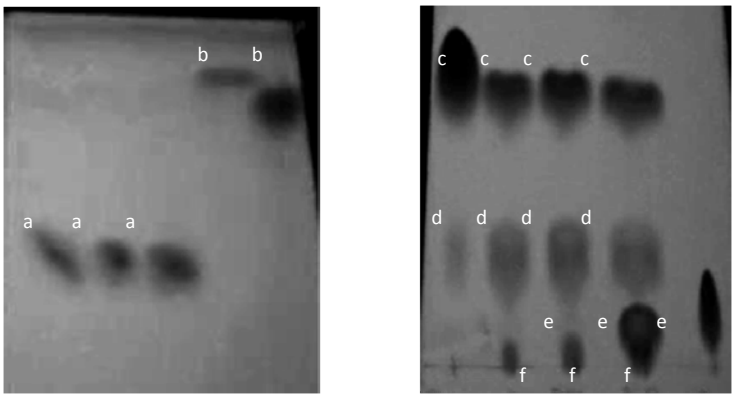

Figure 3-6. Comparison of activity of PFEI and BS2 towards the selection substrates. TLC analysis of biocatalysis with **2b** (left picture) and **3b** (right picture). **1**: **2b**, **2**: blank (biocatalysis without enzyme), **3**: biocatalysis with **2b** and PFEI, **4**: biocatalysis with **2b** and BS2, **5**: **3-PBA**, **6**: **3b**, **7**: blank, **8**: biocatalysis with **3b** and PFEI, **9**: biocatalysis with **3b** and BS2, **10**: **3a**.
[a] **2b**, [b] **3-PBA**, [c] **3b**, [d] impurity from the synthesis reaction, [e] **3a**, [f] impurity of unknown origin.

Table 3-4. Qualitative overview of activity of PFEI and BS2 towards the pre-selection substrates **2b** and **3b**. - : no detectable activity, +: proportional to the estimated activity observed by TLC.

Enzyme	Hydrolysis of 2b	Hydrolysis of 3b
PFEI	-	+
BS2	+++	++

3.2.1.2.2. Selection medium

Due to the fact that clones expressing inactive protein grew in M9 minimal medium supplemented with L-rhamnose and **2b** (Figure 3-4), the ability of *E. coli* to grow on this monosaccharide was investigated. Clones expressing PFEI or inactive protein were cultivated in M9 minimal medium supplemented with and without L-rhamnose and **2b**, and bacterial growth was monitored by OD measurement. All cultures supplemented with L-rhamnose reached similar ODs, independently on esterase activity (Figure 3-7, green and red lines). Cultures without L-rhamnose - and without **2a** supplementation - did not grow (Figure 3-7; black line, crosses) confirming the ability of *E. coli* to grow on L-rhamnose. The presence of **2b** in non-toxic concentrations had no effect on cell growth, because it was not hydrolyzed by either PFEI or the inactive protein.

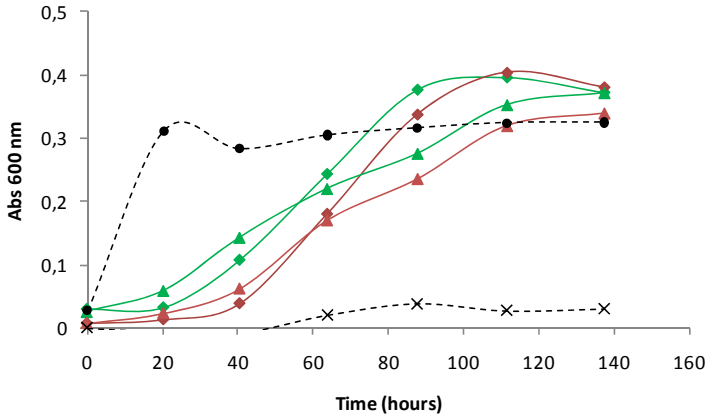

Figure 3-7. Growth curves of *E. coli* DH5α expressing PFEI (green curves) and inactive protein (red curves). Diamonds: M9 minimal medium, L-rhamnose, 10 mM **2b**; triangles: M9 minimal medium, L-rhamnose; circles: positive control, M9 minimal medium, **2a**; crosses: negative control, M9 minimal medium without supplements.

In order to overcome the problem of the utilisation of L-rhamnose as carbon source, an alternative expression system, not rhamnose inducible, was utilised. The use of an *E. coli* strain, which could not use rhamnose as nutrient, would have been an alternative; but

implementation of a 'more universal' selection system was desired and thus, pET vectors were used instead.

3.2.1.3. BS2-pET vector

In conclusion, PFEI was substituted by BS2 as model esterase for the development of the *in vivo* selection system. BS2 was cloned in a pET vector (pET28aΔ*Nco*I) as this is induced by IPTG, which cannot be used as carbon source. The strain *E. coli* DH5α was substituted by *E. coli* BL21 (DE3) as expression strain because T7 RNA polymerase is required for protein expression in pET vectors. The expression of BS2 in pET28Δ*Nco*I was studied at 37°C and 30°C (Figure 3-8). The temperature of 30°C was used for further selection studies because at this condition protein expression is stable over a longer time (Figure 3-8).

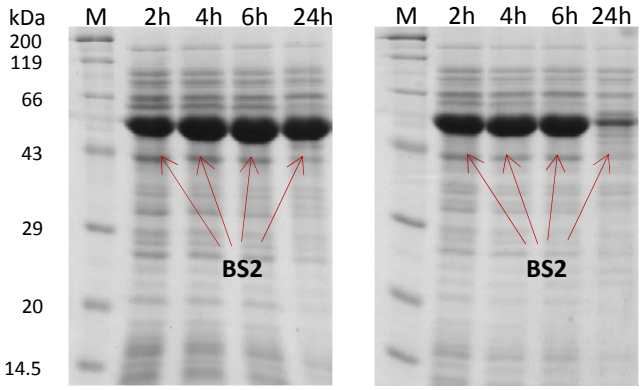

Figure 3-8. Protein analysis by SDS-PAGE of expression of BS2 in pET28aΔ*Nco*I by *E. coli* BL21 (DE3). Soluble fraction from protein expression carried out at 30°C (left gel) and 37°C (right gel) are shown.

Selection simulations with the modified system (model catalyst and expression system) were performed successfully. Again, one culture expressing active esterase and the other culture expressing an inactive construct of BS2 were used. The inactive form was prepared by digestion of the wild type BS2 gene with *Nde*I, as this gene has two restriction sites for *Nde*I (at 1 and 1068 bp). After restriction and ligation in vector pET28aΔ*Nco*I, a fragment of 423 bp was obtained, which coded for a protein without esterase activity. Again, inactivity of the protein expressed was proofed by *p*NPA assay.

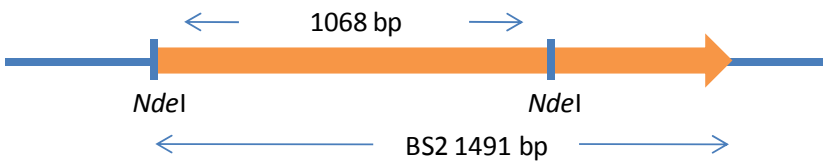

Figure 3-9. BS2 gene with indicated *Nde*I restriction sites.

The new cultivations in pseudo-selection media were performed in M9 minimal medium supplemented with IPTG and 10 mM **2b** (higher concentrations result in a toxic effect). In this case (Figure 3-10, left plot), difference in cell growth was observed in clones expressing active BS2 or inactive protein (Figure 3-10, left plot). Indeed, the clone expressing BS2 (grenn line), which could hydrolyze **2b**, reached a final density similar to the control culture (black line, M9 minimal medium supplemented with 10 mM **2a**).

In cultivations performed in M9 minimal medium supplemented with IPTG, **2a** and 50 µM **3b** (the concentration of **3b** was reduced to avoid ester toxicity) selective growth inhibition dependent on esterase activity was observed as well (Figure 3-10, right plot). Cultures of clones expressing BS2 (green line) did not grow and cultures of clones expressing inactive protein (red line) showed similar growth patterns as the control culture (black line, M9 minimal medium and **2a**).

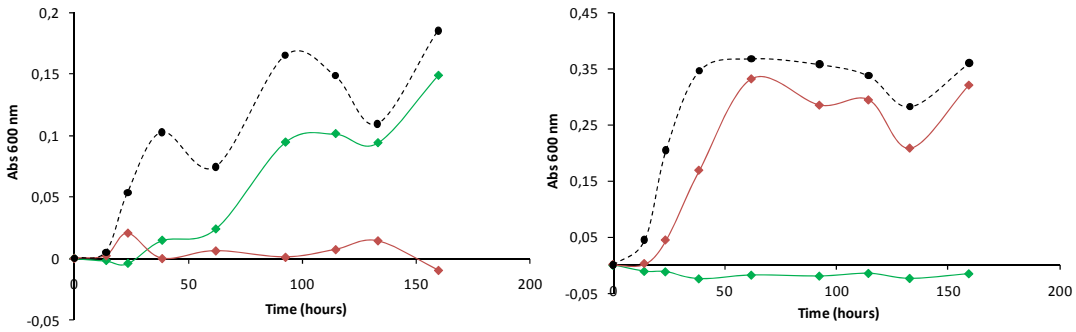

Figure 3-10. Growth in pseudo-selection media. Green diamonds: *E. coli* BL21 (DE3) expressing BS2; red diamonds: *E. coli* BL21 expressing inactive protein; black circles: control cultures, M9 minimal medium, IPTG and **2a**.
Left plot: Pseudo-selection medium supplemented with **2b**.
Right plot: Pseudo-selection medium supplemented with **2a** and **3b**.

The negative OD values in plots from Figure 3-10 are caused by the low substrate solubility. Each OD value is calculated substracting the blank value measured prior to media inoculation. Changes in the suspension over time alter these values affecting

accuracy of the measurement. When no or little cell growth takes place this can lead to negative values.

Despite these positive results, different drawbacks of substrate **3a** and its ester led to the substitution by **5a**. First, the structural difference between **2a** and **3a** generated too distinct pseudo-enantiomeric selection substrates (Scheme 3-6). Second, the antibiotic effect of chloramphenicol is based on its power to inhibit protein biosynthesis in the cell[216] (bacteriostatic effect) and a toxin with bactericidal effect is preferred.

3.2.2. Positive control esterase

As mentioned before (see 3.2), a positive control esterase is necessary for the validation of the *in vivo* selection method. This consists of an esterase which is easy to express in the used *E. coli* strain (as well as the negative control esterase) and highly enantioselective towards the model substrate, **3-PBA**. Although at this time the kinetic resolution of 3-phenylbutanoates by biocatalytic methods had been already reported,[217,218] the enzymes used did not fulfil the prerequisites for the control enzymes. The biocatalysts used were all lipases (from *Burkholderia cepacia*, *Pseudomonas fluorescens* and *Pseudomonas cepacia*) obtained from commercial suppliers because their recombinant expression in *E. coli* has not been established. Hence, the next efforts were directed towards the finding of positive control esterases.

3.2.2.1. Enzyme screening: enantioselectivity towards ethyl esters

To obtain a suitable biocatalyst which efficiently performs a reaction of interest, two strategies can be followed: either a known biocatalyst is modified by protein engineering or the discovery of biocatalysts with the property of interest is attempted.[219] Aiming to find an enantioselective esterase towards 3-phenylbutanoates the second strategy was followed and an enzyme screening was performed. In this, all the recombinant esterases produced in our laboratory together with a library of esterases from the metagenomic origin provided by BRAIN AG (Zwingenberg, Germany) were tested.

In order to increase the probability to find a suitable enzyme candidate, the substrate spectrum was extended to structurally related alkylphenyl carboxylic acid esters also converted by BS2 (this was proofed by biocatalysis and chiral GC analysis). Finally,

ethyl-3-phenylbutanoate (**Et-3-PB**), ethyl-2-phenylbutanoate (**Et-2-PB**) and ethyl-2-phenylpropanoate (**Et-2-PP**) were used in the enantioselectivity screening (Scheme 3-12).

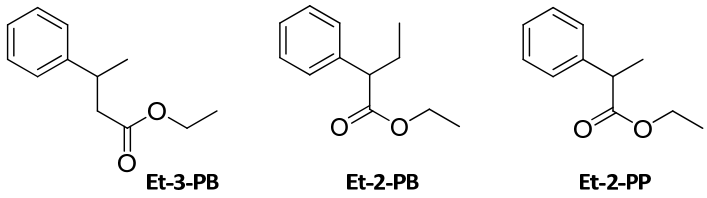

Scheme 3-12. Substrates used in the enzyme screening.

A pH indicator assay developed by Baumann et al.[220] was used to identify active esterases towards the above mentioned substrates, enzymatic activity was detected by colour change in MTPs due to pH decrease after ester hydrolysis (Figure 3-11).

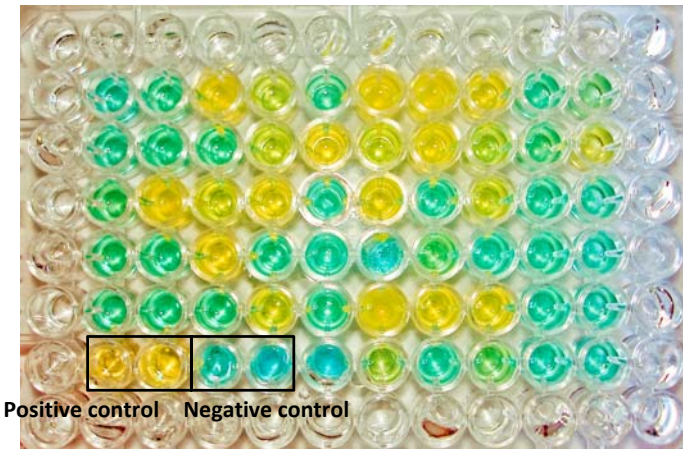

Figure 3-11. Sample of the pH indicator assay used.

Those active enzymes from the initial screen were further evaluated for their enantioselectivity. For this aim, biocatalysis on analytical scale and chiral GC analysis was performed. The best candidates were investigated in detail and the kinetic resolution efficiency was determined by E-value calculation at conversion near to 50%[11] (Table 3-5).

Table 3-5. Results from kinetic resolution of substrates **Et-3-PB**, **Et-2-PB** and **Et-2-PP** with the bests hits found in the enzyme screening.

Substrate	Esterase	T (°C)	ee_s (%)	ee_p (%)	Conversion (%)	E-value	Configuration[a]
Et-3-PB	PestE	30	93	96	49	> 100	(-), *R*
Et-3-PB	CL1	20	93	94	49	> 100	(-), *R*
Et-3-PB	A3	20	93	93	50	96	(+), *S*
Et-2-PB	8	30	98	97	50	> 200	(-), *R*
Et-2-PB	CE	30	88	99	47	> 200	(+), *S*
Et-2-PP	8	20	93	91	51	83	(-), *R*
Et-2-PP	CE	30	92	89	51	61	(+), *S*

[a] Sign of optical rotation and product configuration.

Three enantioselective catalysts in the hydrolysis of **Et-3-PB** were found. The esterase from the hyperthermophilic archaeon *Pyrobaculum calidifontis* PestE[206] and the metagenomic esterase CL1[221] presented (*R*)-preference - they released the (*R*)-acid form - while esterase A3,[222] also from metagenomic origin, showed (*S*)-preference.

Enantioselective esterases in the hydrolysis of **Et-2-PB** and **Et-2-PP** were also found. These originated from the metagenomic library as well, esterase 8[11] efficiently formed the (*R*)-enantiomer of both acids, and esterase CE[222] had inverse enantioselectivity resulting in formation of (*S*)-acids.

Based on these results, selection substrates from the carboxylic acids **3-PBA** and **2-PBA** were synthesized and the enantioselectivity of the selected esterases towards the pre-selection substrates was determined. Selection substrates from **2-PPA** were not synthesized because for this substrate only moderate enantioselectivity was observed.

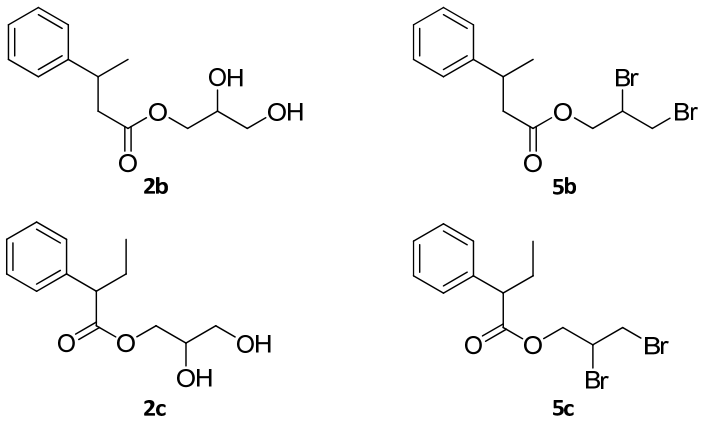

Scheme 3-13. Esters from carboxylic acids **3-PBA** (**2b** and **5b**) and **2-PBA** (**2c** and **5c**).

Esters from **3-PBA** (**2b** and **5b**, Scheme 3-13) and **2-PBA** (**2c** and **5c**, Scheme 3-13) were synthesized by direct esterification with the acyl chloride, following the procedure described in 3.1.2.2.2. Moderate to good yields were obtained (Table 3-6).

Table 3-6. Overview of the yields obtained in the synthesis of selection substrates.

Substrate	Yield (%)
2b	59
5b	85
2c	60
5c	58

3.2.2.2. Hits: enantioselectivity towards selection substrates

The enantioselectivity of esterases PestE, CL1 and A3 towards substrates **2b** and **5b**, and of esterases 8 and CE towards **2c** and **5c** was determined in kinetic resolutions on analytical scale followed by chiral GC analysis (Table 3-7).

Enantiomer separation of **2c** and **5c** was not fully achieved; thus, enantiomeric excess of the product (after derivatization to methyl ester) was determined in order to estimate the enantioselectivity and improve the analysis if results are promising.

Table 3-7. Results of biocatalysis in analytical scale with the selected esterases and the three derivatives of each carboxylic acid.

Substrate	Esterase	T (°C)	ee_s (%)	ee_p (%)	Conversion (%)	E-value	Configuration [a]
Et-3-PBA	PestE	30	93	96	49	> 100	(-), *R*
2b	PestE	30	74	96	43	> 100	(-), *R*
5b	PestE	30	95	78	55	34	(-), *R*
Et-3-PBA	CL1	20	93	94	49	> 100	(-), *R*
2b	CL1	30	92	92	50	79	(-), *R*
5b	CL1	30	71	90	44	40	(-), *R*
Et-3-PBA	A3	20	93	93	50	96	(+), *S*
2b	A3	30	73	74	49	15	(+), *S*
5b	A3	30	25	24	51	2	(+), *S*
Et-2-PBA	8	30	98	97	50	> 200	(-), *R*
2c	8	30	n.d.	97	n.d.	n.d.	(-), *R*
5c	8	30	n.d.	74	n.d.	n.d.	(-), *R*
Et-2-PBA	CE	30	88	99	47	> 200	(+), *S*
2c	CE	30	n.d.	92	n.d.	n.d.	(+), *S*
5c	CE	30	n.d.	91	n.d.	n.d.	(+), *S*

[a] Sign of optical rotation and product configuration.

High enantiomeric excess of the product was observed in hydrolysis of **2c** and **5c** with esterase CE. However, low conversion was estimated comparing the area of the product peaks with those from biocatalysis with esterase 8. Thus, CE was not further used as control esterase due to low activity towards the selection substrates. A3 was neither utilised because the enzyme selectivity towards the selection substrates **2b** and **5b** was low.

Esterases PestE, CL1 and 8 fulfilled the prerequisites to be suitable control esterases, activity and enantioselectivity towards the respective selection substrates was very good to excellent.

As only one substrate is sufficient for development of the system, it was necessary to choose between **3-PBA** and **2-PBA**. Finally, the system was further developed with **3-PBA** as model substrate for many reasons: first, all previous experiments had been performed with derivates of **3-PBA**; second, the chiral analysis of 3-phenylbutanoates had been already successfully established; third, two enantioselective esterases towards 3-phenylbutanoates had been found and the gene encoding esterase PestE was already

available in the laboratory. Esterases CL1 and 8 were supplied by BRAIN AG as protein extract; thus, the genes would have to be requested first.

It is worth to discuss the fact that the enantioselectivity towards 2,3-dibromopropyl esters was in general significantly lower compared to ethyl and glycerol derivates (Table 3-7). Rotticci et al.[223] found a similar effect in kinetic resolutions of secondary alcohols and bromohydrins (Table 3-8) performed with CAL-B as catalyst. They attributed the lower enzyme selectivity towards the bromated substrate to non-steric interactions between enzyme and substrate. Later, in 2005, Park et al.[115] described a similar case where mutants of PFEI with increased enantioselectivity towards halogenated substrates did not show any better selectivity when the halogen group (bromomethyl or chloromethyl) was substituted by an alkyl group (ethyl), which is similar in size but not in electronic density. In this case, they suggested that mostly electronic effects (and not steric effects) had been modified by the amino acid changes which had been introduced. In our case a similar hypothesis can be formulated as glycerol an 2,3-dibromopropanol have a similar size but differ considerably in the electronic environment: probably electronic effects play an important role in the orientation of the alcohol moiety in the alcohol pocket. However, it is still remarkable that the orientation of the alcohol moiety influences so significantly enzyme enantioselectivity towards a chiral centre situated in the acyl moiety.

Table 3-8. Comparison of CAL-B enantioselectivity towards aliphatic alcohols and cyanohydrins performed by Rotticci et al.[223]

Substrate	E-value[a]	$\Delta\Delta G^{\ddagger b}$ (kcal/mol^{-1})	$\Delta\Delta\Delta G^{\ddagger c}$ (kcal/mol^{-1})
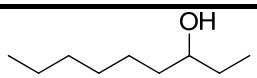	340	3.6	2.4
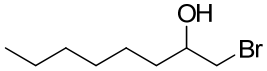	7.6	1.2	
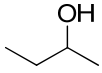	9	1.4	-2.1
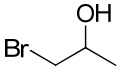	370	3.5	

[a] Enantiomeric ratio calculated at different conversions according to Rakels et al.[47]

[b] Difference of free energy of activation calculated according to Norin et al.[224]

[c] Difference of $\Delta\Delta G^{\ddagger}$ between the aliphatic alcohol and the methyl bromide derivative.

3.2.2.3. Positive controls: CL1 and PestE

Esterases PestE and CL1 were chosen as positive controls for further establishment and validation of the *in vivo* selection system.

If selection occurs, there must be an enrichment of clones expressing enantioselective esterase over clones expressing non-selective catalyst when these are incubated together in selection medium. The viable clones are detected by flow cytometry and sorted out. Therefore, it is necessary to cultivate bacteria expressing positive control esterase and negative control esterase together.

Cultures are often supplemented with antibiotics in order to avoid contamination and loss of plasmid. The plasmid carrying the gene of interest also carries a gene encoding for a protein, which provides antibiotic resistance. In order to make possible the incubation of different clones together, recloning of the PestE gene was necessary. The PestE gene was initially cloned in pET21, a vector with ampicillin resistance; while the BS2 gene (negative control esterase) and CL1 gene were cloned in vectors with kanamycin resistance (pET28 and pET24, respectively). Therefore, the PestE gene was recloned into pET28 to allow cultivation together with BS2 in culture supplemented with kanamycin.

After recloning of PestE, the expression of esterases PestE and CL1 in the *E. coli* strain of interest was analyzed confirming by SDS-PAGE that over-expression was successful (Figure 3-12).

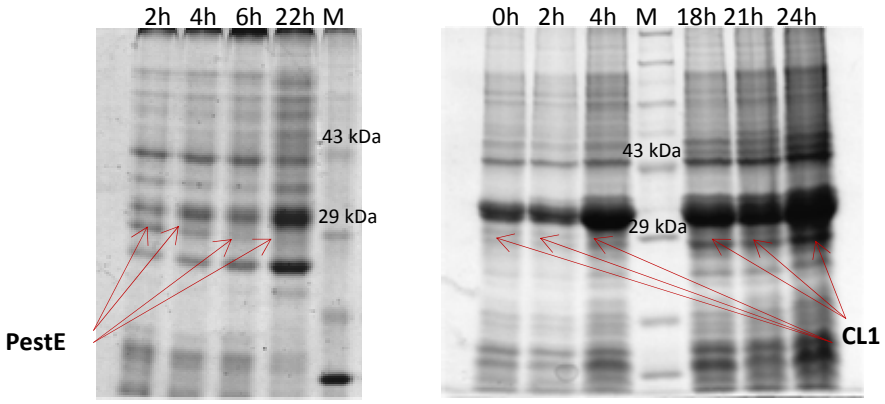

Figure 3-12. Analysis of the soluble fraction after protein expression of PestE (left) and CL1 (right).

3.3. Establishment of the in vivo selection system

3.3.1. Strain optimisation

The change of pre-negative impulse - from **3b** to **5b** - made it necessary to perform further system optimisation.

The *E. coli* strain initially used for protein expression in pET vectors (*E. coli* BL21 (DE3)) had a sensitivity profile towards the selection substrates, which was not adequate. The strain was more sensitive to **2b** than to **5a** (Table 3-9) while in an ideal case, **2b** should be harmless and **5a** toxic. Thus, *in vivo* selection with this strain and these substrates was not possible. Therefore, alternative strains were tested in order to find a better candidate. The strain *E. coli* JM109 (DE3) turned out to be the candidate with the best sensitivity profile towards the selection substrates: it was more tolerant towards the toxic effect of **2b** and **3-PBA** and more sensitive towards the toxin **5a** (Table 3-9). Thus, after confirming good recombinant expression of the control esterases in *E. coli* JM109 (DE3), this strain was selected as expression host.

Table 3-9. Sensitivity profile of the above mentioned *E. coli* strains.

Substrate	MIC (mM)	
	E. coli BL21 (DE3)	*E. coli* JM109 (DE3)
5a	> 15	≤ 10
5b	> 15	> 15
3-PBA	5-7	10-15
2b	5-7	10- 15

3.3.2. Solubility optimisation

For an effective selection with negative impulse higher concentrations of **5a** were necessary, compared to **3a** (10 mM towards 3 µM), for growth inhibition in *E. coli*. Thus, higher concentrations of **5b** in selection medium were required (10 mM of **5b** towards 50 µM of **3b**). The low solubility of substrate **5b** became a problem. As general procedure, all substrates were stored (short-term storage) as 1 M solutions in ethanol. A given volume of these solutions was added to selection media to achieve the required concentration in each case. When 10 mM **5b** was required in the selection medium, the amount of ethanol (1% final concentration) added in this strategy was not effective as

substrate co-solvent. The prozent of ethanol necessary to solubilise this concentration of **5b** would be lethal for the cells, so the use of an alternative co-solvent was required. Further organic co-solvents were tested (Table 3-10) without success. As alternative, β-cyclodextrin was used and dispersion of the selection substrates in the aqueous medium was reached, but the emulsion formed made the monitoring of cell growth by OD measurement impossible. Thus, the development of the selection system was further performed following bacterial growth by flow cytometry.

Up to 10 mg/ml β-cyclodextrin were added to selection medium and bacterial growth analysis confirmed that this substance did not affect cell growth. It was not toxic and *E. coli* cells could not use it as carbon source.

Table 3-10. Co-solvents tested for dispersion of 10 mM **5b** in aqueous medium.

Co-solvent	MIC (%)
Acetonitrile	10-20
Dioxane	1-2
DMF	2-3
DMSO	5-10
Ethanol	3
Isopropanol	3
THF	10-20
β-cyclodextrin	n.d.[a]

[a] 10 mg/ml was the highest concentration of β-cyclodextrin used and it did not affect cell growth.

3.3.3. Cell counting: optimisation of pre-selection substrates concentration

3.3.3.1. Racemic substrates

Bacterial growth was further monitored by means of cell concentration with the help of a flow cytometer and expressed in counts/ml. This system, although more time-consuming, was more reliable than OD measurement (Figure 3-13). This allowed a better adjustment of the optimal substrate concentration, as growth could be determined more accurately. The toxicity of **5a** was determined via flow cytometry and it was found out that 5 mM was already toxic for cells although not sufficient for complete inhibition of bacterial growth.

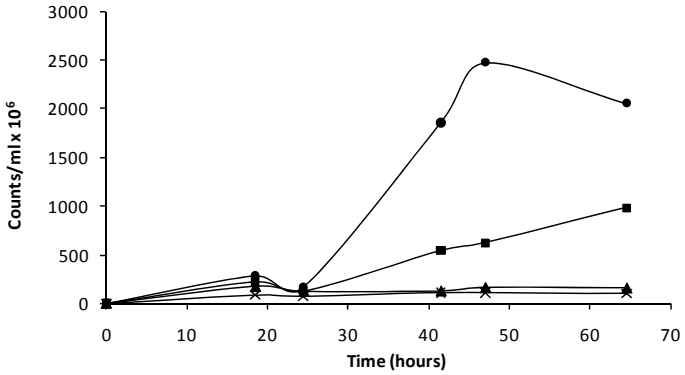

Figure 3-13. Growth curves of *E. coli* JM109 (DE3) in M9 minimal medium supplemented with 10 mM **2a** and different concentrations of **5a**. Circles: 0 mM **5a**; squares: 5 mM **5a**; triangles: 10 mM **5a** and crosses: 15 mM **5a**.

Next, cultures of *E. coli* JM109 (DE3) cells expressing esterase BS2 were used in order to verify the hypothesis of the selection principle: growth is possible when **2b** is hydrolyzed and growth is inhibited when **5b** or both **2b** and **5b** are hydrolyzed (Figure 3-14).

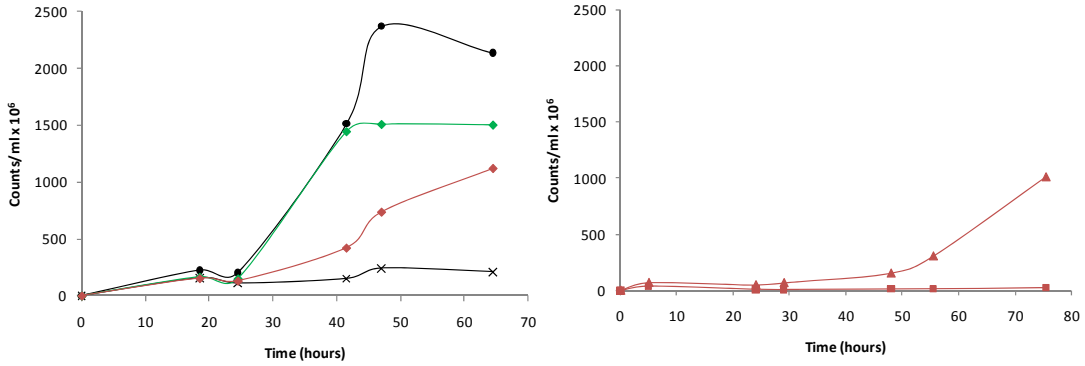

Figure 3-14. Growth curves of *E. coli* JM109 (DE3) expressing BS2 in control cultures. All media were composed of M9 minimal medium, IPTG and β-cyclodextrin.
Left plot- Circles: 10 mM **2a**; green diamonds: 10 mM *rac*-**2b**; red diamonds: 10 mM *rac*-**2b** and 10 mM *rac*-**5b**; crosses: no additional substrates.
Right plot- Triangles: 10 mM *rac*-**2b** and 10 mM *rac*-**5b**; squares: 10 mM *rac*-**2b** and 20 mM *rac*-**5b**.

These results confirmed that *E. coli* JM109 (DE3) can grow from the glycerol released after hydrolysis of 10 mM **2b** (Figure 3-14, left plot, green line) but cannot use either IPTG or β-cyclodextrin as nutrient (Figure 3-14, left plot, black line, crosses). In order to

achieve complete growth inhibition by simultaneous hydrolysis of **2b** and **5b**, the concentration of **5b** was increased from 10 mM to 20 mM (Figure 3-14, right plot). This increase on concentration was possible because β-cyclodextrin was used to facilitate homogeneous dispersion of substrate.

Once the *in vivo* selection system had been established with the racemic form of substrates **2b** and **5b** (for practical and economical reasons), tests with pure enantiomers and control esterases were performed.

3.3.3.2. Pure enantiomers

Development of the *in vivo* selection with pure enantiomers of **2b** and **5b** was performed with enantioselective and non-enantioselective control esterases. PestE was the enantioselective control esterase used for these initial experiments and for optimisation of enantiopure substrate concentration. Thus, *E. coli* JM109 (DE3) cells expressing PestE were cultivated in selection medium (supplemented with (*R*)-**2b** and (*S*)-**5b**) and anti-selection medium (supplemented with (*S*)-**2b** and (*R*)-**5b**). Again, optimisation of substrate concentration was required and this was performed by toxicity assays with pure enantiomers of **2b** and **5b** in M9 minimal medium supplemented with **2a**.

In the case of **5b**, no detectable differences in the MIC between *rac*-**5b**, (*R*)-**5b** and (*S*)-**5b** were observed. In contrast, the (*R*)-form of **2b** was more toxic than the (*S*)-form (Table 3-11). Thus, the concentration of **2b** in selection medium was reduced to 5 mM.

The potential selective blocking of metabolic routes by the (*R*)-enantiomer of **2b** could explain its higher toxic effect. It has been previously described in the literature[225] that *Rhodococcus rhodochrous* PB1 metabolizes selectively (*R*)-3-phenylbutyric acid as it can only grow on the (*R*)-enantiomer of this acid. In a similar way, *E. coli* could selectively incorporate the (*R*)-form of **2b** in its metabolism whilst blocking metabolic pathways. Indeed, (*R*)-**3-PBA** is structurally similar to some L-amino acids which are metabolized by *E. coli*, like tyrosine and phenylalanine.[226]

Table 3-11. MICs determined for racemic form and pure enantiomers of **2b**.

Substrate	MIC (mM)
(*rac*)-**2b**	~ 15
(*R*)-**2b**	≥ 5
(*S*)-**2b**	≥ 15

Now, cells expressing PestE or BS2 were cultivated separately in selection and anti-selection medium (5 mM (*R*)-**2b**/20 mM (*S*)-**5b** and 5 mM (*S*)-**2b**/20 mM (*R*)-**5b**, respectively). Bacterial growth was monitored by flow cytometry. As shown in Figure 3-15 only the culture expressing esterase PestE in selection medium (green circles) could proliferate. The same clone in anti-selection medium (red circles) hydrolyzed (*R*)-**5b** over (*S*)-**2b** due to the enzyme enantioselectivity and released more toxin than energy source, which hindered bacterial growth. Cells expressing BS2 (green and red crosses) did not grow on any of the selection media; this fact demonstrates that when both pseudo-enantiomers are hydrolyzed at similar rates by non-enantioselective enzymes the toxicity of the released **5a** hampers bacterial growth.

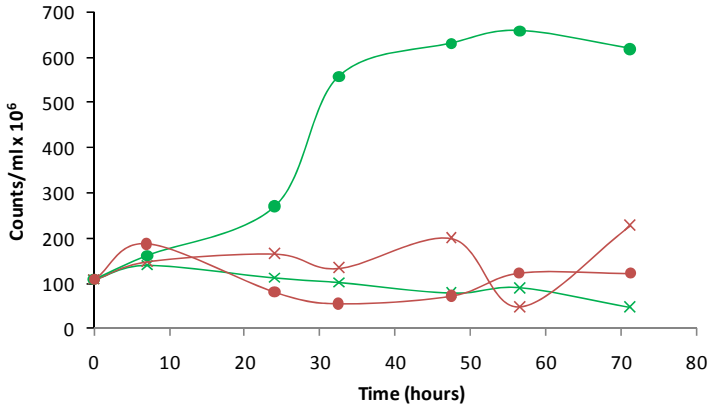

Figure 3-15. Growth curves in selection media. Green lines: selection medium; red lines: anti-selection medium. Circles: *E. coli* JM109 (DE3) cells expressing PestE, crosses: *E. coli* JM109 (DE3) cells expressing BS2.

3.4. Establishment of the flow cytometric detection method

As described above, cultivation of cells expressing PestE and BS2 separately, showed different bacterial growth depending on the enantioselectivity of the expressed esterase and on the used pair of pseudo-enantiomers (selection or anti-selection medium). Thus, establishment of a selection medium, which linked cell survival to enzyme enantioselectivity, had been achieved.

In theory, incubation of a mixture of enantioselective and non-enantioselective esterases would result in enrichment of the clones expressing enantioselective enzymes. However, there are cells which circumvent the selection pressure and survive despite expressing non-enantioselective esterase. In order to minimize these false positive results, a more sensitive detection strategy than growth on agar plates was planned: analysis by flow cytometry using differential dyes followed by cell sorting. For this aim, the finding of a suitable protocol to distinguish between different physiological status of *E. coli* was necessary.The application of cell cytometers for the differentiation of bacterial cells in different physiological status is increasing and as consequence, many protocols to perform this task have been described in the last decade.[227-229] However, these techniques are based on modified protocols developed originally for eukaryotes. Due to the smaller size and different composition and permeability of cell wall in prokaryotes, the finding of the best technique for the microorganism of interest and the pertinent toxin, becomes a challenge.[230] Different alternatives were tested trying to find the best and simplest methodology.

3.4.1. PI staining

A general method for cell staining is the use of fluorescent dyes. There are two types of dyes, some can penetrate all cell membranes and other dyes can only penetrate into cells with permeabilised membranes. In this strategy, a nucleic acid stain specific for damaged cells was used for determination of the physiological state of *E. coli*. Propidium iodide (PI), which binds to DNA and emits red fluorescence, was the dye of choice. PI penetrates more readily in cells with permeabilised membranes than in intact cells. Thus, it is possible to translate the signal of red fluorescence intensity (FL2) into an indication of the bacterial physiological condition. As PI does not penetrate intact membranes, viable cells would not be affected by DNA staining.

In the preliminary assays, samples taken from an exponentially growing culture were analyzed as a control for viable cells, and samples from the same culture after permeabilization (heat treatment: 95°C for 10 min) were analyzed as control for dead cells. Difference in red fluorescence intensity between the samples was observed, although separation between both populations was low (Figure 3-16).

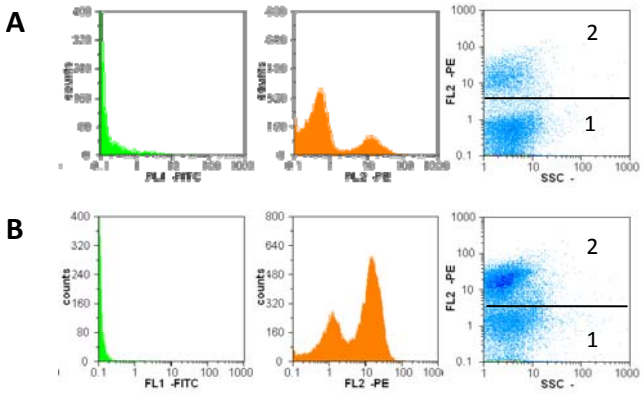

Figure 3-16. Preliminary assays with PI staining. A: viable cells, B: permeabilized cells. 1: Population of viable cells, 2: Population of dead cells.

When cultures of cells expressing BS2 and PestE were analyzed after incubation in medium supplemented with toxin (**5a**), cellular damage was not observed (Figure 3-17), most cells were detected as viable. Probably, **5a** does not affect cell membrane in the same way as high temperature and thus its effect cannot be detected only by PI staining.

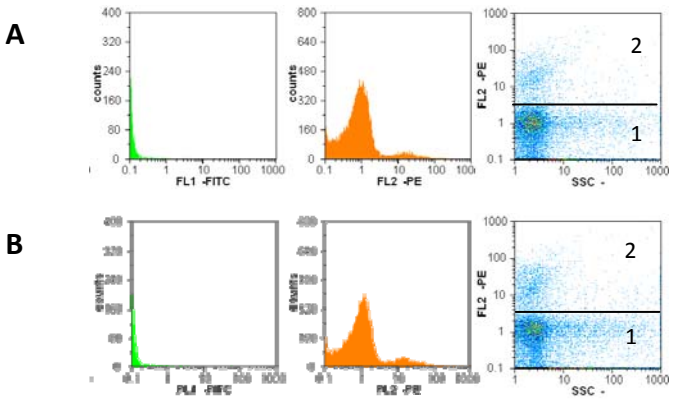

Figure 3-17. A: BS2 expressing cells incubated overnight in M9 minimal medium supplemented with 5 mM **2a** and 10 mM **5a**. B: PestE expressing cells incubated overnight in M9 minimal medium supplemented with 5 mM **2a** and 10 mM **5a**. 1: viable cells and 2: dead cells.

3.4.2. GFP/PI

Due to the small size of *E. coli* (0.5 x 1-3 µm)[231] it is easier to distinguish these cells from the background in flow cytometry analysis when they emit fluorescence, rather than relying solely on forward and side scatter signals.[181] Thus, the co-expression of the green fluorescent protein (GFP)[205] with the esterases of interest was performed, in order to make all cells emit a basal green fluorescence helping detection. The green fluorescence

(FL1) of GFP combined with the selective red fluorescence (FL2) of PI has been reported as a method to detect bacterial physiological state,[227] and thus this strategy was followed in a second attempt.

When expressing GFP, the methodology of heating cells to use them as control for non-viable bacteria was not used, because it caused loss of FL1 signal, probably because of GFP denaturation. Thus, *E. coli* cells expressing GFP were directly transferred to M9 minimal medium supplemented with glycerol in presence and absence of **5a**. Samples were removed after different incubation times, stained with PI and analyzed by flow cytometry. The results obtained were encouraging (Figure 3-18), good separation between viable and dead cell populations, and between cells and background, was achieved in FL1/FL2 histograms.

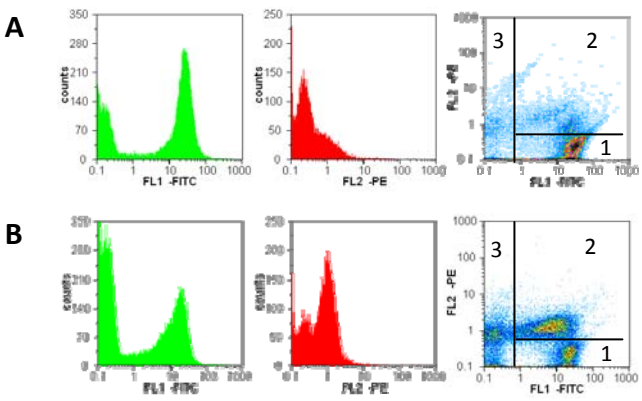

Figure 3-18. Flow cytometric analysis of *E. coli* JM109 (DE3) expressing GFP in M9 minimal medium supplemented with 5 mM **2a** (A) and with 5 mM **2a** + 10 mM **5a** (B). 1: viable cells, 2: dead cells, 3: background.

The results obtained with GFP-expressing cells could not be reproduced with cells co-expressing BS2 and GFP due to the drastic decrease in FL1 intensity. The amplification of FL1 signal was attempted but it involved loss of signal quality, which led to diffuse and broading peaks (Figure 3-19). Thus, the separation between bacterial populations, and between cells and background, became worse.

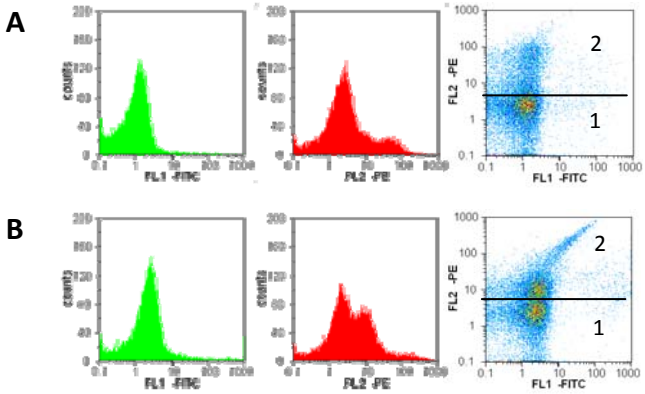

Figure 3-19. Flow cytometric analysis of *E. coli* JM109 (DE3) expressing GFP and BS2 in M9 minimal medium supplemented with 5 mM **2a** (A) and with 5 mM **2a** + 10 mM **5a** (B). 1: viable cells, 2: dead cells. The background cannot be distinguished.

Protein analysis of the different populations (Figure 3-20) indicated that the reason for the decrease in FL1 emission lies in the reduction of GFP expression when the protein is co-expressed together with BS2.

For the co-expression of GFP and BS2, each gene was cloned in one vector and these were sequentially transformed in one cell (competent cells carrying one plasmid were prepared, and these were transformed with the second plasmid). Two pET vectors with different antibiotic resistance were used in a first attempt: BS2-pET28a (kanamycin resistance) and GFP-pET11a (ampicillin resistance). In order to achieve better expression of both proteins, a second co-expression strategy was followed. Vectors with different replication origin were used: BS2-pET28a and GFP-pALTER CDC42. With this system the expression of GFP increased but the expression of BS2 decreased as well (Figure 3-20).

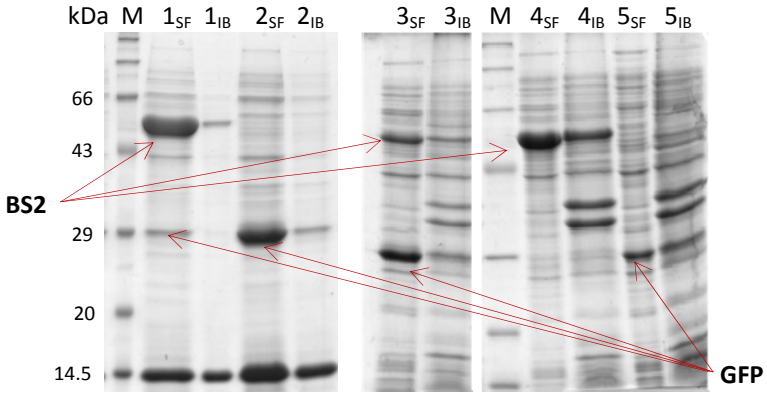

Figure 3-20. SDS-PAGE analysis of GFP and/or BS2 expression. M: marker; 1: GFP-pET11a and BS2-pET28a; 2: GFP-pET11a, 3: GFP-pALTER CDC42 and BS2-pET28a; 4: BS2-pET28a; 5: GFP-pALTER DCD42. $_{SF}$ soluble fraction, $_{IB}$ inclusion bodies.

In order to overcome the problem of enzyme co-expression, the use of a bacterial strain with the GFP gene inserted in genomic DNA[232] was attempted. The strain was kindly donated by Prof. Sorensen, but after cell cultivation no green fluorescence could be detected in this culture.

Further attempts to obtain good protein co-expression, like the use of pET-Duet vectors (Novagen) were not performed because there was no guarantee that after the selection process the GFP fluorescence would remain constant. When cells are incubated in a carbon deficient medium, they first metabolize proteins which are not necessary for cell survival to obtain energy which can be used for vital functions.[233] In this case, GFP and the esterase would be catabolized under starvation conditions (selection conditions). Different clones in selection medium would have different nutritional deficiencies, and would consume GFP and esterase at different rates. Different levels of GFP in each cell would lead to uncontrolled differences in FL1 emission. Thus, further strategies were attempted in order to obtain a reliable and reproducible system for determination of the physiological status of *E. coli.*

3.4.3. Double-dye system

As mentioned before, the systems generally used to selectively stain bacterial populations according to their viability are composed by two dyes: one can penetrate intact and damaged cell membranes and stains all cells, the second dye can only penetrate into damaged cells and stains these.

Due to the failure of the systems described above, the general strategy of double staining was tested. Here, the expression of GFP was replaced by a fluorescent dye aiming to control more accurately the fluorescence levels and not to overload the cell machinery with over-expression of two proteins. The drawback of this strategy is that staining affects cell viability and this leads to lower recovery of the viable cell population after flow cytomertric analysis and cell sorting.

Two combinations of dyes were tested for the differentiation of *E. coli* JM109 (DE3) populations: Syto9/PI[228] and DIBAC/PI.[229] Again, cells taken from a fresh M9 minimal medium-glycerol culture were used as positive control (viable cells), and cells taken from the same culture with permeabilized membrane by heating at 95°C for 10 min were used

as negative control (dead cells). Bacterial analysis with the double-dye systems was not very successful in the first attempts (Figure 3-21). Separation between the populations was not complete, and this led to bad differentiation between samples with viable and dead cells.

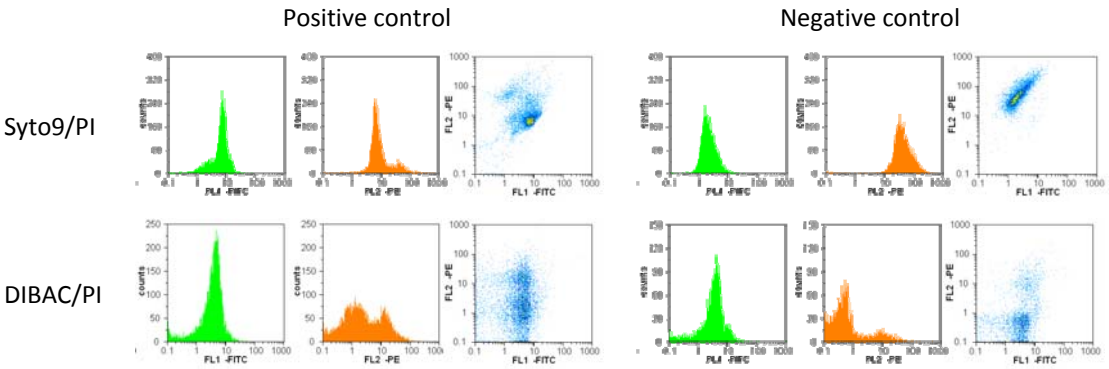

Figure 3-21. Flow cytometry analysis by double-staining systems Syto9/PI and DIBAC/PI. Figures 3-21 and 3-22 show the same samples, analyzed without and with crosstalk compensation.

Results improved significantly when crosstalk compensation was performed.[234] Settings in flow cytometry analysis were modified in order to minimize the green fluorescence signal in the red fluorescence channel and vice versa. Thus, good separation between populations was achieved in both cases (Figure 3-22).

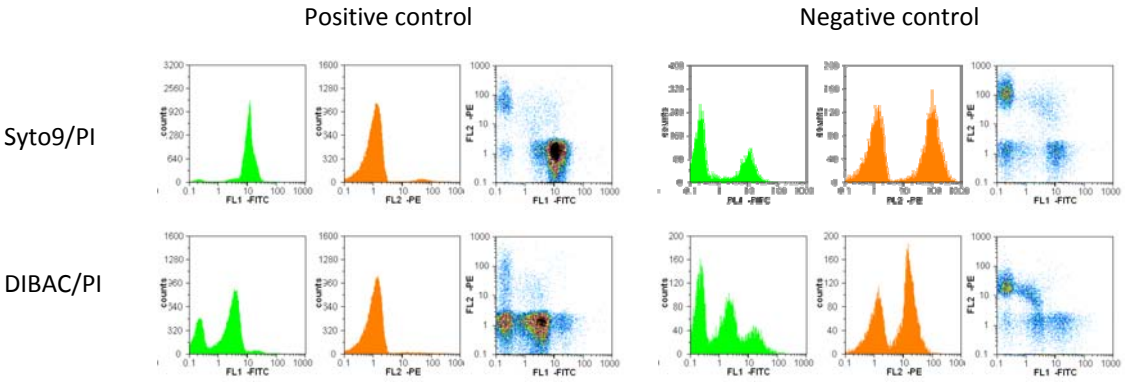

Figure 3-22. Flow cytometry analysis by double-staining systems Syto9/PI and DIBAC/PI with crosstalk compensation.

The combination Syto9/PI was selected for further experiments because the best separation of bacterial populations and background was achieved. The differences with DIBAC/PI staining were more difficult to interpret as other populations appeared as well.

Hence, cultures of *E. coli* JM109 (DE3) expressing esterase BS2, PestE or CL1 in M9 minimal medium supplemented with **2a** and in presence or absence of **5a** were prepared, samples were taken at different time periods and these were analysed by flow cytometry for viability determination. After 6 hours incubation the difference between viable and non-viable cultures could be clearly detected (Figure 3-23).

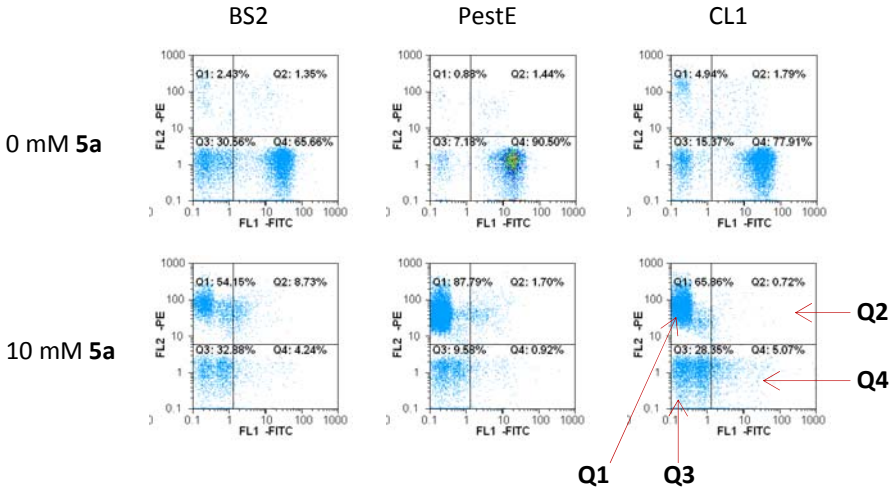

Figure 3-23. Viability analysis of *E. coli* expressing esterases BS2, PestE and CL1 after incubation in M9 minimal medium with 5 mM **2a** in presence or absence of toxin **5a**.

Analysis of histograms representing FL1/FL2 plots resulted in detection of four quadrants, which represented four different populations:

Quadrant 1 (**Q1**) – signal for dead cells, which emit high FL2 and low FL1. The decrease of FL1 emission in these cells occurs because Syto9 and PI bind competitively to DNA, and PI displaces the previously bound Syto9 molecules.

Quadrant 2 (**Q2**) - probably signal for cells in intermediate physiological status, which would constitute a part of the false positives. This population has not been further investigated as only the most viable clones are interesting for selection.

Quadrant 3 (**Q3**) - background signal emitted by the particles present in cultivation medium, buffer and sheath fluid. The buffer was sodium phosphate buffer used to dilute 1/100 (v/v) samples prior to flow cytometry analysis. Sample dilution is necessary due to the high sensibility of flow cytometric analysis; high concentration of particles can saturate the detector and the precision of the analysis decreases. Sheath fluid is the mobile phase, which transports the sample through the flow cytometer.

The intensity of the background signal (Q3) was difficult to control. Attempts to reduce it were made by filtering the buffer before sample dilution. The background signal was reduced, but still varied from sample to sample, and increased significantly when the selection medium was an emulsion (Figure 3-26).

Quadrant 4 (**Q4**) – signal for viable cells. These emit high FL1 intensity and low FL2 intensity as only minor amount of PI penetrates and binds to the DNA of these cells. Thus, no displacement of Syto9 occurs.

The proportion of the different cell populations Q1, Q2 and Q4 was calculated for cultures expressing esterases BS2, PestE and CL1 in presence and absence of toxin **5a**. Similar behaviour was observed in all cases: high percentage of viable cells in absence of toxin, and high percentage of dead cells in presence of toxin (Figure 3-24). The independence of enzyme expressed to culture sensitivity to toxin is an important factor to reduce false positive and false negative results in the assay.

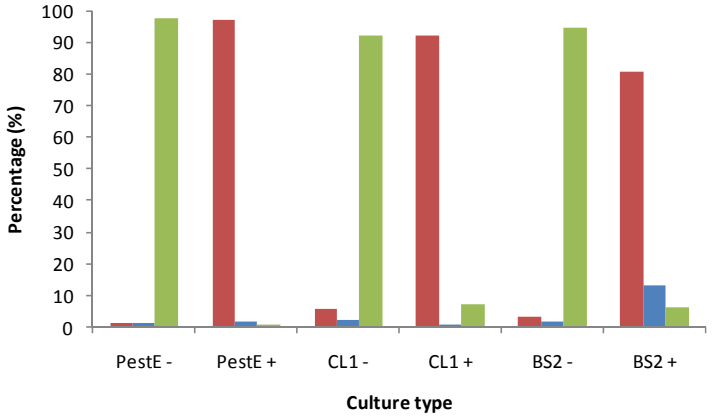

Figure 3-24. Graphic representation of population distribution in the different cultures used in presence (+) and absence (-) of **5a**. Red bars: Q1, blue bars: Q2, green bars: Q4.

With the successful establishment of a system to determine cell viability, all components and protocols for the '*in vivo* selection system and flow cytometry analysis' had been established. Next, validation of the optimised system was attempted.

3.5. Validation of the in vivo selection system

The validation procedure was first established with *E. coli* cultures expressing one of both esterases, BS2 or PestE, as controls. After incubation in selection medium, samples were

taken after different time periods (2, 4, 6, 24 and 48 hours), stained with Syto9/PI and analyzed via flow cytometry in order to determine the viability of the culture. In samples taken after 24 hours incubation, a clear difference between both cultures was observed. Hence, this time point was set as reference for further experiments. When the cell cultures were incubated with **2a** and **5a**, effects were detected already after 6 hours. However, it is obvious that changes require longer time in selection medium because hydrolysis of esters **2b** and **5b** must occur for release of the carbon source (**2a**) or the toxin (**5a**).

After 24 hours incubation in selection medium with **2b** and **5b**, almost the whole cell population expressing esterase BS2 was dead, while cell survival was observed in culture expressing esterase PestE (Figure 3-25). These results are in agreement with the growth curves made for cultures expressing these enzymes in selection media (Figure 3-15).

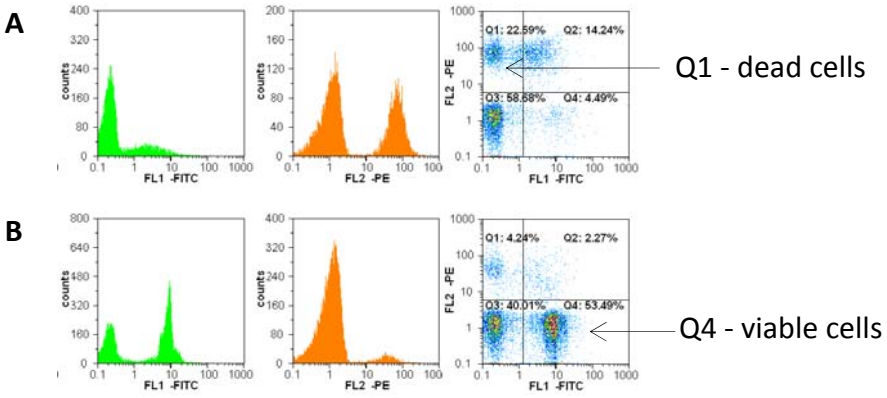

Figure 3-25. Analysis of cell cultures expressing esterase BS2 (A) or PestE (B) in selection medium.

The use of flow cytometry reduced incubation time in selection medium. Bacterial viability could be analyzed by differential cell staining instead of determination of bacterial growth by OD measurement. If cell division/proliferation in selection medium is not required, enzyme expression here is not necessary either (cells transferred to selection medium have previously expressed the esterase), and the inducer is no longer required as a component of the selection medium. This allows the screening of libraries cloned in all kind of vectors, also in those which are induced by L-rhamnose or L-arabinose (alternative carbon sources), because their presence in selection medium is not required.

As previously mentioned, the background signal in the flow cytometer was high in selection medium, due to the emulsion formed by dispersion of substrate **5b** in aqueous medium. This is evidenced by the higher intensity of Q3 in both analyses in Figure 3-25, and by the presence of particles with different characteristics than cells in FSC/SSC

histograms (Figure 3-26). These particles increased the noise/signal ratio and could not be eliminated, but they did not affect analysis because good separation of the background signal had been established.

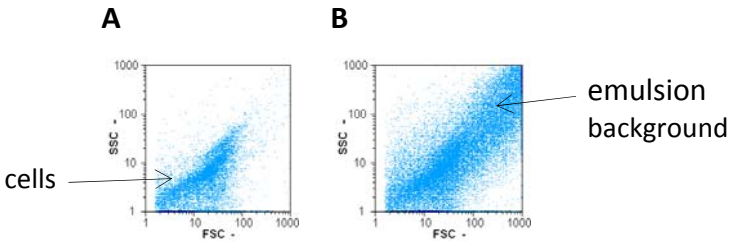

Figure 3-26. FSC/SSC histogram showing the higher background in selection medium. A: cell culture with OD = 0.1 in M9 minimal medium; B: cell culture with OD = 0.1 in M9 minimal medium supplemented with β-cyclodextrin and selection substrates **2b** and **5b** (selection medium)

After establishment of the validation procedure with esterases BS2 and PestE, mixtures of positive (PestE or CL1) and negative (BS2) control esterases in different proportions (1/1, 1/10 and 1/100) were incubated in the selection media (selection and anti-selection medium). Samples were taken after 24 hours incubation, stained and analyzed via flow cytometry. This allowed separation of cells attending to their physiological status and the most viable clones (quadrant 4) were sorted out and platted on agar. The colonies were identified in order to calculate the enrichment of the enantioselective variant (positive control) over the non-enantioselective one (negative control).

For the analysis of the plated clones, gene identification by PCR with vector specific primers followed by agarose gel electrophoresis was carried out. The gene coding for BS2 (1.5 kb) is bigger than the genes coding for PestE (1 kb) and CL1 (1 kb), so differentiation of negative and positive control can be performed attending to the size of the fragment amplified. Nevertheless, this method did not offer a high throughput approach and was time and material consuming. PCR with gene-specific primers or analysis of the protein size would be alternative strategies, but the throughput would be still low.

Fortunately, the promiscuous catalytic activity [235,236] of BS2 served for the elaboration of a fast and easy-to-perform detection method. BS2 has promiscuous amidase activity[237] (additionally to the esterase activity) which can be detected via overlay assay specific for amidase activity. Thus, all selected clones platted on agar were analyzed simultaneously differentiating BS2 from PestE and CL1 by the colour of the colonies (Figure 3-27).

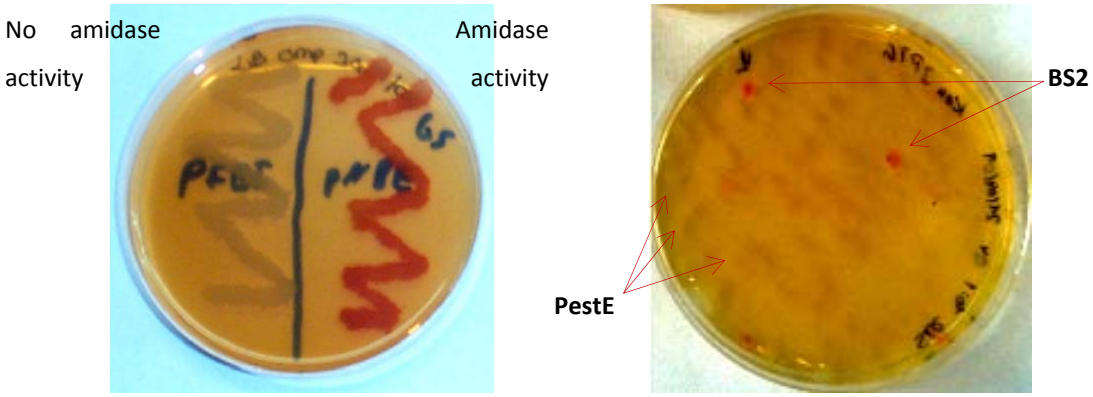

Figure 3-27. Left plate: example of the overlay assay for amidase activity with active and inactive enzymes. Right plate: replica plate of a selected population where the majority of PestE (yellow colonies) over BS2 (red colonies) can be seen.

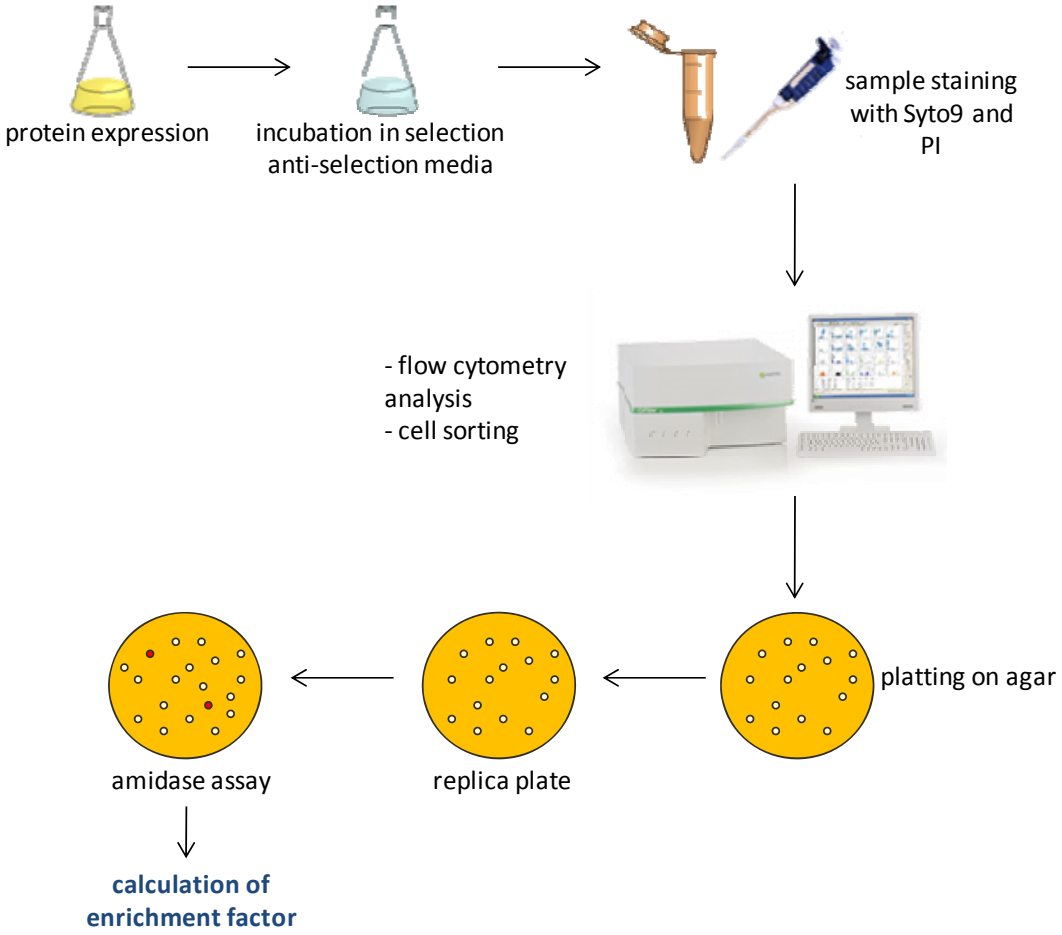

Figure 3-28. General scheme of the procedure for validation of the *in vivo* selection system.

After incubation of PestE/BS2 and CL1/BS2 mixtures in selection media and cell sorting of the viable population, between 100 and 200 clones grew usually on agar plates supplemented with kanamycin (LB-Kan). These were identified as PestE/CL1 or BS2 via

overlay assay for amidase activity, and the enrichment factor of the enantioselective esterase over the non enantioselective one was calculated (Table 3-12). The expected enrichment of PestE or CL1 over BS2 was confirmed.

Table 3-12. Enrichment data of the positive control esterase (PestE or CL1) over the negative control esterase (BS2) after incubation in selection medium and cell sorting.

Initial % positive control (PC)[a]	Final % PC[b]	Enrichment factor (EF)[c]	Theorically maximal EF
50	91.5 ± 4.6	1.8 ± 0.1	2
10	93.8 ± 2.5	9.4 ± 0.2	10
1	88.3 ± 5.6	88.3 ± 5.8	100

[a]Initial % of the positive control in the mixture.

[b]Final % of the positive control in the mixture.

[c]Enrichment factor calculated as: final % PC / initial % PC

The mixtures incubated in anti-selection medium were plated on LB-Kan as well and very few colonies appeared in all cases (zero to five colonies). Thus, no calculation of any kind of enrichment ratio was possible. These results agree with the growth curves of PestE and BS2 in anti-selection medium (Figure 3-15), both clones did not grow because the hydrolysis of **5b** released the toxin **5a**.

These results confirm the reliability of the *in vivo* selection method coupled to flow cytometry as a tool for the identification of enantioselective esterases in a mixture. After the validation of the method, analysis of a real mutant library was attempted.

3.6. Analysis of PFEI mutant library

Although esterase BS2 was used for the validation of the *in vivo* selection method, its utilisation as model catalyst for the evolutionary process was not considered because computational analysis of its active site gave evidence that it is too large for the straightforward development of enantioselectivity towards 3-phenylbutanoates, and *in silico* screening for hot spots was not successful. In contrast to this, PFEI displays better prerequisites to achieve the goal. Thus, a mutant library of *Pseudomonas fluorescens* esterase I (PFEI) generated by site-directed mutagenesis[116] was analyzed. In this library, residues W28, V121, F198 and V225 were saturated as it had been previously reported that these positions influence the enantioselectivity of the enzyme towards chiral

carboxylic acids.[115] Using a chromogenic screening method to determine E_{app} in MTPs, a mutant with enhanced enantioselectivity towards **Et-3-PB** had been already found.[116] In this way, if no mutant is found using the *in vivo* selection strategy, the method would be invalid. Hence, this experiment served as direct proof of concept.

Prior to selection, the ability of the library to hydrolyze the selection substrates **2b** and **5b** was tested and confirmed by GC analysis. The wild type esterase PFEI is inactive towards selection substrate **2b** but some of the generated mutants could hydrolyze it; thus, the library was suitable for *in vivo* selection. Next, the mutant library of PFEI was expressed in *E. coli* JM109 (DE3) cells in LB medium and 10^8 clones were washed and transferred to selection medium. Aliquots of selection medium were taken after 24 hours, stained and analyzed via flow cytometry. Events identified as viable cells (Q4) were sorted out and platted on LB-Kan (Figure 3-29).

It is worth to mention that the screened PFEI library was cloned in pGASTON (L-rhamnose inducible vector, ampicillin resistance). Instead of sub-cloning, protein expression was performed in LB medium prior to selection, and aliquots of this culture were washed and transferred to inductor-free (L-rhamnose free) selection medium. The cell sorting method for selection of viable clones allowed shorter incubation times compared with the measurement of cell growth over days; thus, inducer is not necessary in selection medium and any inducer for protein expression can be used.

After incubation of the library in selection medium, flow cytometry analysis and cell sorting; 28 colonies grew on LB-Kan. When this procedure was performed in anti-selection medium, 12 colonies grew on LB-Kan. These 40 colonies were all transferred to one microtiter plate (MTP) and further analyzed.

In MTP format esterase activity and enantioselectivity (E_{app}) of each of the 40 selected clones was determined with a photometric high-throughput screening method based on the hydrolysis of *p*-nitrophenyl esters. After hydrolysis of *p*-nitrophenyl-3-phenylbutanoate, the released *p*-nitrophenolate has yellow colour, which can be quantified to follow the reaction course. When *p*-nitrophenyl esters of pure enantiomers are used separately, the enzyme enantioselectivity can be estimated as $E_{app.}$[129] Using this methodology, eight promising clones were identified and investigated in kinetic resolutions in analytic scale.

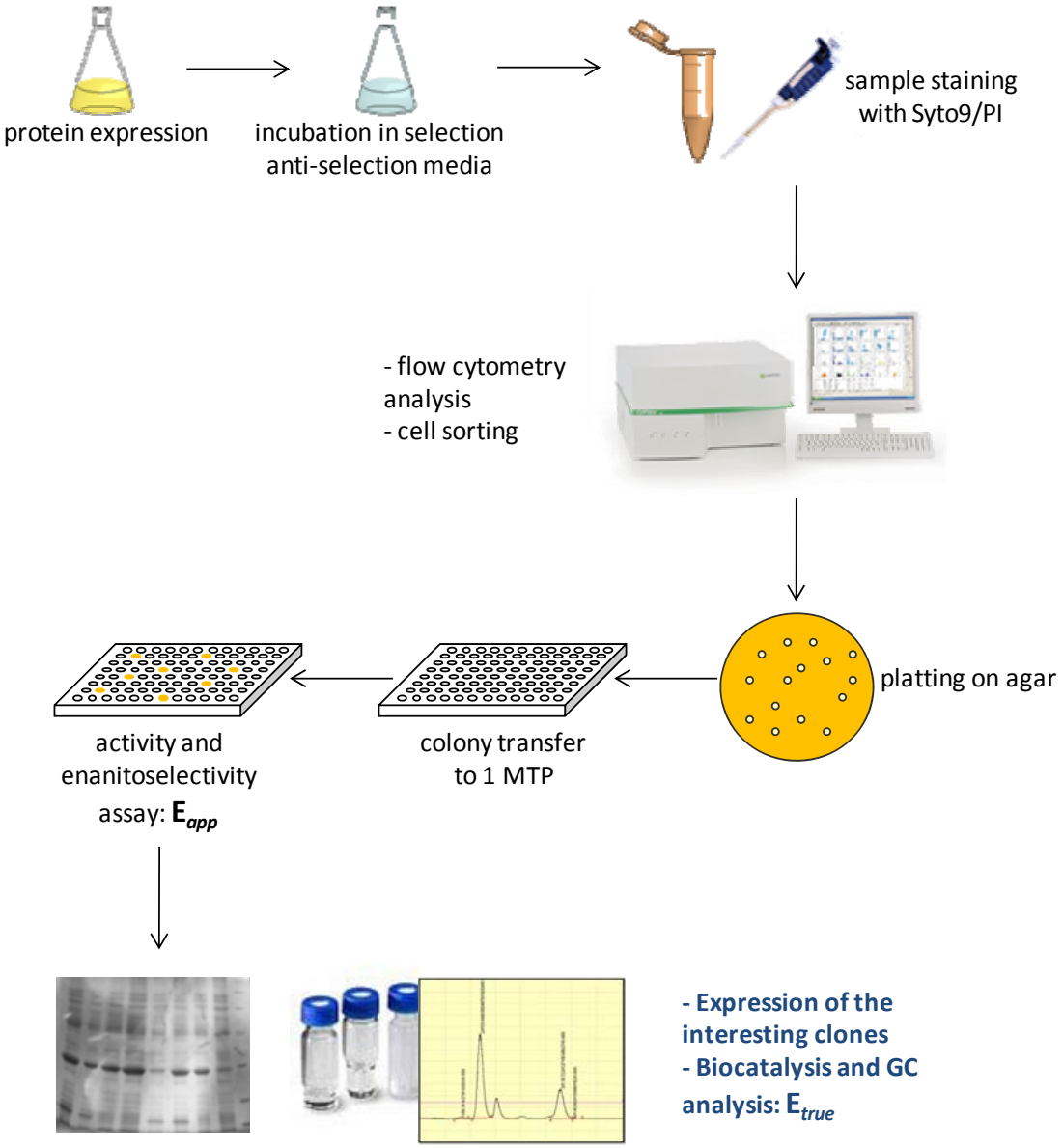

Figure 3-29. General scheme of the *in vivo* selection method coupled to flow cytometry in analysis of a mutant library.

3.6.1. Characterisation of the interesting clones

Interesting clones found by screening with *p*-nitrophenolates were sequenced and expressed on larger scale (50 ml flasks). The enzyme enantioselectivity was determined in biocatalysis of **Et-3-PB** in analytical scale by chiral GC analysis. By this procedure E_{true} was determined (Table 3-13).

All selected clones were (*R*)-selective and originated from the aliquot incubated in selection medium. No (*S*)-selective clones were found after incubation neither in selection nor in anti-selection medium. The homo-selectivity might me caused by the positions of

the saturated amino acids, which might be not adequate for inversion of enzyme enantioselectivity. These positions were identified by Park et al.,[115] who increased the enantioselectivity of PFEI towards methyl-3-bromo-2-methylpropionate, but did not invert it. As wildtype PFEI has (*R*)-preference towards **Et-3-PB**, the enantioselectivity in this case has been increased as well. Jochens et al.[116] analyzed this library with a MTP-based screening method to identify mutants with increased enantioselectivity towards our model substrate, **Et-3-PB**. Here, the best mutant they found had E ~ 80 with (*R*)-selectivity, and no (*S*)-selective clones were identified either.

Table 3-13. Selected clones: amino acid changes and calculated E-values.

Mutant	**Amino-acid changes**	**E_{app} [a]**	**E_{true} [b] / conv %**
C4	V121I, F198G, V225A	80	1 / 61
E7	V121S	>200	3 / 23
E8	V121S, F198G, V225A	6	48 / 50
F5	V121I, F198C	5	15 / 47
G6	V121I, S156T, Y163H (stop codon)	14	13 / 12

[a] E_{app} from screening with pure enantiomers of *p*-nitrophenyl-3-phenylbutanoate.

[b] E_{true} from biocatalysis in analytical scale with *rac*-ethyl-3-phenylbutanoate.

After gene sequencing it turned out that the eight clones were actually five different mutants. Clones C4, C8 and G4; and clones D7 and E7, had the same nucleotide exchanges. The performance of these five mutants in enzymatic kinetic resolutions will be discussed below.

Mutants C4 and E7 displayed high enantioselectivity towards *p*-nitrophenyl-3-phenylbutanoate, and no selectivity towards the ethyl ester (**Et-3-PB**). On the other hand, mutants E8 and F5 showed low to moderate E_{app} values towards *p*-nitrophenyl-3-phenylbutanoate but moderate to good enantioselectivities towards the ethyl ester. Differences in enantioselectivity (and activity) of the selected mutants towards assay substrates and real substrates have been previously reported[238] and these are the main disadvantage of using substrate analogues in high throughput analysis. Despite this, the method has been proven to be effective as enantioselective catalysts have been selected.

The sequence analysis of mutant G6 revealed a stop codon at position 163, so 109 amino acids of the 272 that constitute PFEI were not expressed. Among them, residues Asp222 and His251, which are part of the catalytic triad, are missing. The resulting protein still retained hydrolytic activity (Table 3-13) probably because other amino acids participated

in the catalysis. Examples of protein mutants where other amino acids have overtaken the catalytic role have been previously reported.[179]

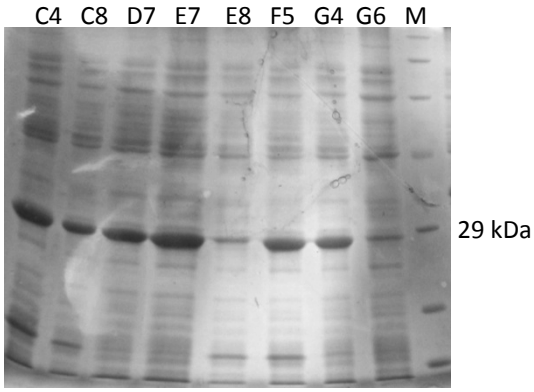

Figure 3-30. Protein analysis of the identified mutants after *in vivo* selection and chromogenic screening in MTPs.

Mutants C4, E7, E8 and F5 were purified and their enantioselectivity towards substrates **2b** and **Et-3-PB**, as cell extract and purified enzyme, was determined (Table 3-14). Mutants C4 and E7 showed no enantioselectivity when E_{true} was determined. The activity of purified E7 could not be determined because the protein precipitated after purification and lost activity. Mutants E8 and F5 showed good enantioselectivity towards both substrates, both as whole cell and in purified form. In both cases the enantioselectivity towards substrate **Et-3-PB** increased significantly when purified catalyst was used. This fact cannot be explained because when biocatalysis with whole cells was performed, background esterase activity of the *E. coli* strain used was tested and not detected. Substrate auto-hydrolysis has not been observed either. Product racemisation could be the cause of the decrease of enantioselectivity when cell extract is used for biocatalysis, but no specific search for this activity has been performed to confirm this theory.

Table 3-14. Data from the biocatalysis with selected mutants towards substrates **2b** and **Et-3-PB.**

Mutant	**E_{true} 2b**		**E_{true} Et-3-PB**	
	cell lysate	pure protein	cell lysate	pure protein
C4	4	4	3	1
E7	2	n.d.	4	n.d.
E8	25	16	50	> 100
F5	13	15	18	80

n.d. not determined.

Aiming to find a molecular explanation for the increased enantioselectivity of clones E8 and F5, *in silico* studies of the orientation of each enantiomer in the active site of the mutants were performed. The results obtained could not clearly explain the increase in enantioselectivity. In both cases, the different enantiomers orientate always with the phenyl ring pointing in similar direction. The orientations with the lowest energy for each enantiomer differ in the orientation of the methyl group, which could be the reason of the enantioselectivity. In mutant E8, the methyl group of (*S*)-**Et-3-PB** points to the side chain of tryptophan, this might impede the orientation of this enantiomer. On the contrary, the methyl group of (*R*)-**Et-3-PB** is placed in an area without steric hindrance and thus, this enantiomer might fix better in the active site. In mutant F5 each enantiomer of **Et-3-PB** is orientated very different compared to mutant E8. The (*S*)-form of **Et-3-PB** is pointing to residues 198 and 121; but in F5 interactions with the side chain of isoleucin might difficult correct substrate orientation. (*R*)-**Et-3-PB** is oriented oppositely, being the methyl group of the substrate again orientated to an area free of steric hindrance (Figure 3-31).

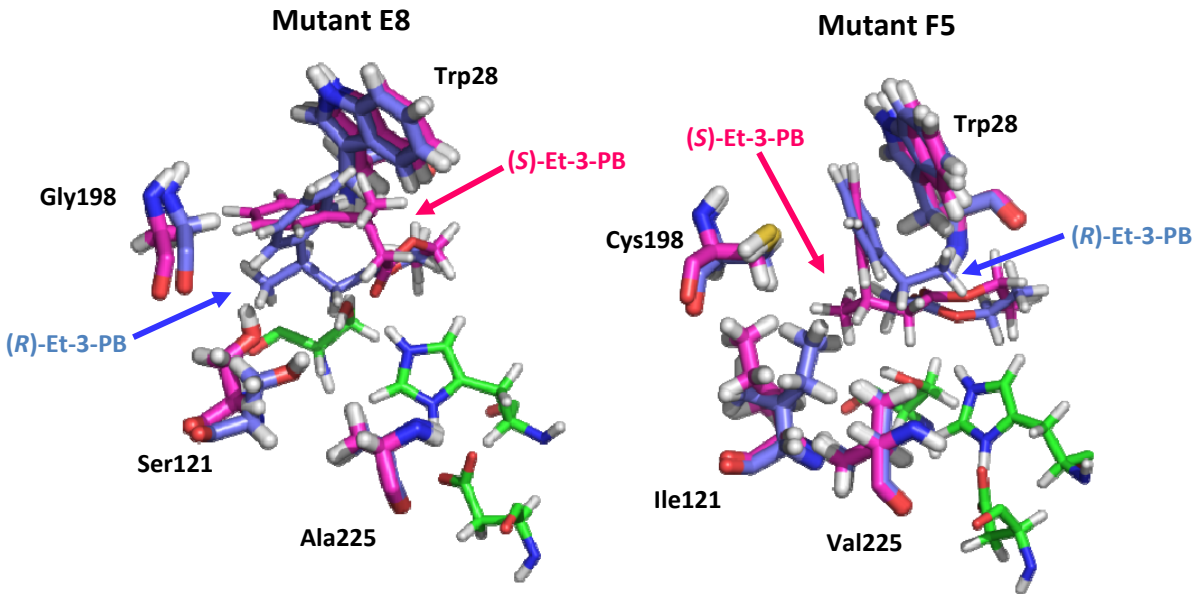

Figure 3-31. Homology model of mutants E8 and F5 with (*R*)-**Et-3-PB** (blue sticks) and (*S*)-**Et-3-PB** (pink sticks) docked in the active site. A productive orientation of each enantiomer in the active site is shown. Residues 28, 121, 198 and 225 are represented as blue or pink sticks, the residues forming the catalytic triad are represented as green lines.

When this PFEI mutant library was screened previously using a chromogenic method, clone F5 was the best mutant found whilst E8 was missed. The *in vivo* selection strategy

coupled to flow cytomery detection of the viable clones reduced the analysis effort down to 40 clones, which could be investigated in more detail, and a more selective mutant was found (E ~ 80 towards E > 100).

Most of the false positive clones obtained after *in vivo* selection and cell sorting, were inactive proteins, rather than active but non-enantioselective. These inactive selected clones are probably truncated products (where a stop codon is inserted, like in the case of G6) resulting into the transcription of shorter proteins which are less arduous for the cell to express. These cells suffer from lower metabolic stress and have better chances to survive in the selection media than cells expressing active non-selective esterases. However, it has already been shown that inactive clones can be easily identified in the chromogenic screening for activity and enantioselectivity. An alternative strategy would consist in selecting for activity prior to selection for enantioselectivity. Incubating the library after protein expression in M9 minimal medium supplemented with *rac*-**2b**, inactive clones could be removed from the medium and these selected clones could be selected again for enantioselectivity. Whether this strategy is better than the chromogenic screening is unknown.

3.7. Preliminary studies on selective in vivo evolution

It has been fully demonstrated that the designed system, based on *in vivo* selection coupled to flow cytometry, is suitable for identification of enantioselective esterases. Selection in liquid medium has advantages compared to selection on agar plates: higher throughput with lower material consumption, better contact between substrate and cell, etc. Another advantage of selection in liquid medium is that simultaneous enzyme evolution and selection is in theory possible. Hypothetically, cells carrying the gene and expressing the protein of interest could be subjected to *in vivo* mutation. The mutant library would be expressed and selective substrate hydrolysis would occur, cell survival being linked to enzyme activity. Design of this selective *in vivo* evolution strategy was attempted.

In this system, where evolution and selection are simultaneously performed, the use of inducer for protein expression is more restricted. Alternative carbon sources for *E. coli*, like L-rhamnose, are unsuitable, because here the inducer must be present in the selection

medium as well. Thus, the use of alternative expression systems, like pET vectors, or the use of auxotrophic strains is necessary.

The chemical mutagen N-methyl-N-nitrosoguanidine (MNNG) was chosen to generate the *E. coli* mutants. MNNG is a methylating agent classified as S_N-1 type, it decomposes to form a methyl diazonium cation that methylates DNA generating mainly N^7-methylguanine, N^3-methyladenine and O^6-methylguanine[239] (Scheme 3-14).

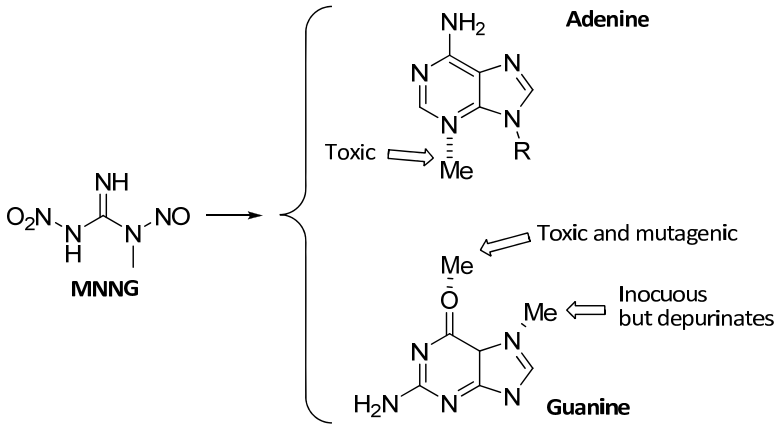

Scheme 3-14. Structure of MNNG and the most common base methylations.

Esterase BS2 cloned in a pET vector was the enzyme used in this project because the wildtype hydrolyzes both selection substrates (**2b** and **5b**), and this was considered an important issue for the beginning of the selection. Esterase PFEI has a smaller active site more suitable for engineering of enantioselectivity, but wildtype PFEI does not convert the positive impulse **2b**. Thus, cultures of *E. coli* JM109 (DE3) cells carrying the plasmid BS2-pET28Δ*Nco*I in LB medium and M9 minimal medium + glycerol supplemented with different MNNG concentrations were prepared. The effect of MNNG on these cells was studied observing two parameters: cell survival and mutagenic effect.

The effect of MNNG on cell survival was determined monitoring cell growth by OD measurement. The toxic effect of MNNG was higher when cells were incubated in M9 minimal medium + glycerol than when these were cultivated in LB medium (Figure 3-32). Cells are likely more sensitive when they are cultivated in nutrient limited media.

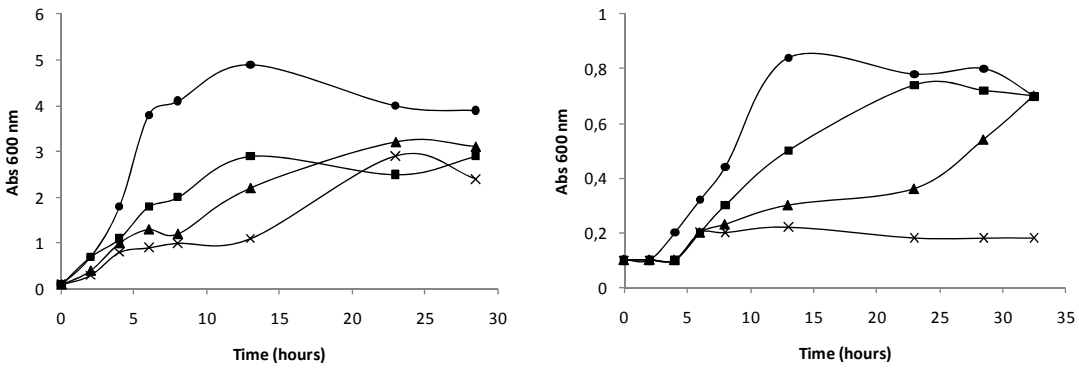

Figure 3-32. Growth curves of *E. coli* JM109 (DE3) in LB medium (left plot) and M9 minimal medium + glycerol (right plot) supplemented with different concentrations of MNNG: circles 0 µg/ml; squares 50 µg/ml; triangles 100 µg/ml and crosses 200 µg/ml.

The mutation rate was estimated calculating the percentage of clones with high decrease or lost of activity. For this aim, samples taken from the cultures at different times were plated on agar. Replica plates for protein expression on agar plates were performed and esterase activity was estimated by overlay assay. Good mutagenic effect was observed by cultivations with 50 and 100 µg/ml MNNG, with 40-50% of the clones with high loss of activity (Figure 3-33), so selective *in vivo* evolution experiments were performed in selection medium supplemented with these concentrations of MNNG.

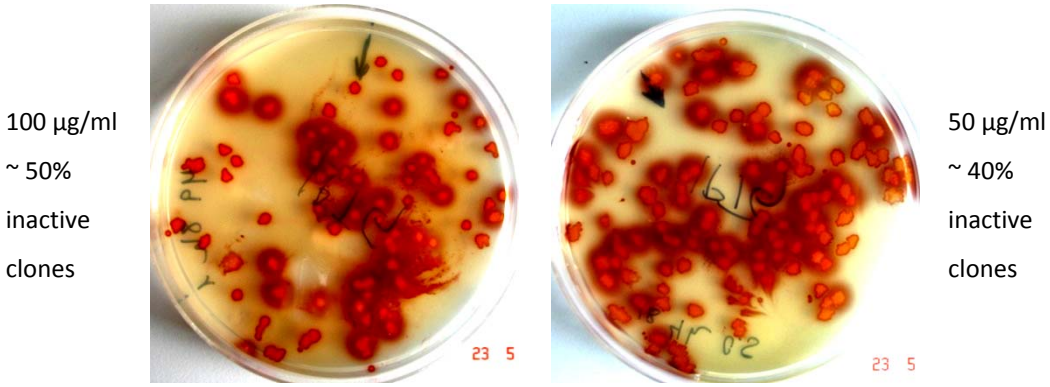

Figure 3-33. Overlay assay for esterase activity of clones after cultivation in M9 minimal medium + glycerol supplemented with 100 µg/ml (left picture) and 50 µg/ml (right picture) MNNG. The percentage of inactive clones has been calculated as inactive colonies/total colonies.

E. coli cells expressing BS2 were transferred at OD = 0.1 to M9 minimal medium supplemented with selection substrates (*R*)-**2b** and (*S*)-**5b**, β-cyclodextrin as co-solvent, IPTG to maintain esterase expression and MNNG for the generation of mutations. Samples were taken from these cultures after 24, 48 and 72 hours and different volumes

were platted onto agar (100-200 μL), but no colonies grew on any of the plates. The control culture supplemented with M9 minimal medium, β-cyclodextrin, IPTG and glycerol grew, so the culture was initially vital. Probably, selective and evolutive conditions simultaneously applied form a too hostile environment for *E. coli* to survive. High system optimisation is required to adapt the *in vivo* selection system into a selective *in vivo* evolution system.

The substitution of MNNG by a milder mutagene, like UV light might be more successful. Thus, mutagenic conditions could be applied intermittently, decreasing the stress in the cell culture. If a mutator strain was used the mutagen concentration in medium could be decreased or this could be even disregarded. This option might ease the development of the selective *in vivo* evolution system.

Probably, search of a suitable esterase for this selective *in vivo* evolution is necessary as well. Esterase PFEI has an active site with an appropriate size to engineer enantioselectivity but it does not hydrolyze the pre-selection substrate **2b**. On the contrary, esterase BS2 hydrolyses both pre-selection substrates at good rates, but the form of its active centre makes the increase of enantioselectivity towards 3-phanylbutanoates difficult. If the finding of the appropriate parent esterase for this substrate is not straightforward, another alternative would be the change of model substrate for strategy development.

4. RESULTS AND DISCUSSION – CHAPTER II:

CRYSTALLIZATION, STRUCTURE ELUCIDATION AND ANALYSIS OF PestE

4. CRYSTALLIZATION, STRUCTURE ELUCIDATION AND ANALYSIS OF PestE

An esterase of the hyperthermophilic archaeon *Pyrobaculum calidifontis*, the PestE, was identified and recombinant expressed in *E. coli* by Prof. Atomi´s group.[206] This esterase is highly enantioselective towards the model substrate used for the development of the previously described *in vivo* selection system -3-phenyl butyric acid, **3-PBA**- and was used as control esterase for system validation. Apart from this particular application, PestE has further interesting characteristics, which make of it a valuable candidate with many possibilities in the biocatalytical industry.

PestE is resistant to both, extreme temperatures and organic solvents[240] (miscible and immiscible with water), it is one of the few known hydrolases which shows activity towards tertiary alcohols[241] and it has been successfully immobilized on Celite,[242] so catalyst recycling is possible.

Aiming to expand the knowledge about this esterase, crystallization and structure elucidation of the enzyme was attempted. Availability of information about protein structure would allow analysis of the structural basis of properties like enantioselectivity and thermostability. In addition, protein engineering with this catalyst can be more effectively performed with knowledge about structure and reaction mechanism as significant domains can be detected and specifically randomized.

4.1. PestE purification

The high stability of PestE allows easy purification. Enough amounts of protein in high purity were obtained following the purification protocol previously established by Hotta et al.[206]

After cell disruption and centrifugation, supernatant (soluble fraction of cell extract) was heated to 80°C for 20 min. This step should precipitate most of the *E. coli* proteins, as *E. coli* is a mesophilic microorganism, leading to higher PestE concentrations in the soluble fraction. After cell extract heating and centrifugation a precipitate was observed, which should be consisted of most *E. coli* proteins. However, when the soluble fraction of cell extract was analyzed by SDS-PAGE, small differences in the purity of PestE before and

after heat treatment were observed (Figure 4-1, A). Probably longer incubation times at 80°C or higher temperatures are required to obtain a more effective precipitation of *E. coli* proteins.

The cell extract was further purified by anion exchange chromatography (AEC). Esterase containing fractions could be identified by detection of esterase activity via qualitative *p*NPA. These active fractions were collected in three separated batches corresponding to their estimated purity deduced by the purification chromatogram (see Figure 4-1, B). These batches were analyzed via SDS-PAGE and effective purification of PestE could be observed. However, higher sample purity increases the success probability in a crystallization screening. Thus, fractions 15-24 were collected and further purified. Fractions 25-32 were not added to the mixture because the purity degree of this sample was lower.

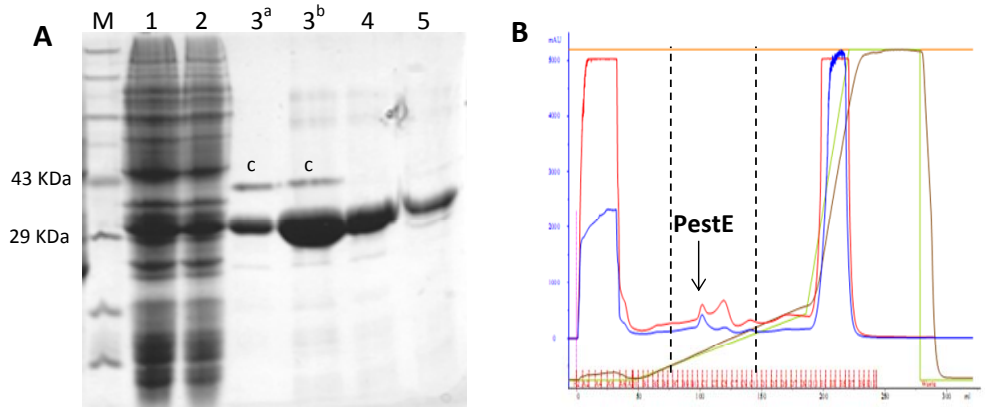

Figure 4-1. A: SDS-PAGE analysis of cell lysate before and after different purification steps. M: marker, 1and 2: cell lysate. 1: before heat purification; 2: after heat purification, 3-5: fractions from AEC. 3: 20-24; 4: 15-19 and 5: 25-32.

[a] 2 µL sample volume loaded, [b] 5 µL sample volume loaded, [c] non-denaturated PestE.

B: chromatogram of purification by AEC. The active fractions collected and analyzed via SDS-PAGE are delimited by discontinuous lines. Blue line: abs_{280nm}, maximum absorbance of proteins, red line: abs_{260nm}, maximum absorbance of DNA, brown line: conductivity, green line: % NaCl.

Next, protein purification by gel filtration (GF) was performed. This procedure separates molecules attending to their size. A clear protein peak was observable in the GF chromatogram (Figure 4-2, B) which was identified as PestE by qualitative *p*NPA and SDS-PAGE analysis (Figure 4-2, A). The remaining NaCl from purification by AEC could be separated from the sample by this procedure as well. In SDS-PAGE analysis,

together with the expected PestE band (at ~ 29 kDa) a second band (at ~ 43 kDa) was observed in some samples. As it showed esterase activity and its intensity was reduced with longer denaturation times prior to SDS-PAGE analysis, it was assumed to be non-denaturated PestE. However, this can not be concluded for sure without protein identification by mass spectrometry.

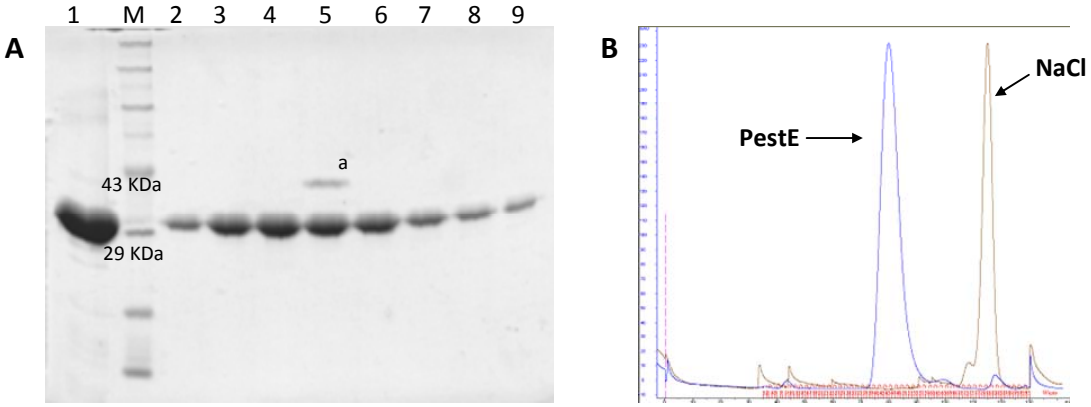

Figure 4-2. A: SDS-PAGE analysis of cell lysate before and after GF. M: marker, 1: fractions 15-24 from purification by AEC; 2-9: significant fractions from purification by GF.
[a] non-denaturated PestE.
B: GF chromatogram. Blue line: abs_{280nm}, the blue peak corresponds to PestE, every second fraction corresponding to it was analyzed via SDS-PAGE. Brown line: conductivity, the brown peak corresponds to eluted NaCl.

4.2. PestE crystallization and structure elucidation

After concentration of the protein solution by ultrafiltration, 250 µL solution with a concentration of 32 mg/ml PestE were obtained. A first crystallization screening with 300 different conditions was set at 20°C with a crystallization robot (HTPC, CyBio, Jena, Germany) using the sitting-drop-diffusion method in 96-well plates. Promising crystals were found, and the conditions were optimized in 24-well plates by vapour diffusion using the hanging-drop method. At the condition 30% MPD, 10% PEG 4000, 0.1 M imidazole pH 8, small irregular crystals appeared after four days (Figure 4-3, A). At the condition 30% ethanol, 10% PEG 6000, 0.1 M sodium acetate, colourless crystals in the form of thin layers appeared after four days as well (Figure 4-3, B).

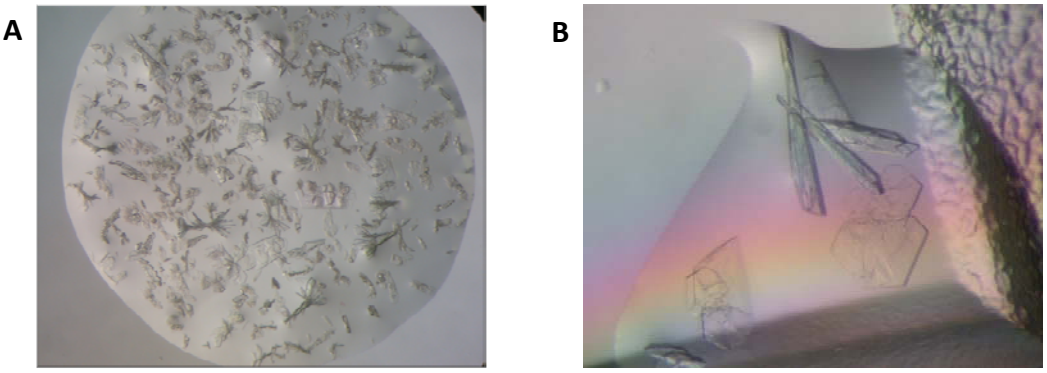

Figure 4-3. Best conditions out of the optimisation screening in 24-well plates. A: 30% MPD, 10% PEG 4000, 0.1 M imidazole pH 8. B: 30% ethanol, 10% PEG 6000, 0.1 M sodium acetate.

Further optimisation was carried out with the hanging-drop method and PestE crystals suitable for data collection were obtained at the condition 30% MPD, 10% PEG 6000, 0.1 M sodium acetate (Figure 4-4). Diffraction data collection and crystallographic computing was performed by Dr. Gottfried Palm from the research group of Prof. Dr. Hinrichs, Greifswald University.

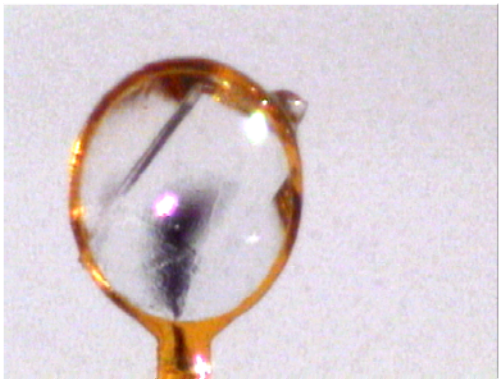

Figure 4-4. PestE crystal used for the collection of the diffraction data. The picture shows the crystal already assembled in a ring for diffraction data collection.

PestE was classified by Hotta et al.[206] as a member of the hormone-sensitive-lipase family (HSLs) of the esterase/lipase superfamily on the basis of the amino acid sequence identity (30% identity). The structure of PestE corresponds to a canonical α/β-hydrolase fold with a cap-domain (Figure 4-5).

The active site of PestE is composed by the typical catalytic triad present in carboxyl esterases: Ser157, His284 and Asp254. The catalytic Ser is found within the conserved amino acid motif GXSXG (where X is any amino acid) located in the apex of the

nucleophilic elbow[51] between β5 and α5 (Figure 4-5). The oxyanion hole is composed of Gly85 and Gly86 within the conserved sequence motif HGGG(M,F,W) (amino acid residues 83-87) and Ala158. Between the cap structure and the C-terminal site of the central β-sheet a tunnel-like cavity (around 11 Å in diameter) is located. The active site is located within this cavity, and two main accesses to it can be observed: the wider channel is surrounded by αI, αII and loop αVI-αVII, the narrower channel is bordered by αVI, αVII and loop βIII-αIII. There is a third smaller access to the tunnel between the loops, α-III and α-XI.

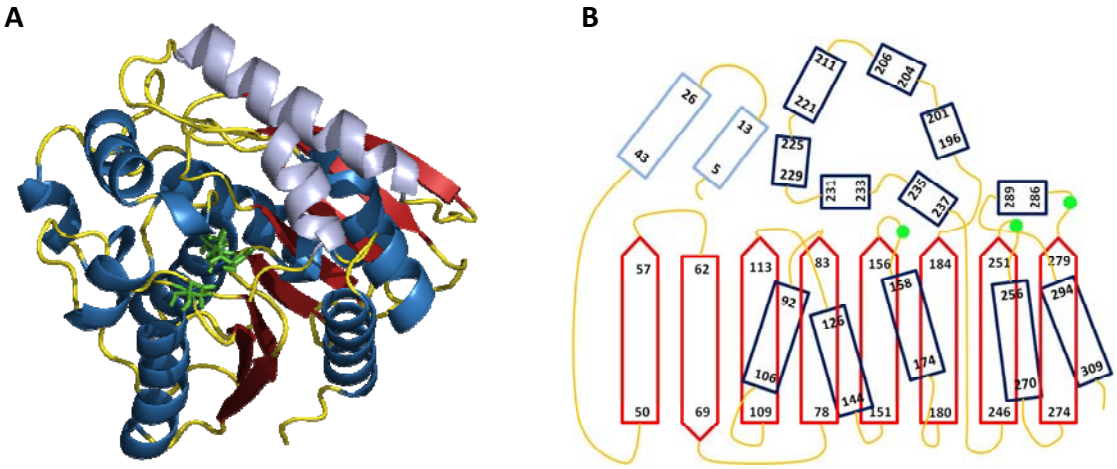

Figure 4-5. A: Overall fold of the PestE generated using PyMol.[243] α-helices are shown in blue (helices forming the cap domain are light blue) and β-strands in red. The amino acid residues of the catalytic triad are shown as green sticks: Ser157, Asp254 and His284.

B: Secondary topology of the PestE fold. The α-helices as blue cylinders (α1: 5-13; α2: 26-43; α3: 92-106; α4: 126-144; α5: 158-174; α6: 196-201; α7: 204-206; α8: 211-221; α9: 225-229; α10:231-233; α11:235-237; α12:256-270; α13: 286-289; α14: 294-309) and the β-strands are shown as red arrows (β1: 50-57; β2: 62-69; β3: 78-83; β4: 109-113; β5: 151-156; β6: 180-184; β7: 246-251; β8: 274-279). Secondary structure assignments were obtained from Pymol.[243]

The quaternary structure of PestE is a dimer in solution as determined by gel filtration (estimated to 53 kDa, Figure 4-2). This oligomerization has also been observed in closely related esterases (EstE1,[244] BFAE,[245] heroin esterase,[246] Est E7[247] and AFEST[248]). Oligomerization reduces the solvent accessible surface of PestE and it probably contributes to protein stabilization as this effect occurs commonly in thermostable

enzymes, while structural related esterases from mesophiles, like EstE5[249], stay as monomers.

4.3. Structural basis for enantioselectivity towards 3-phenylbutanoates

Aiming to understand the molecular reasons for the enantioselectivity of PestE towards 3-phenylbutanoates, automated docking and molecular dynamic simulations were performed using the different enantiomers of ethyl-3-phenylbutanoate (**Et-3-PB**, Figure 4-6). The potential energies of the substrates obtained after 1 ns simulations and energy minimization of the first transition state (TI1) matched the experimental results.

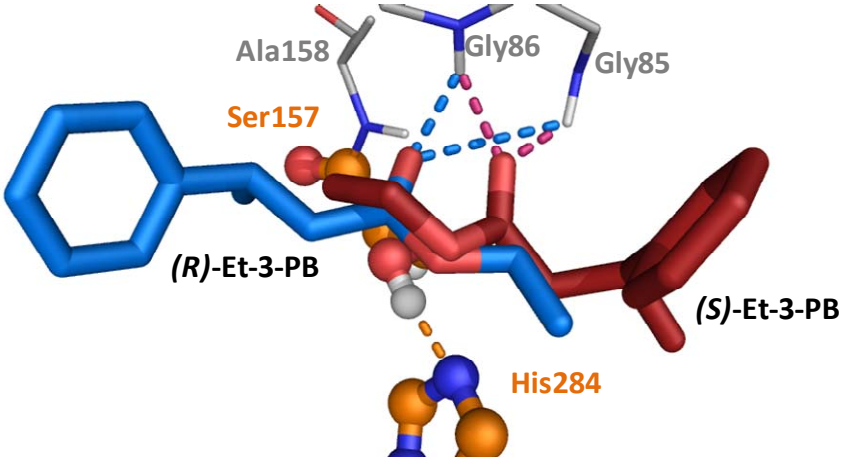

Figure 4-6. Close view of both enantiomers of **Et-3-PB** and their orientation in the active site.

Two different orientations of each enantiomer in the active site with significant energy differences were found (Figure 4-7 and Table 4-1). The TI1 for the (*R*)- and (*S*)-enantiomer with the lowest energy favors the (*R*)-enantiomer and match with the experimentally calculated high enantioselectivity. The energies of the TI1 suggest that the (*R*)-enantiomer orientates principally with the phenyl ring pointing into the narrow tunnel, while the (*S*)-enantiomer orientates preferably with the phenyl ring in the wide hydrophobic channel. For effective catalysis the orientation of the (*R*)-enantiomer is more likely. Mechanistically, the release of the alcohol and generation of the acyl enzyme follows the TI1 (see 1.2.3.1.2.) and ethanol (in the case of ethyl ester) will leave the

active site through the hydrophobic, wide tunnel which is only possible for the orientation of the (*R*)-enantiomer of **Et-3-PB**.

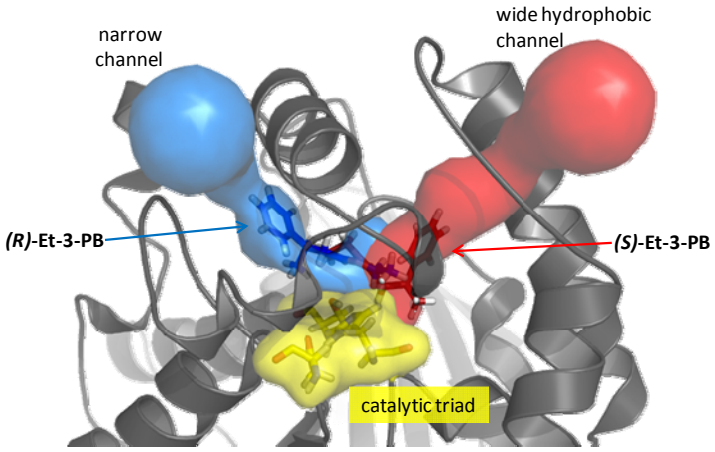

Figure 4-7. Representation of wide and narrow access channels into the active site of PestE with the enantiomers of **Et-3-PB** in the orientation with the lowest energy.

Table 4-1. Calculated energy of the TI1 for each enantiomer in each orientation.

	A	**B**
(*R*)-**Et-3-PB**	- 493.40 kJ/mol	- 472.08 kJ/mol
(*S*)- **Et-3-PB**	- 457.68 kJ/mol	- 473.98 kJ/mol

A: phenyl ring pointing into the narrow channel.

B: phenyl ring pointing into the wide channel.

These results provide a molecular explanation for the high enantioselectivity observed in the biocatalysis experiments. While the acyl moiety of **Et-3-PB** needs to be oriented in the small channel, the alcohol leaving group is pointing to the larger access tunnel.

5. SUMMARY AND CONCLUSIONS

5. SUMMARY AND CONCLUSIONS

During this PhD thesis, an *in vivo* selection system coupled to flow cytometry analysis and cell sorting for the identification of enantioselective esterases has been established. For the development of the selection medium, positive and negative impulses have been designed, and the pre-impulses have been synthesized. Initially, substrates **2b** and **3b** were used as pre-impulses in the selection medium. However, **3b** was finally substituted by **5b** because this substrate had higher structural similarity to **2b**. Furthermore, the toxin released after hydrolysis, **5a**, had bactericide effect, while **3a** had only bacteriostatic effect. The presence of co-solvents in the culture medium has been optimized as well in order to achieve good substrate dispersion allowing cell survival. The addition of β-cyclodextrin made possible the dispersion in medium of concentrations of **5b** high enough for negative selection to take place (20 mM).

Together with the design of the selective culture medium, adequate control esterases for the establishment of the strategy were identified. Esterase PFEI, which had been used in previous work on this subject, was substituted by BS2 because PFEI did not convert the pre-selection substrate **2b**. The expression system was modified as well and pET vectors were used instead of pGASTON because these do not use L-rhamnose as inducer of protein expression, which is an alternative carbon source. In addition to BS2, which is the negative control esterase (not enantioselective towards the model substrate, **3-PBA**), enantioselective esterases were searched in order to use them as positive controls for system validation. Esterases CL1 and PestE were identified in an enzyme screening as high enantioselective towards 3-phenylbutanoates and recombinant expressed in the *E. coli* strain used for selection (*E. coli* JM109 (DE3)).

In addition to the *in vivo* selection system, a strategy based on flow cytometry and cell sorting has been optimized to enable the detection of the desired clones. Thus, a suitable staining technique to differentiate cell viability, cell damage and cell death caused by toxin **5a** was implemented. The combination of DNA stains Syto9 and PI was chosen as staining method because the use of alternative less aggressive detection methods (PI staining, GFP expression combined to PI staining) failed and further dye combinations (DIBAC/PI) did not provide clear results.

Once established, the reliability of this assay has been demonstrated in two different ways. First, the enantioselective esterases PestE or CL1 and the non-selective esterase

BS2 (control esterases) were incubated together (BS2 with PestE, or BS2 with CL1) in selection medium. After flow cytometry analysis and sorting of the viable population, enrichment of the enantioselective enzyme over the non-selective BS2 has been proven. Second, 10^8 clones of a mutant library of PFEI (which contained mutants active towards substrate **2b**) were *in vivo* selected, and the clones sorted after flow cytometry analysis were investigated for improved enantioselectivity. Two mutants with high enantioselectivity towards **Et-3-PB** (E ~ 80 and E > 100) and with moderate enantioselectivity towards the pre-impulse **2b** (E ~16 and E ~15) were found. Analysis of the same library by E_{app} determination using a MTP-based screening method and enantiopure chromogenic substrates (*p*-nitrophenyl-3-phenylbutanoate), resulted in the finding of a mutant with E ~ 80 towards ethyl-3-phenylbutanoate.[116] After *in vivo* library selection, this mutant was found and additionally a mutant with E > 100 was identified as well. Thus, this method has demonstrated to be more effective. Moreover, the analysis of 10^8 clones by the here described methodology takes only three days and is low time consuming; the strategy consists of library expression, incubation of the clones in selective medium, cell staining, flow cytometric analysis and sorting of the interesting candidates. The colonies that grow on agar plates after this process are investigated more in detail, reducing the analytic effort from 10^8 clones to some dozens.

Compared to the method described by Boersma et al.[179] (see 1.4.2.2.), our strategy uses a structurally more similar pseudo-enantiomeric couple. In addition, Boerma et al. use an auxotrophic *E. coli* strain for aspartate as expression host, because their selection is based on this amino acid; this limits the possibilities of recombinant protein expression as only one *E. coli* strain can be used. The selection method described here uses a carbon source as positive impulse. Thus, any *E. coli* strain can be used as expression host as long as the sensitivity towards the selection substrates (**2b**, **5a** and **5b**) is adequate. Compared to the other existing *in vivo* selection method for enantioselectivity, described by Reetz et al.[180] (see 1.4.2.2.), our method has the advantage of using *E. coli* as expression host. Reetz et al. used a pseudo-enantiomeric couple with very high similarity, but it was only effective for selection in *Pichia pastoris*. The use of *Pichia pastoris* for the expression of mutant libraries is quite limited because due to the low transformation yield of this organism, only effective expression of small libraries is achieved. These strategies[179,180] selected the most viable clones after *in vivo* selection, based on growth on agar plates. The outcome in

both cases was rather modest as low enantioselectivities were achieved (E-values below 10, the enantiopreference was inverted in both cases).

The here reported *in vivo* selection process is performed completely in liquid medium instead of on agar plates. Apart from making the library amenable to flow cytometric analysis, this simplifies the simultaneous combination of mutation and selection procedures, making the development of a selective *in vivo* evolution strategy theoretically possible. In this way, mutant generation and *in vivo* selection of the interesting clones could be performed at the same time. If several mutation & selection rounds take place without the need of individualization of the clones, high quality libraries can be created without any need of knowing about the protein structure or the reaction mechanism. This strategy is a faster and more economical alternative to the genetic complementation selection systems and screening techniques currently used. Aiming to achieve this challenging goal, the first attempts of selective *in vivo* evolution have been performed using the chemical mutagen MNNG, and guidelines for future system optimisation have been established.

In addition, enantioselective esterases towards 3-phenylbutanoates and other arylalkyl carboxylic acids have been discovered during this work and its application in kinetic resolutions in analytical and preparative scale has been performed. One of these esterases, the PestE, which displays interesting features for wide industrial applications, has been crystallized allowing elucidation of its structure. Experimental results about the enantioselectivity of this enzyme towards **Et-3-PB** could be supported by *in silico* studies and a hypothesis about its thermostability has been formulated. The availability of the crystal structure of PestE allows more reliable *in silico* studies on the identification of significant residues for modification of enzyme properties, broadening the possibilities of engineering this enzyme.

6. MATERIALS AND METHODS

6. MATERIALS AND METHODS

6.1. Materials

6.1.1. Chemicals and consumables

Unless otherwise stated, all chemicals and consumables were purchased from the commercial suppliers ABCR (Karlsruhe), Fischer Scientific (Schwerte), Greiner (Solingen), Roth GmbH (Karlsruhe), Sarstedt (Nümbrecht), Sigma-Aldrich (Taufkirchen), StarLab (Ahrensburg) and VWR (Darmstadt) and used without further purification.

Fermentas (St. Leon-Rot)	GeneJET™ Plasmid Miniprep Kit
GE Healthcare (Freiburg)	XK 16/20 column, Q Sepharose™, HiLoad™ 16/60 Superdex 200 pg, IMAC SepharoseTM 6 Fast Flow columns
Interchim S.A. (Frankfurt)	BC Assay Protein Quantification Kit
Millipore GmbH (Schwalbach)	Centricons® 10 KDa
Novagen (Darmstadt)	BugBuster™ Protein Extraction Reagent
Qiagen GmbH (Hilden)	QIAprep Spin® Miniprep Kit
	QIAquick™ Gel Extraction Kit
Stratagene (La Jolla, USA)	QuikChange™ Site-directed Mutagenesis Kit

6.1.2. Strains

For recombinant expression of proteins, for growth/toxicity assays and for the establishment and validation of the *in vivo* selection system several *E. coli* strains were used (Table 6-1).

Table 6-1. The above described *E. coli* strains were used.

Species	Strain	Genotype	Supplier
Escherichia coli	DH5α	supE44 ΔlacU169(F80lacZΔM15) hsdR17 recA1 endA1 gyrA96 thi-1 relA1	Clontech
Escherichia coli	BL21 (DE3)	F^- ompT $hsdS_B$ (r_B^- m_B^-) gal dcm (DE3)	Novagen
Escherichia coli	JM109 (DE3)	recA1 endA1 gyrA96 thi-1 hsdR17 supE44 relA1 Δ(lac-proAB) F'[traD36 $proAB^+$ $lacI^q$ lacZΔM15] (DE3)	Promega

6.1.3. Genes and plasmids

Site-directed mutagenesis was performed in vector pET28a from Novagen (C296A and C297T) in order to substitute the *Nco*I restriction site by an *Nde*I restriction site. The modified vector was named pET28aΔ*Nco*I and was used for further cloning experiments.

The gene of the esterase from *Bacillus subtilis* DSM402 (BS2)[50] was available in our laboratory in the vector pGASTON (ampicillin resistance) fused with six histidin codons on C-terminus (His_6-tag). Site-directed mutagenesis had been performed in BS2 (T1069C) in order to delete one *Nde*I restriction site by a silent mutation. The modified gene was named BS2Δ*Nde*I and was cloned into vector pET28aΔ*Nco*I with kanamycin resistance and a T7 promoter fused with a His_6-tag.

The gene of esterase CL1[221] was kindly supplied by BRAIN AG (Zwingenberg, Germany) in the vector pET24a with kanamycin resistance and a T7 promoter. It has been used without further recloning.

The gene of the thermostable esterase from *Pyrobaculum calidifontis* (PestE)[206] in vector pET21a with ampicillin resistance and a T7 promoter was a kind gift from Prof. H. Atomi (Kyoto University, Japan). The PestE gene was cloned into the vector pET28aΔ*Nco*I with kanamycin resistance and a T7 promoter.

The gene of the green fluorescent protein (GFP) was used in two different expression vectors. GFP was cloned in vector pET11a with ampicillin resistance and a T7 promoter, this gene was a kind gift from Prof. Hinrichs (University of Greifswald, Germany). The gene of GFP was also cloned in pALTER CDC42, which is a derivative from the original pAlter-ExII vector (Promega), where the chloramphenicol resistance has been deleted. This vector has tetracycline resistance and a T7 promoter. Plasmid pALTER CDC42l

containing the GFP gene was a kind gift from Susanne Brakmann (University of Dortmund, Germany).

The gene of the esterase I from *Pseudomonas fluorescens* (PFEI)[250] was available in our laboratory in vector pGASTON with ampicillin resistance and a promoter inducible by L-rhamnose,[251] it was C-terminally fused with a His_6-tag. In the PFEI gene site-directed mutagenesis had been performed in order to delete two *Nar*I restriction sites situated at 363 and 726 bp by silent mutations.[214] This PFEIΔ*Nar*I gene was used as template for the construction of the site-directed mutant library.[116]

The plasmids used are listed in Table 6-2. All vectors but pALTER CDC42 (p15A ori) have replication origin type ColE1.

Table 6-2. The plasmids used in this project are summarized below.

Vector	**Resistance**	**Supplier**
pGASTON	Amp^r	Henke[251]
pET-28a(+)	Kan^r	Novagen
pET-24a(+)	Kan^r	Novagen
pET-11a	Amp^r	Novagen
pALTER CDC42	Tet^r	Brakmann and Grzeszik[252]
pET-21a(+)	Amp^r	Novagen

6.1.4. Primers

All primers used were provided by MWG Biotech (Martinsried) or Biomers (Ulm).

6.1.4.1. Sequencing primers

Table 6-3. Plasmids used for gene sequencing.

Name	Sequence	Use
pGAS-FW	5′-CAT CAT CAC GTT CAT CTT TCC CTG-3′	forward primer for pGASTON vector
pGAS-RV	5′-TTT CAC TTC TGA GTT CGG CAT GG-3′	reverse primer for pGASTON vector
T7- Promoter	5′-TAA TAC GAC TCA CTA TAG GG-3′	forward primer for all pET vectors
T7- Terminator	5′-CTA GTT ATT GCT CAG CGG T-3′	reverse primer for all pET vectors

6.1.4.2. QuikChange™ primers

Table 6-4. Primers used for site-directed mutagenesis. Mutations are bold and the new restriction site created is underlined.

Name	Sequence	Use
QCpET28aBs2-FW	5′-GAT GAT GAT GGC TGC **AT**A TGG TAT ATC TCC TTC TTA AAG-3′	replacement of *NcoI* restriction site by *NdeI* restriction site
QCpET28aBs2-RV	5′-CTT TAA GAA GAT ATA CCA T**AT** GCA GCA GCC ATC ATC ATC-3′	

6.1.5. Enzymes

All restriction enzymes, polymerases and ligases were provided by the commercial suppliers: Promega (Mannheim), Roboklon (Berlin), New England Biolabs GmbH (Frankfurt am Main) and Fermentas (St. Leon-Rot).

Following recombinant hydrolases of metagenomic origin were used as cell lysate stabilized with glycerol: Est 1, Est 4, Est 5, Est 7, Est 8, Est 10, Est 12, Est 15, Est 16, Est 17, Est 20, Est 22, Est 24, Est 25, Est 27, Est 28, Est 29, Est 31, Est 32, Est 34, Est 37, Est

38, Est 40, Est 42, Est 43, Est 44, Est 49, Est 51, Est 56, Est 57, Est 58, Est 59, Est 63, Est 67, Est 74, Est 91, Est 99, Est 101, Est 114, Est 118, Est 124, Est 125, Est 135, Est 139, Est 140, Est 141, Est 143, Est 144, Est 145, Est 147, Est 148, Est 149, Est M43dM-1-2, Est M10bA1, Est M8cA5, Est M3dH5, Est M48c05, Est M43dH1, Est A3, Est CL1, Est CL2, Est CE, Lip 5 and Lip 8. All of them were kindly provided by BRAIN AG (Zwingenberg).

The used recombinant esterases which were available in our laboratory are summarized in Table 6-5.

Table 6-5. Recombinant esterases used in this PhD Thesis.

Esterase	Organism
BS2	*Bacillus subtilis*
BsubE	*Bacillus subtilis*
PestE	*Pyrobaculum calidifontis*
SDE	*Streptomyces diastatochromogenes*
BsteE	*Bacillus stearothermophilus*
PFEI	*Pseudomonas fluorescens* SIK WI
PFEII	*Pseudomonas fluorescens* DSM 50106

6.1.6. Media, additives and inducers

6.1.6.1. General media

Luria-Bertani medium/LB medium[253]

1% (w/v) NaCl

1% (w/v) tryptone

0.5% (w/v) yeast extract

Filled with dest. water and sterilized in autoclave at 121°C for 21 min.

LB-SOC medium

Addition of 10% (v/v) of 10 x SOC solution to sterile LB medium

10 x SOC solution: 0.2% (w/v) KCl
2.0% (w/v) $MgCl_2$
2.0% (w/v) $MgSO_4$
4.0% (w/v) glucose

M9 minimal medium

10% (v/v) 10 x M9 salt solution, sterile
0.2% (v/v) 1 M $MgSO_4$ x $7H_2O$, sterile
0.1% (v/v) 100 mM $CaCl_2$ x $2H_2O$, sterile
Filled with dest. water, sterile

10 x M9 salt solution: 76.5 g Na_2HPO_4 x $2H_2O$
30.0 g KH_2PO_4
5.0 g NaCl
10.0 g NH_4Cl

Filled to 1000 ml with dest. water, pH adjusted to 6.6 and sterilized at 121°C for 21 min.

For agar plates 1.5% agar was added before sterilization. When agar plates with antibiotics were prepared, the corresponding antibiotic was added to the adequate concentration after the LB-agar solution had cooled down to 40°C.

6.1.6.2. In vivo selection media

Pseudo-selection media

M9 minimal medium with antibiotic (Amp or Kan)
5 mM **2b**[a] or 0.5 mM **3b**[b] or 20 mM **5b**[a, b]
0.2% (w/v) L-rhamnose or 0.1 mM IPTG
[a]medium supplemented with 10 mg/ml β-cyclodextrin
[b]medium supplemented with 5 mM glycerol

Selection medium

M9 minimal medium with antibiotic (Amp or Kan)

5 mM (*R*)-**2b**

20 mM (*S*)-**5b**

10 mg/ml β-cyclodextrin

0.1 mM IPTG (when cell growth was determined)

Anti-selection medium

M9 minimal medium with antibiotic (Amp or Kan)

5 mM (*S*)-**2b**

20 mM (*R*)-**5b**

10 mg/ml β-cyclodextrin

0.1 mM IPTG (when cell growth was determined)

Positive selection control

M9 minimal medium with antibiotic (Amp or Kan)

5 mM **2a**

10 mg/ml β-cyclodextrin

0.1 mM IPTG (when cell growth was determined)

Negative selection control

M9 minimal medium with antibiotic (Amp or Kan)

5 mM **2a**

10 mM **5a**

10 mg/ml β-cyclodextrin

0.1 mM IPTG (when cell growth was determined)

6.1.6.3. Additives and inducers

Antibiotics

ampicillin (Amp)	Standard solution: 100 mg/ml in water
	Final concentration: 100 μg/ml

kanamycin (Kan)	Standard solution: 50 mg/ml in water
	Final concentration: 50 µg/ml
tetracyclin (Tet)	Standard solution: 5 mg/ml in 70% ethanol
	Final concentration: 10 µg/ml

Inducers

L-rhamnose	Standard solution: 20% (w/v) in water
	Final concentration: 0.2% (w/v)
IPTG	Standard solution: 0.1 M in water
	Final concentration: 0.1 mM

Co-solvents

β-cyclodextrin	Standard solution: 100 mg/ml in M9 minimal medium
	Final concentration: 10 mg/ml

6.1.7. Buffers and solutions

6.1.7.1. Cell washing, cell disruption and separation of inclusion bodies

50 mM sodium phosphate buffer pH 7.4[253]

11.3 ml 1 M NaH_2PO_4 solution

32.7 ml 1 M Na_2HPO_4 solution

The combined 1 M stock solutions are diluted to 1000 ml with dest. water and pH is adjusted to 7.4 if necessary. The buffer was sterilized if needed. Phosphate buffer of lower strength was prepared diluting this concentration with dest. water and adjusting the pH.

Triton X-100 solution

50 mM sodium phosphate buffer pH 7.4

0.1% (v/v) Triton X-100

Lysis buffer

50 mM sodium phosphate buffer pH 8.0

300 mM NaCl

Addition of 1mg/ml lysozyme and 1 U/ml DNase before use.

6.1.7.2. Preparation of competent cells

6.1.7.2.1. Chemically competent cells

Buffer RF1

100 mM RbCl

50 mM $MnCl_2$

30 mM CH_3COOK

10 mM $CaCl_2$

15% (v/v) glycerol

pH is adjusted to 5.8 with 0.2 M acetic acid and the solution is sterilized by filtration (0.2 μm diameter).

Buffer RF2

10 mM RbCl

75 mM $CaCl_2$

10 mM 3-(N-morpholino) propane sulfonic acid

15% (v/v) glycerol

The pH is adjusted to 6.8-7.0 and the solution is sterilized by filtration (0.2 μm diameter).

6.1.7.2.2. Electro-competent cells

10% (v/v) glycerol

Filled with milliQ water and sterilized in autoclave at 121°C for 21 min.

6.1.7.3. Agarose gel electrophoresis

Agarose gel

0.1‰ ethidium bromide solution

Agarose (0.8-1.5% final concentration)

1 x TAE buffer

50 x TAE buffer

242 g Tris

57.1 ml acetic acid

100 ml 0.5 M EDTA

Filled to 1000 ml with dest. water, pH adjusted to 8.0. TAE buffer of lower strength was prepared diluting this concentration with dest. water.

Agarose gel loading buffer

10 x TAE buffer

0.25% (w/v) bromophenol blue

30% glycerol

DNA marker

1 kb DNA ladder from Roth (0.5 - 10 kb)

6.1.7.4. Protein purification

6.1.7.4.1. Heat precipitation

20 mM Tris/HCl pH 8.0

2.428 g Tris base

Filled to 1000 ml with dest. water, pH adjusted to 8.0

6.1.7.4.2. Anion Exchange Chromatography

Equilibration/Wash buffer

20 mM Tris/HCl pH 8.0

Elution buffer

20 mM Tris/HCl pH 8.0

0 M to 1 M NaCl

Column cleaning buffer

20 mM Tris/HCl pH 8.0

1 M NaCl

Column storage buffer

20% ethanol

0.2 M CH_3COONa

6.1.7.4.3. Gel Filtration

Equilibration/Wash buffer

20 mM Tris/HCl pH 8.0

Elution buffer

20 mM Tris/HCl pH 8.0

0 mM and 200 mM NaCl

Column rinsing buffer

20 mM Tris/HCl pH 8.0

1M NaCl

Column storage solution

20% ethanol

6.1.7.4.4. His-tag purification

Equilibration/Wash buffer

50 mM sodium phosphate buffer pH 7.5

500 mM NaCl

Elution buffer

50 mM sodium phosphate buffer pH 7.5

500 mM NaCl

300 mM Imidazole

Column cleaning buffer

20% ethanol

Column storage solution

20% ethanol

6.1.7.5. SDS-Polyacrylamide gel electrophoresis

4 x Upper Tris

0.5 M Tris-HCl pH 6.8

0.4% (w/v) SDS

4 x Lower Tris

1.5 M Tris-HCl pH 8.0

0.4% (w/v) SDS

APS

10% (w/v) ammonium persulfate solution in dest. water

Acrylamide solution

30% (w/v) acrylamide-, bisacrylamide solution (37.5:1)

Stacking gel

1 ml 4 x Upper Tris

520 µL acrylamide solution

2.47 ml dest. water

40 µL APS

4 µL TEMED

Resolving gel

2 ml 4 x Lower Tris

3.33 ml acrylamide solution

2.67 ml dest. water

40 µL APS

4 µL TEMED

SDS-Loading buffer

20% (w/v) glycerol

6% (w/v) 2-mercaptoethanol

0.0025% (w/v) bromophenol blue

Filled with 1 x Upper Tris

10 x SDS-Running buffer

30.3 g Tris

144 g glycerol

10 g SDS

Filled with dest. water, pH adjusted to 8.4

Protein marker

RotiMark® Standard from Roth (molecular weight from 14 to 200 kDa)

Low range marker from Sigma (molecular weight from 6.5 to 66 kDa)

6.1.7.6. Coomassie blue staining of SDS-Polyacrylamide gels

Staining solution

0.1% (w/v) Coomassie Brilliant Blue G250

30% (v/v) ethanol

10% (v/v) acetic acid

Filled with dest. water

Destaining solution

30% (v/v) methanol

10% (v/v) acetic acid

Filled with dest. water

6.1.7.7. Activity assays

6.1.7.7.1. Esterase activity staining for SDS polyacrylamide gel

Renaturation solution

100 mM Tris buffer pH 7.5

0.5% (v/v) Triton X-100

Solution A

8 mg α-naphthyl acetate

2 ml acetone

18 ml 50 mM sodium phosphate buffer pH 7.4

Solution B

20 mg Fast Red TR

20 ml 50 mM sodium phosphate buffer pH 7.4

6.1.7.7.2. Overlay assay for esterase activity

10 ml 0.5% (w/v) agarose solution (in water)

160 µL Fast Red solution (80 mg/ml in DMSO)

80 µL α-naphthyl acetate solution (40 mg/ml in DMF)

6.1.7.7.3. Overlay assay for amidase activity

10 ml 0.5% (w/v) agarose solution (in water)

100 µL Fast Blue solution (89 mg/ml in DMSO)

80 µL N-acetyl-aminonaphthalene solution (40 mg/ml in DMF)

6.1.7.7.4. pNPA assay

50 mM sodium phosphate buffer pH 7.4

*p*NP solution (10 mM in DMSO)

*p*NPA solution (10 mM in DMSO)

Enzyme solution

6.1.7.7.5. pH assay for esterase activity screening in MTPs

Screening wells

20 µL substrate (**Et-3-PB**, **Et-2-PB** or **Et-2-PP**) stock solution (200 mM in DMSO)

5 µL BTB solution (16 mM in 16% ethanol)

30 µL esterase solution in sodium phosphate buffer with/without glycerol

145 µL 5 mM sodium phosphate buffer pH 7.4

Positive control

20 µL acids (**3-PBA**, **2-PBA** or **2-PPA**) stock solution (10-200 mM in DMSO)

5 µL BTB solution

145 µL 5 mM sodium phosphate buffer pH 7.4

Negative control

5 µL BTB solution

5 mM sodium phosphate buffer pH 7.4

6.1.7.7.6. Enantioselectivity screening with p-nitrophenyl-3-phenylbutanoates

100 µl 50 mM sodium phosphate buffer pH 7.4

30 µl (*R*)/(*S*)-*p*-nitrophenyl-3-phenylbutanoate solution (1 mM in acetonitrile)

30 µl enzyme solution

6.1.7.8. Biocatalysis

50 mM sodium phosphate buffer pH 7.4

20-40 mM substrate

0-10% DMSO or 10 mg/ml β-cyclodextrin

6.1.7.9. TLC detection

Cer-reagent

2.5% (w/v) $H_3[P(Mo_3O_{10})_4]$ x H_2O

1% (w/v) $Cer(SO_4)_2$

8% (v/v) conc. H_2SO_4

Filled with dest. water and filtered

6.1.8. Equipment

Autoclave	V-120, Systec (Wettenberg)
Balances	R180D and AC120S, Sartorius (Göttingen)
Centrifuges	Multifuge 3 S-R, Labofuge 4000R, Biofuge fresco and Biofuge pico, Heraeus (Hanau)
Crystallization robot	HTPC, CyBio (Jena)
DNA-electrophoresis	Sub-Cell® G and Mini-Sub Cell® GT, BioRad (Munich) Power supply unit: EPS 301, Amersham Pharmacia Biotech (Uppsala, Sweden)
Electroporator	MicroPulser, BioRad (Munich)
Flow cytometer	Partec CyFlow®Space flow cytometer with cell sorter, Partec GmbH (Münster)
Fluorimeter	Varioskan, Thermo Electron (Langenselbold)
GC	GC-14A, Shimadzu (Duisburg) GC-2010, Shimadzu (Duisburg) GC-MS-QP2010, Shimadzu (Duisburg)
HPLC	Hitachi Elite LaCrom, Hitachi High Technologies America (San Jose, USA)
Incubator	Friocell and Incucell, MMM Medcenter-Einrichtungen GmbH (Gräfelfing)
Incubation shakers	Incubator noctua IH50, shaker noctua K15/500, Noctua GmbH (Mössingen) Unitron, Infors AG (Bottmingen, Switzerland)
Lyophilisator	Alpha 1-2, Christ GmbH (Osterode am Harz)
Magnetic stirrer	IKAMAG® safety control, IKA Labortechnik (Staufen)

Microbiological cabinets	HeraSafe KS15, Thermo Electron (Langenselbold)
pH-meter	Microprocessor HI 9321, Hanna Instruments (Kehl am Rhein)
Protein electrophoresis	Minigel-Twin, Biometra GmbH (Göttingen) Power supply unit: EPS 301, Amersham Pharmacia Biotech (Uppsala, Sweden)
Rotating evaporators	Laborota 4000, Heidolph (Kehlheim) Vacuum pump system, Vaccubrand (Wertheim)
Speed Vac	Thermo Fischer Scientific (Langensenbold)
Thermocyclers	T-Personal, Biometra GmbH (Göttingen) Touchgene Gradient, Techne (Cambridge, UK)
Thermomixer	Thermomixer comfort, Eppendorf (Hamburg)
TLC	Färbekasten nach Hellendahl (85x35x95 mm), Roth (Karlsruhe)
Ultrasonic apparatus	Sonoplus HD2070 and UW2070, Bandelin (Berlin)
UV-VIS spectrophotometer	UVmini 1240, Shimadzu (Duisburg)
Vortexer	Vortex-Genie® 2, Scientific Industries (Bohemia, NY, USA)

6.1.9. Special computer programs

Both, the analysis of nucleotide sequences and the *in silico* cloning experiments were performed with the help of VectorNTI® from Invitrogen. The analysis of protein structures and interactions substrate-protein was carried out with PyMol[243] (www.pymol.org).

6.2. Methods

6.2.1. Microbiological methods

6.2.1.1. Conservation of E. coli strains and clones

All *E. coli* strains and clones were conserved as 40% glycerol stock at -80°C for long term storage. The different clones were stored streaked on agar plates at 4°C for short

term storage. Every two weeks the correspondent competent cells were transformed with the appropriate DNA and new agar plates were streaked.

6.2.1.2. Overnight culture

Either 3 ml or 5 ml sterile LB medium in cultivation tubes was supplemented if needed with antibiotics and inoculated with a single colony. The culture was incubated at 30°C or 37°C and 200 rpm overnight.

6.2.1.3. Protein expression

6.2.1.3.1. Expression of PFEI mutants in MTP-scale

The clones which grew on LB-Amp agar plates after *in vivo* selection and cell sorting were transferred to 96-well plates supplemented with 180 µl LB-Amp medium and incubated overnight at 37°C and 200 rpm. After incubation overnight, mutants were grown in microtiter plates by adding 50 µl of cell culture to 150 µl of fresh LB-Amp medium. After 4 h incubation at 37°C at 200 rpm protein expression was induced by adding 20 µl of a L-rhamnose solution (1% w/v). Cells were incubated for additional 16 h at 30°C and 200 rpm and then centrifuged for 45 min and 1935 x g. The pellet was resuspended in 100 µl 50 mM sodium phosphate puffer pH 7.4 containing 1% v/v BugBuster™ (Novagen), and DNase (1 U/ml) was added to each well and incubated for 1 h at 37°C and 200 rpm. Soluble fraction and pellet were separated by centrifugation for 45 min at 1935 x g and 4°C.

6.2.1.3.2. Protein expression in flasks

For expression of the esterases used, different volumes of LB medium (10-500 ml) supplemented with the appropriate antibiotics were inoculated with 0.1% (v/v) overnight culture. The culture was incubated at 37°C and 200 rpm and bacterial growth was monitored by periodic determination of the optical density at 600 nm. When the culture had reached OD_{600nm} = 0.5-0.7 protein expression was induced by addition of either 0.2% L-rhamnose or 0.1 mM IPTG (final concentration). Samples were taken before the induction as well as at different time intervals after it, in order to analyze the expression course. Sample volume was normalized to 2 ml with OD_{600nm} = 1. Cells were washed

twice with 50 mM sodium phosphate buffer pH 7.4 and resuspended in 200 µL of the same buffer. Cell lysis was carried out by sonication (1 min at 30% power, or 10 sec at 50% power) and the pellet was separated from the soluble fraction by centrifugation for 10 min at 16000 x g and 4°C.When cultures of higher volume were prepared (300-500 ml), cell lysis was performed by sonication for 10 to 20 min at 50% power. Pellet was separated from soluble fraction by centrifugation for 30 min at 4500 x g and 4°C.

6.2.1.4. Growth/toxicity assays

6.2.1.4.1. Growth/toxicity assays in MTP-scale

Each well was filled with 250 µL of cultivation medium and inoculated with 2 µL overnight culture. Triplicates of each sample were prepared. Two wells were inoculated and the non-inoculated well was used as control for culture contamination. The peripheral wells of each MTP were filled with 200 µL of 50 mM sodium phosphate buffer pH 7.4 in order to prevent evaporation. The MTPs were incubated at 30°C or 37°C and 200 rpm in a plastic box with wet tissues to generate a water saturated atmosphere. Bacterial growth was monitored by measuring the OD_{600nm} at different intervals. The substances used and their concentrations are summarized in Table 6-6 and Table 6-7.

Table 6-6. Substances used and their concentration in media for growth assays in MTPs.

Substance	Concentration (mM)
Glucose	5-30
Glycerol	5-30
1a	5-300

Table 6-7. Substances used and their concentration in media for toxicity assays in MTPs.

Cosolvent	Concentration (%)	Substance	Concentration (mM)
Acetonitrile	1-20	**3-PBA**	0.6-60
Isopropanol	1-20	**2b**	0.4-40
Ethanol	1-20	**3a**	$1.5\ 10^{-4}$-0.15
DMSO	1-20	**3b**	0.1-1
DMF	1-20	**4a**	1.3-130
THF	1-20	**4b**	2-450
Dioxane	1-20	**5a**	0.46-46
		5b	2-20
		6a	0.23-230
		7a	0.24-240

6.2.1.4.2. Growth/toxicity assays in flasks

For growth and viability assays in 100 ml flasks, 10 ml of M9 minimal medium supplemented with the correspondent substances were incubated at 30°C or 37°C and 200 rpm. Bacterial growth was monitored either by measuring the OD_{600nm} at different intervals or by cell counting and cell vitality analysis using the Partec CyFlow® Space flow cytometer (Partec GmbH, Münster). The substances used and their concentration are summarized in Table 6-8 and Table 6-9.

Table 6-8. Substances used and their concentration in media for growth assays in flasks.

Substance	Concentration (mM)
Glucose	5-30
Glycerol	5-30
1a	5-300
β-cyclodextrin	$9\ 10^{-4}$-$9\ 10^{-3}$

Table 6-9. Substances used and their concentration in media for toxicity assays in flasks.

Substance	Concentration (mM)
5a	1-20
5b	5-40
8a	20-100
8b	20-80
9a	20-100
9b	20-80

6.2.1.5. In vivo selection

6.2.1.5.1. Pseudo-selection media in MTP-scale

192-194 µL M9 minimal medium

2 µL 20% L-rhamnose solution

2 µL *E. coli* culture after enzyme expression

2-4 µL **2b**/**3b**[a] solution in ethanol (1-20 mM **2b**, 0.2-0.7 mM **3b,** final conc.)

[a]when pseudo-selection medium contained **3b**, M9 minimal medium was supplemented with 5 mM **2a**.

Triplicates were made, positive control (M9 minimal medium +5 mM **2a**) and negative control (M9 minimal medium + 5 mM **2a** and 5 µM **3a**) were present in each MTP. Bacterial growth was monitored by determination of OD_{600nm} at different times using the correspondent well before inoculation as blank value.

6.2.1.5.2. Pseudo-selection media in cultivation tubes

865-885 µL M9 minimal medium

5-40 µL **2b**/**5b**[a] solution in ethanol (stock solution 1 M)

100 µL β-cyclodextrin solution in M9 minimal medium (10 mg/ml final conc.)

10 µL *E. coli* culture after esterase expression washed and resuspended in M9 minimal medium at OD = 10 (OD = 0.1 in the cultivation tube)

[a]pseudo-selection medium with substrate **5b** was supplemented with 5 mM **2a**

Positive control (M9 minimal medium + 5 mM **2a**) and negative control (M9 minimal medium + 10 mM **5a**) were present in each experiment and parallel analyzed. Cell growth and cell viability was analyzed by flow cytometry.

6.2.1.5.3. Selection and anti-selection media

Experiments with selection and anti-selection media were performed in cultivation tubes with 1 ml culture volume.

865 µL M9 minimal medium

20 µL (*S*)-**5b** and 5 µL (*R*)-**2b** solutions in ethanol (1 M) in selection medium

20 µL (*R*)-**5b** and 5 µL (*S*)-**2b** solution in ethanol (1 M) in anti-selection medium

100 µL β-cyclodextrin solution (10 mg/ml final conc.)

10 µL *E. coli* cells after esterase expression in LB medium, washed and resuspended in M9 minimal medium at OD = 10 (OD = 0.1 in selection and anti-selecion medium)
Cultures were inoculated with an *E. coli* culture after esterase expression for 10-16 hours at 30°C and incubated at 30°C and 200 rpm in selection and anti-selection medium. Samples were taken after different times and cell viability was analyzed via flow cytometry. Parallel to the selection experiments, positive (5 mM **2a**) and negative (5 mM **2a**, 10 mM **5a**) control cultures were inoculated and analyzed.

6.2.1.6. Flow cytometer analysis and cell sorting

6.2.1.6.1. Cell counting

Aliquots of 10 µL were removed from the cultures after different time periods. Syto9 (5 µM final conc.) was added to stain bacterial DNA and the mixture was incubated for 10-30 min at 30°C. The sample was diluted by addition of 990 µL 50 mM sodium phosphate buffer (pH 7.5, sterile filtered) and after mixing thoroughly, cell counting was performed setting green fluorescence (FL1) as trigger factor for analysis.

6.2.1.6.2. Cell viability analysis and cell sorting

Aliquots of 10 µL were removed at different time periods from the cultures. PI (1 µg/ml final conc.) and Syto9 (5 µM final conc.) were added and the mixture was incubated at 30°C for 10-30 min.[254] Analysis parameters were optimized to minimize the interference of background signal and to obtain optimal separation of living and death cells signals, and between these and the background, in the two parameter histograms (Table 6-10 and Table 6-11). Living cells were sorted out and grown on LB-Kan agar plates.

Table 6-10. Analysis parameters used in cell viability analysis by Syto9/PI staining.

Parameter	Gain	Log	Lower limit	Upper limit
FSC	125	log3	80	999.9
SSC	230	log3	10	999.9
FL1	300	log4	10	999.9
FL2	400	log4	10	999.9

Table 6-11. Compensation settings for minimization of signal crossover.

	FSC	SSC	FL1	FL2	IC
FSC	-	-	-	-	-
SSC	-	-	-	-	-
FL1	-	-	-	8.0	0.1
FL2	-	-	402.2	-	0.9

6.2.2. Molecular biology methods

6.2.2.1. Plasmid isolation

For plasmid isolation from *E. coli* cultures the GeneJET™ Plasmid Miniprep Kit from Fermentas was used. For this aim 5 ml overnight cultures were used and the protocol described by Fermentas was followed.

http://www.fermentas.com/profiles/kits/pdf/coa_k0502.pdf

The elution of plasmid DNA was performed with 50 µL of elution buffer previously warmed up to 95°C and cooled down to 70°C.

6.2.2.2. Polymersase Chain Reaction

6.2.2.2.1. Site directed mutagenesis (QuikChange™)

This reaction was performed to modify the pET28a vector. The restriction site *NcoI* was substituted by *NdeI* in order to clone the BS2 gene in this vector without N-terminal His_6-tag. For this aim, the protocol described in the QuikChange™ Site-Directed Mutagenesis Kit from Stratagene was followed.

http://www.stratagene.com/manuals/200508.pdf

PCR mixture (50 µL)

5 µL 10 x PCR buffer

0.5 µL template (14 ng DNA)

1.5 µL primers (15 pmol each)

1 µL dNTPs

1 µL *Pfu* Turbo (1U, Invitrogen)

39.5 µL milliQ water

Table 6-12. Temperature programm for the site-directed mutagenesis reaction.

Cycle number	Step	Temperature (°C)	Time
1	Denaturation	95	1 min
2-19	Denaturation	95	50 sec
	Annealing	55.3-67.2[a]	50 sec
	Elongation	72	6 min
20	Final Extension	72	7 min

[a] annealing temperatures tested: 55.3, 57.8, 60.4, 62.8, 65.5 and 67.2°C.

As control, 10 µL of the reaction mixture were analyzed by electrophoresis in 1% agarose. The PCR product was directly transformed into electro-competent *E. coli* DH5α cells by electroporation.

6.2.2.2.2. Colony PCR

This reaction was used either as control of the ligation processes (in order to differentiate between religated and gene-containing plasmids) or for identification of the clones sorted out by flow cytometry during validation of the *in vivo* selection system. At least 20 colonies were analyzed each time.

PCR mixture (5 µl)

0.5 µL 10 x PCR buffer

0.07 µL primers (0.7 pmol each)

0.15 µL DMSO

0.1 µL dNTPs

0.05 µL *Taq* polymerase

4.06 µL milliQ water

Colonies were picked with a tooth pick and added separately to the reaction microtubes mixing thoroughly.

Table 6-13. Temperature program for the colony PCR.

Cycle number	Step	Temperature (°C)	Time
1	Denaturation	95	3 min
2-6	Denaturation	95	45 sec
	Annealing	55	30 sec
	Elongation	72	1 min/ kb
7-32	Denaturation	95	45 sec
	Annealing	50	30 sec
	Elongation	72	1 min/ kb
33	Final Extension	72	7 min

The reaction products were afterwards analyzed by electrophoresis using 1% agarose.

6.2.2.3. Digestion

The restriction enzymes used and their recognition sequence are summarized in Table 6-14. The digestion time varied from 2 hours for standard restriction enzymes to 10-20 min for Fast Digest® restriction enzymes from Fermentas.
http://www.fermentas.com/fastdigest/index.html

Table 6-14. List of restriction enzymes used and their recognition sequence. The restriction site is indicated with a vertical arrow.

Restriction enzyme	Specifity 5´→ 3´
*Nde*I	G↓GATCC
*Bam*HI	A↓AGCTT
*Hind*III	CA↓TATG

Digestion mixture (20 µL)

2 µL 10 x digestion buffer

8-15 µL DNA

2 µL *Nde*I

1 µL *Bam*HI / *Hind*III

7-0 µL milliQ water

6.2.2.4. Agarose gel electrophoresis

The agarose solution in buffer is heated until it becomes fluid. Ethidium bromide solution is added after the solution cools down to 40-50°C. This solution is poured into a gel form and it solidifies at RT for around 20 min. The solid gel is introduced in an electrophoresis chamber filled with 1 x TAE buffer and the DNA samples previously mixed with loading buffer are loaded. An electric current of 85 V is applied and the electrophoresis is performed until the bromophenol blue has covered 2/3 of the gel. The DNA fragments can be visualized with UV light. The DNA size and quantity can be estimated with the help of DNA markers.

6.2.2.5. Purification of DNA from agarose gels

In order to purify the DNA after agarose gel electrophoresis, the band of interest was extracted from the gel and the QIAquick® Gel Extraction Kit (Qiagen, Hilden) was used according to user´s manual.
http://www1.qiagen.com/Products/DnaCleanup/GelPcrSiCleanupSystems/QIAquickGelExtractionKit.aspx

6.2.2.6. Ligation

Insert and vector were previously digested with the appropriate restriction enzymes in order to generate compatible ends. The ligation was catalyzed by T4 DNA Ligase.

Ligation mixture (20 µL)
2 µL 10 x ligation buffer
2 µL ligase
10-13 µL insert
6-3 µL vector

Vector and insert were added in molar concentration ratios of 1:3 and 1:5. The reaction mixture was incubated 16 hours at 16°C or 2 hours at RT. Afterwards the reaction product was immediately transformed in competent *E. coli* cells.

6.2.2.7. Preparation of competent cells

6.2.2.7.1. Chemically competent E. coli cells

The rubidium chloride method[255] was used for the preparation of chemically competent *E. coli* cells. LB medium (100 ml) was inoculated with an overnight culture and incubated at 37°C and 200 rpm until the culture had reached OD_{600nm} = 0.3-0.4. Cells were then harvested, chilled on ice for 15 min, and centrifuged at 4°C for 25 min at 4000 x g. The pellet was resuspended in 20 ml ice cold RF1 buffer, incubated at 4°C for 15 min and centrifugated at 4°C for 25 min at 4000 x g. The pellet was resuspended in 4 ml RF2 buffer, incubated at 4°C for 15 min and distributed in 50 µL aliquots. These aliquots were immediately frozen in dry ice and stored at -80°C.

6.2.2.7.2. Electro-competent E. coli cells

LB medium (500 ml) was inoculated with an overnight culture and incubated at 37°C and 200 rpm until the culture had reached OD_{600nm} = 0.3-0.4. Cells were harvested, chilled on ice for 15 min and centrifuged at 4000 x g for 20 min. The pellet was washed three times with 500 ml, 250 ml and 20 ml ice cold 10% glycerol solution in milliQ water. Finally the pellet was resuspended in 2 ml ice cold 10% glycerol solution in milliQ water and distributed in 50 µL aliquots. These aliquots were immediately frozen in dry ice and stored at -80°C.

6.2.2.8. Transformation

6.2.2.8.1. Transformation of chemically competent E. coli cells

To a 50 µL aliquot of *E. coli* cells, 1-10 µL DNA solution were added and the mixture was incubated for 30 min on ice. Cells were permeabilized by heat shock (30 sec at 42°C) and chilled on ice for 5-10 min. Next, 300 µL LB-SOC medium were added to the cells and incubated for 1-3 hours at 37°C and 200 rpm. Different volumes of the culture were platted on agar supplemented with an adequate antibiotic and incubated overnight at 37°C.

6.2.2.8.2. *Transformation of electro-competent E. coli cells*

To a 50 µL aliquot of *E. coli* cells, 0.1-1 µL DNA solution with low salt concentration was added. The mixture was incubated 1 min on ice and immediately transferred to an ice cold electroporation cuvette. Electroporation was performed for 5 ms at 2500 mV in a MicroPulser (BioRad). Right after the electronic impulse 1 ml LB-SOC medium was added to the cells. The mixture was incubated at 37°C and 200 rpm for 1-3 hours. Afterwards different volumes of the culture were platted on agar supplemented with the pertinent antibiotic and incubated overnight at 37°C.

6.2.3. Biochemical methods

6.2.3.1. SDS-PAGE

According to general procedure,[256] stacking and resolving gel were made and poured into the gel form. Soluble and insoluble fractions were always separately analyzed.

Soluble fraction: 10 µL samples were mixed with 5 µL loading buffer and heated at 95°C for 10 min. Samples containing the thermostable esterase PestE were heated for 1 hour.

Insoluble fraction: The pellet was resuspended with 500 µL 0.1% Triton X-100 solution and incubated at 37°C for 10 min. It was washed twice with 500 µL 50 mM sodium phosphate buffer (pH 7.4) and resuspended in 20 µL loading buffer. This mixture was heated at 95°C for 10 min. When samples containing the thermostable esterase PestE were analyzed, this mixture was heated for 1 hour.

The gels ran at 200 V until the bromophenol blue band had reached the front of the gel. The protein bands were visualized by Coomassie Brilliant Blue staining. Standards for protein size were present in all gels.

6.2.3.2. Coomassie staining

For visualization of the protein bands, SDS gels were soaked in Coomassie Brilliant Blue staining solution and incubated at RT for 30-60 min. Background and excess stain was then eluted soaking the gels two times in destaining solution for 30 min and overnight in dest. water.

6.2.3.3. SDS esterase activity staining

The esterase activity staining[257] is based on the esterase catalyzed hydrolysis of α-naphthylacetate to acetic acid and α-naphthol. The released α-naphthol conjugates with Fast Red forming a red azo dye. After SDS-PAGE, the resulting gel is incubated one hour in renaturation solution for protein refolding. Next, the gel is soaked in a 1:1 mixture of solutions A and B (see 6.1.7.7.1.) until red bands become visible.

6.2.3.4. Overlay activity assays

Overlay assays are used for fast identification of active clones on agar plates. First, the agar plate has to be replicated onto another agar plate containing inducer for the protein expression. The replica plate is incubated for several hours until colonies have grown.

6.2.3.4.1. Overlay assay for esterase activity

The agarose solution containing Fast Red and α-naphthylacetate is poured over the replica plate. Colonies presenting esterase activity will hydrolyze the α-naphthylacetate releasing α-naphthol which can, in combination with Fast Red, form a red azo compound which will stain the colonies differentiating them from the inactive ones (no esterase expression or expression of inactive esterase).

6.2.3.4.2. Overlay assay for amidase activity

The agarose solution containing Fast Blue and N-acetyl aminonaphthalene is poured over the replica plate. Colonies presenting amidase activity will hydrolyze the N-acetyl aminonaphthalene releasing aminonaphthol which can combine with Fast Blue forming a brownish azo dye which will stain the colonies differentiating them from the inactive ones.

6.2.3.5. Protein purification

6.2.3.5.1. Heat precipitation

After cell lysis by sonication in presence of 1U/ml DNase, the cell extract was heated at 80°C for 20 min. The precipitated proteins were separated by centrifugation at 4°C for 30 min at 4000 x g and the supernatant was used for further purification steps.

6.2.3.5.2. Anion exchange chromatography

Purification by anion exchange chromatography was performed on Q-Sepharose (GE Healthcare) on an "XK 16/20" column (17 ml volume, Amersham Pharmacia) in 20 mM Tris-HCl pH 8.0 with a gradient from 0 to 1 M NaCl. Qualitative *p*NPA in MTP was performed in order to identify the esterase containing fractions and these were collected and concentrated to 5 ml volume.

6.2.3.5.3. Gel filtration

The gel filtration chromatography was performed with a "HiLoad 16/60 Superdex 200 pg" column (120 ml volume, GE Healthcare) and 20 mM Tris, pH 8.0 as elution buffer. The column was charged with 5 ml protein solution and 1 ml fractions were eluted. The fractions active towards *p*NPA were collected again and concentrated by ultrafiltration to 32 mg/ml protein.

6.2.3.5.4. His-tag purification

The PFEI mutants selected and expressed in flasks were His-tag purified by Äkta purifier using 1 ml or 5ml IMAC SepharoseTM 6 Fast Flow columns (GE Healthcare). The protein was eluted from the column with sodium phosphate buffer (50 mM, pH = 7.5, 500 mM NaCl) containing 300 mM imidazol. To remove imidazol from the solution, the protein was desalted using a 60 ml Q-Sepharose (G-25) column.

6.2.3.6. Ultrafiltration

The ultrafiltration was performed with Centricon® Plus-20 centrifugal filter units with an Ultracel-PL membrane of 10 kDa-cut off (Millipore), which were used according to manufacturer´s instructions.

6.2.3.7. Determination of the protein content

The BC Assay: Protein Quantification Kit (Uptima Interchim) was used for determination of the protein content according to user's manual.
http://www.interchim.fr/ft/4/40840A.pdf

6.2.3.8. Protein crystallization

6.2.3.8.1. *Crystallization by sitting drop method*

The first screening for crystallization conditions was performed by this method in 96-well plates at 20°C. Each well contained a mixture of 0.3 µL protein solution (10 mg/ml) and 0.3 µL reservoir solution equilibrated against 40 µL reservoir solution.

6.2.3.8.2. *Crystallization by hanging drop method*

The best conditions obtained from the above described method were optimized by vapour diffusion in 24-well plates at 20°C, with 2 µL protein solution and 2 µL reservoir solution equilibrated against 500 µL reservoir solution.

6.2.3.9. pNPA assay

This assay, for the quantification of esterase activity in liquid medium, is based in the esterase catalyzed hydrolysis of *p*-nitrophenyl acetate to acetic acid and *p*-nitrophenol. At the neutral pH in which the assay is performed, *p*-nitrophenol is essentially ionized and its anion has yellow color which can be quantified photometrically at 410 nm. The amount of reactives required for assay in cuvette of in MTP-scale is summarized in Table 6-15.

Table 6-15. Composition of the *p*NPA performed in cuvette or in MTP-scale.

Components	µl in cuvette	µl in MTPs
Phosphate buffer	850	180
pNPA solution (10 mM DMSO)	100	15
Protein solution	50	5

Absorbance at 410 nm is monitored for 60 sec and the hydrolytic activity towards *p*NPA can be calculated as:

Activity (U/ml) = [(Δabs/Δt)/ε]·dilution in cuvette or well·dilution of protein solution

For calculation of ε (extinction coefficient) a standard curve with 10 µL *p*-nitrophenol solution and 990 µL buffer is done representing Δabs/Δc (c: 0.1-0.02 mM). The slope of the line is the extinction coefficient.

The spontaneous *p*NPA hydrolysis (blank value) will be subtracted from Δabs/Δt.

Esterase activity can also be qualitatively detected observing which wells turn yellow within seconds.

6.2.3.10. pH assay for activity screening

This assay[220] was used in the screening of active esterases towards **Et-3-PB**, **Et-2-PB** and **Et-2-PP**. Each well contained 145 µl 5 mM sodium phosphate buffer pH 7.4, 20 µl substrate solution (200 mM in DMSO), 5 µl BTB solution and 30 µl enzyme solution. Positive and negative controls were present in each screening plate. Esterase activity was evidenced by color change from blue to yellow, this was evaluated after 24 and 48 hours of incubation at 30°C and 400 rpm in a thermomixer.

6.2.3.11. Enantioselectivity screening with p-nitrophenyl-3-phenylbutanoates

After cell harvest, two times 30 µl of each well were transferred into two microtiter plates each containing 100 µl 50 mM phosphate buffer pH 7.4. The activity of the mutants in both plates was measured by following the absorbance at 410 nm for 10 min after adding 30 µl substrate solution ((*R*)-or (*S*)-3-*p*-nitrophenyl-3-phenylbutanoate, 1 mM in acetonitrile). Afterwards the plates were incubated for an additional hour at 37°C and the absorbance was measured again as a one-point-measurement. Activity of mutants was

determined from the first 10 min for variants showing high activity and from initial absorbance and absorbance after 60 min for those showing low activities.

6.2.4. Biocatalysis

6.2.4.1. Biocatalysis in analytical scale

The enantioselectivity towards **Et-3-PB**, **Et-2-PB** and **Et-2-PP** of the esterases identified as active with the pH-assay was checked in 2 ml reaction microtubes. To a stirred solution of the ethyl esters (0.076 mmol of **Et-3-PB** or **Et-2-PB**, or 0.15 mmol of **Et-2-PP**) in 1.8 ml 50 mM sodium phosphate buffer pH 7.4, 200 µL enzyme solution or cell extract was added. The addition of 10% DMSO in order to increase enantioselectivity was checked in selected cases. Aliquots of 300 µL were taken after different reaction times, acidified with 1N HCl, extracted three times with diethyl ether and dried over sodium sulfate.

Biocatalysis in analytical scale was also performed with the pre-selection substrates **2b** and **5b**. To a stirred solution of **2b** or **5b** (0.08 mmol) in 1.8 ml 50 mM sodium phosphate buffer pH 7.4 with β-cyclodextrin (10 mg/ml) as cosolvent, 200 µL cell extract, purified enzyme or resting cells (OD = 10-20) were added. Aliquots of 300 µL were taken after different reaction time periods, acidified with 1N HCl, extracted three times with ethyl acetate and dried over sodium sulfate.

In both cases the organic layer was evaporated under N_2 atmosphere or in a Speed Vac (Thermo Fisher Scientific), and carboxylic acids were converted in their methyl esters to allow determination of enantiomeric excess of substrate and product in one run.

6.2.4.2. Biocatalysis in preparative scale

To a 40 mM solution (~1 g) of **Et-3-PB**, **Et-2-PB** or **Et-2-PP** in 50 mM sodium phosphate buffer pH 7.4, esterase (lyophilisate dissolved in buffer, comparable units to biocatalysis in analytical scale) was added. The reactions were performed in 500 ml Erlenmeyer flasks and incubated at 20°C and 250 rpm. Samples were taken after different times, acidified with 1N HCl, extracted with diethyl ether and analyzed by TLC in order to estimate the reaction conversion. When conversion was estimated to be 50% the reaction was stopped, acidified with 1 N HCl and extracted three times with diethyl ether. Substrate and product were purified through silica gel chromatography (*n*-hexane: ethyl

acetate, 5:1) and verified by ^{1}H-NMR. The enantiomeric excess was checked by HPLC (carboxylic acid) or gas chromatography (ethyl ester).

6.2.5. Chemical methods

6.2.5.1. Analytics

6.2.5.1.1. Chiral CG methods

Method 1:

T program 90°C, isotherm

Column Heptakis-(2,3-di-*O*-acetyl-6-*O*-*t*-butyldimethylsilyl)-β-cyclodextrin

Substances **Et-3-PB** and **Me-3-PB**

Method 2:

T program 70°C, isotherm

Column Heptakis-(2,6-*O*-di-*O*-methyl-3-*O*-pentyl)-β-cyclodextrin

Substances **Et-2-PB**, **Me-2-PB**, **Et-2-PP** and **Me-2-PP**

Method 3:

T program 90°C for 35 min. Increase in 2°C/min until 120°C for 60 min

Column Heptakis-(2,3-di-*O*-acetyl-6-*O*-*t*-butyldimethylsilyl)-β-cyclodextrin

Substance **2b** and **Me-3-PB**

Method 4:

T program 90°C for 35 min. Increase in 2°C/min until 125°C for 60 min

Column Heptakis-(2,3-di-*O*-acetyl-6-*O*-*t*-butyldimethylsilyl)-β-cyclodextrin

Substance **5b** and **Me-3-PB**

6.2.5.1.2. Chiral HPLC methods

Method 5:

Mobile phase *n*-hexane/isopropanol 97:3 for 30 min at RT

Column Chiracel OD-H 250 mm x 4.6 mm column

Substances **3-PBA**, **2-PBA** and **2-PPA**

6.2.5.1.3. Preparation of methyl esters from carboxylic acids

Samples taken from the biocatalysis, after extraction in organic solvent and evaporation of it, were resolved in 900 µL diethyl ether and 100 µL methanol. Addition of 20 µL TMS-diazomethane[258] and incubation at RT for 30 min in an open microtube was performed, for derivatization of carboxylic acids into their methyl esters. After this time, 40 µL glacial acetic acid were added and this mixture was incubated open at RT for another 30 min. The complete neutralization of TMS-diazomethane is evidenced by color change of the solution from yellow to colorless. The solvent is evaporated under nitrogen atmosphere or in a Speed Vac. A complete conversion of carboxylic acids into their methyl esters is expected.

6.2.5.2. Organic synthesis

6.2.5.2.1. Azeotropic esterification

The carboxylic acid (1 equiv.) was stirred with the alcohol (3 equiv.) at 110°C in toluene as solvent with some drops of sulfuric acid as catalyst. Water formed in the esterification reaction was removed by a Dean-stark trap until completion. Next, the solvent was evaporated and the product was purified by silica gel chromatography (*n*-pentane/ethyl acetate). This procedure was used for the preparation of the ethyl esters **Et-3-PB**, **Et-2-PB** and **Et-2-PP**. These compounds have been previously characterized.[259]

6.2.5.2.2. Deprotection of ***1b***

Strategy 1:[260] 50 mg **1b** (0.18 mmol) were stirred in 1 ml TFA solution (75% in water) at RT for 6 hours. The reaction product was further analyzed by TLC (hexane/ethyl acetate, 5:1) and it was observed that the ester bond had been hydrolyzed.

Strategy 2:[260] 20 mg **1b** (0.07 mmol) and 1 equiv. PPTS (12.4 mg) were stirred in methanol at RT. The reaction was supposed to be completed after 30 min, but no deprotection was observed by TLC analysis. Hence the mixture was stirred for 48 hours performing TLC analysis in between, but still no conversion of **1b** to **2b** occurred. The reaction was repeated with more substrate and 3 and 10 equiv. PPTS without success.

Strategy 3:[261] 100 mg **1b** (0.36 mmol) and 5% mol PTSA (~3 mg) were stirred in 2 ml acetone at RT for 36 hours. This strategy for the deprotection of **1b** also failed.

6.2.5.2.3. Esterification of acyl chloride

The carboxylic acids **3-PBA** and **2-PBA** were activated by forming its acyl chloride. For this aim, 1.5 equiv. of thionyl chloride was added drop by drop to 1 equiv. of the carboxylic acid solved in DCM at 4°C. The reaction was catalyzed with some drops of DMF. After addition of all components, the reaction mixture was stirred for two hours at RT and the product was purified by vacuum distillation. The yield of this reaction is quantitative.

The acyl chloride (1 equiv.) was solved in THF and added drop by drop to 2-3 equiv. of the correspondent alcohol (the excess will be higher if the alcohol presents multiple alcohol functions, in order to prevent poly-esterification) with THF as solvent and 10 equiv. of TEA to neutralize the HCl formed. The reaction mixture was stirred for two hours and a white precipitate was formed (triethylammonium chloride). After completion, the white precipitate was filtered, and the solid was washed with THF. After solvent evaporation, the reaction product was further purified by silica gel chromatography (*n*-pentane/ethyl acetate).

Following this procedurethe following products were obtained:

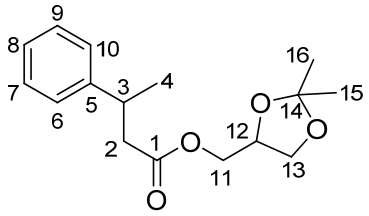

Product: **1b**, colorless oil.

Mass: 1.3 mg (4.8 mmol)

Yield: 40%

M.W. = 278.34

^{1}H-NMR ($CDCl_3$): δ 1.30 (d, J = 6.9 Hz, 3H, H-4); 1.35 (s, 3H, H-15 or H-16); 1.41 (s, 3H, H-15 or H-16); 2.57-2.69 (m, 2H, H-2); 3.25-3.31 (m, 1H, H-3); 3.57-3.61 (dd, J_1 = 6.15 Hz, J_2 = 2.38 Hz, 1H, H-13); 3.93-3.97 (dd, J_1 = 6.39 Hz, J_2 = 2.14 Hz, 1H, H-13); 4.01-4.12 (m, 2H, H-11); 4.16-4.22 (m, 1H, H-12); 7.18-7.31 (m, 5H, H-6/H-7/H-8/H-9/H-10).

^{13}C-NMR ($CDCl_3$): δ 21.9 (q, C-4); 25.4 (q, C-15 or C-16); 26.7 (q, C-15 or C-16); 36.5 (d, C-3); 42.7 (t, C-2); 64.4 (t, C-11); 66.3 (t, C-13); 73.5 (d, C-12);

109.7 (s, C-14); 126.5 & 126.7 & 128.5 (5 x d, C-6/C-7/C-8/C-9/C-10); 145.5 (s, C-5); 172.1 (s, C-1).

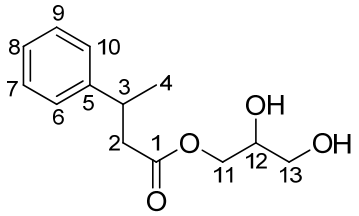

Product: **2b**, colorless oil.

Mass: up to 5 g (21 mmol)

Yield: 55-59%

M.W. = 238.28

m/z (%) = 118 (100); 105 (93); 91(16); 77 (15); 79 (12).

^{1}H-NMR ($CDCl_3$): δ 1.28 (d, *J* = 6.8 Hz, 3H, H-4); 2.54-2.67 (m, 2H, H-2); 3.19-3.31 (m, 1H, H-3); 3.37-3.41 (m, 1H, H-12); 3.51 (bs, 2H, H-13); 3.63 (bs, 1H, H-OH); 3.75 (bs, 1H, H-OH); 4.00 (d, *J* = 5.3 Hz, 2H, H-11); 7.15-7.30 (m, 5H, H-6/H-7/H-8/H-9/H-10).

^{13}C-NMR ($CDCl_3$): δ 21.8 (q, C-4); 36.4 (d, C-3); 42.5 (t, C-2); 63.1 (t, C-13); 64.8 (t, C-11); 69.9 (d, C-12); 126.4 & 126.6 & 128.4 (5 x d, C-6/C-7/C-8/C-9/C-10); 145.2 (s, C-5); 172.6 (s, C-1).

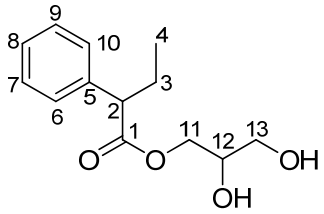

Product: **2c**, light yellow oil.

Mass: 1 g (4.2 mmol)

Yield: 59%

M.W.= 238.28

m/z (%) = 91 (100); 119 (62); 165 (12); 146 (11); 41 (10)

^{1}H-NMR ($CDCl_3$): δ 0.9 (t, *J* = 7.18 Hz, 3H, H-4); 1.75-1.89 (m, 1H, H-3); 2.04-2.18 (m, 1H, H-3); 2.27 (bs, 1H, H-OH); 2.56 (bs, 1H, H-OH); 3.41-3.48

(m, 1H, H-13); 3.52-3.59 (m, 1H, H-13); 3.49 (t, *J* = 7.55 Hz, 1H, H-2); 3.77-3.87 (m, 1H, H-12); 4.12-4.17 (m, 2H, H-11); 7.24-7.35 (m, 5H, H-6/H-7/H-8/H-9/H-10).

^{13}C-NMR ($CDCl_3$): δ 12.1 (q, C-4); 26.4 (t, C-3); 53.3 (d, C-2); 63.2 (t, C-13); 65.3 (t, C-11); 70.0 (d, C-12); 127.4 & 127.8 & 128.7 (5 x d, C-6/C-7/C-8/C-9/C-10); 138.7 (s, C-5); 174.5 (s, C-1).

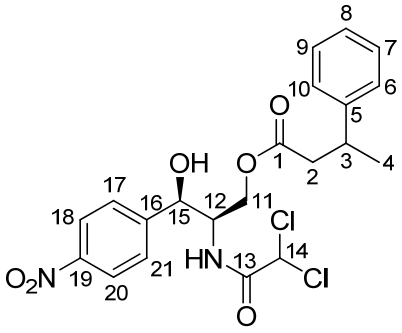

Product: **3b**, yellow oil.

Mass: 1.1 g (2.3 mmol)

Yield: 25%

M.W. = 469.32

^{1}H-NMR ($CDCl_3$): δ 1.32 (d, *J* = 6.9 Hz, 3H, H-4); 2.63-2.74 (m, 2H, H-2); 3.23-3.32 (m, 1H. H-3); 3.46 (s, 1H, H-OH); 3.98-4.02 (m, 1H, H-11); 4.16-4.24 (m, 1H, H-11); 4.33-4.38 (m, 1H, H-12); 4.45 (s, 1H, H-NH); 5.71 (s, 1H, H-14); 6.81 (d, *J* = 9.03 Hz, 1H, H-15); 7.09-7.28 (m, 5H, H-6/H-7/H-8/H-9/H-10); 7.39 (d, *J* = 8.66 Hz, 2H, H-17 & H-21); 8.15 (d, *J* = 8.79 Hz, 2H, H-18 & H-20).

^{13}C-NMR ($CDCl_3$): δ 22.3 (q, C-4); 36.9 (d, C-3); 42.7 (t, C-2); 54.0 (d, C-12); 62.0 (t, C-11); 66.0 (d, C-14); 69.8 (d, C-15); 123.5 (2 x d, C-18 & C-20); 126.6 & 126.7 & 126.8 (5 x d, C-6/C-7/C-8/C-9/C-10); 128.6 (2 x d, C-17 & C-21); 145.1 (s, C-19); 147.2 (s, C-5); 147.7 (s, C-16); 164.3 (s, C-13); 172.9 (s, C-1).

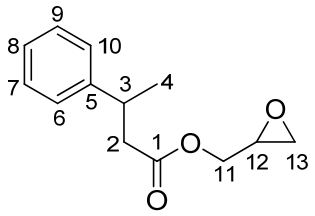

Product: **4b**, light yellow oil.

Mass: 800 mg (3.6 mmol)

Yield: 46%

M.W. = 220.26

m/z (%) = 118 (100); 105 (93); 121 (23), 91(16); 77 (15).

^{1}H-NMR ($CDCl_3$): δ 1.32 (d, J = 6.8 Hz, 3H, H-4); 2.52-2.72 (m, 2H, H-2); 2.76-2.81 (m, 1H. H-13); 3.07-3.15 (m, 1H, H-13); 3.23-3.35 (m, 1H, H-3); 3.84-3.91 (m, 1H, H-12); 4.31-4.37 (m, 2H, H-11); 7.17-7.33 (m, 5H, H-6/H-7/H-8/H-9/H-10).

^{13}C-NMR ($CDCl_3$): δ 21.9 (q, C-4); 36.5 (d, C-3); 42.7 (t, C-2); 44.6 (t, C-13); 49.3 (d, C-12); 64.8 (t, C-11); 126.5 & 126.8 & 128.5 (5 x d, C-6/C-7/C-8/C-9/C-10); 145.4 (s, C-5); 172.0 (s, C-1).

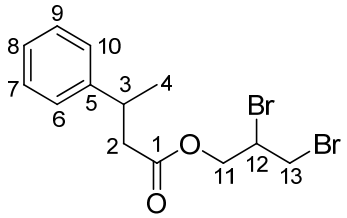

Product: **5b**, light yellow oil.

Mass: up to 7 g (19.2 mmol)

Yield: 70-80%

M.W. = 364.07

m/z (%) = 121 (100); 105 (84); 118 (55); 163 (44); 117 (18).

^{1}H-NMR (CDCl3): δ 1.33 (dd, J_1 = 0.8 Hz, J_2 = 7.1 Hz, 3H, H-4); 2.58-2.75 (m, 2H, H-2); 3.22-3.36 (m, 1H, H-3); 3.49-3.68 (m, 2H, H-13); 4.15-4.24 (m, 1H, H-12); 4.36-4.47 (m, 2H, H-11); 7.17-7.33 (m, 5H, H-6/H-7/H-8/H-9/H-10).

^{13}C-NMR ($CDCl_3$): δ 22.0 (q, C-4); 32.1 (d, C-3); 36.5 (t, C-2); 42.5 (t, C-13); 46.8 (d, C-12); 64.9 (t, C-11); 126.5 & 126.7 & 128.5 (5 x d, C-6/C-7/C-8/C-9/C-10); 145.2 (s, C-5); 171.5 (s, C-1).

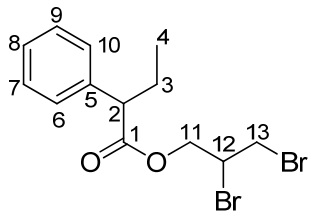

Product: **5c**, light yellow oil.

Mass: 1.6 g (4.4 mmol)

Yield: 58%

M.W.= 364.07

m/z (%) = 91 (100); 119 (82); 41 (14); 77 (8); 163 (6).

^{1}H-NMR ($CDCl_3$): δ 0.92 (t, *J* = 7.18 Hz, 3H, H-4); 1.77-1.92 (m, 1H, H-3); 2.07-2.21 (m, 1H, H-3); 3.49-3.55 (t, *J* = 7.55 Hz, 1H, H-2); 3.59-3.70 (m, 2H, H-13); 4.21-4.29 (m, 1H, H-12); 4.46-4.49 (m, 2H, H-11); 7.23-7.36 (m, 5H, H-6/H-7/H-8/H-9/H-10).

^{13}C-NMR ($CDCl_3$): δ 12.1 (q, C-4); 26.3 (t, C-3); 46.7 (t, C-13); 53.3 (d, C-2); 65.0 (d, C-12); 65.1 (t, C-11); 127.4 & 128.0 & 128.6 (5 x d, C-6/C-7/C-8/C-9/C-10); 138.5 (s, C-5); 173.2 (s, C-1).

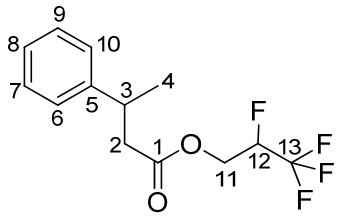

Product: **8b**, colorless oil.

Mass: 320 mg (1.1 mmol)

Yield: 55%

M.W. =278.24

m/z (%) = 105 (100); 118 (53); 51 (18); 77 (15); 278 (8).

^{1}H-NMR ($CDCl_3$): δ 1.31 (d, J = 7.18 Hz, 3H, H-4); 2.60-2.75 (m, 2H, H-2); 3.21-3.33 (m, 1H, H-3); 4.33-4.42 (m, 2H, H-11); 5.58 (dt, J_1 = 53.25, J_2 = 4.15, 1H, H-12); 7.18-7.32 (m, 5H, H-6/H-7/H-8/H-9/H-10).

^{13}C-NMR ($CDCl_3$): δ 21.8 (q, C-4); 36.5 (d, C-3); 42.2 (t, C-2); 59.4 (t, C-11); 109.0 (d, C-12); 115.65 (s, C-13); 126.6 & 128.6 & 129 (5 x d, C-6/C-7/C-8/C-9/C-10); 145 (s, C-5); 170.7 (s, C-1).

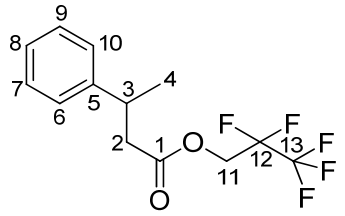

Product: **9b**, light red oil.

Mass: 173 mg (0.6 mmol)

Yield: 73%

M.W. = 296.23

m/z (%) = 105 (100); 118 (48); 77 (16); 296 (12); 239 (9).

^{1}H-NMR ($CDCl_3$): δ 1.31 (d, J = 6.80 Hz, 3H, H-4); 2.60-2.76 (m, 2H, H-2); 3.25-3.32 (m, 1H, H-3); 4.36-4.45 (m, 2H, H-11); 7.17-7.32 (m, 5H, H-6/H-7/H-8/H-9/H-10).

^{13}C-NMR ($CDCl_3$): δ 21.7 (q, C-4); 36.3 (d, C-3); 42.1 (t, C-2); 59.0 (t, C-11); 112.0 (s, C-12); 118.4 (s, C-13); 126.6 & 128.6 (5 x d, C-6/C-7/C-8/C-9/C-10); 145.0 (s, C-5); 170.6 (s, C-1).

Compounds (*R*)- and (*S*)-*p*-nitrophenyl-3-phenylbutanoate were synthesized by Anita Gollin. These substrates have been previously charachterized.[116]

7. LITERATURE

7. LITERATURE

1. Collet, A., Brienne, M.J. & Jacques, J. (**1980**). Optical resolution by direct crystallization of enantiomer mixtures. Chem. Rev. *80*, 215-230.

2. Mason, S. (**1986**). The origin of chirality in nature. Trends Pharmacol. Sci. *7*, 20-23.

3. Crossley, R. (**1992**). The relevance of chirality to the study of biological activity. Tetrahedron *48*, 8155-8178.

4. Teo, S.K., Colburn, W.A., Tracewell, W.G., Kook, K.A., Stirling, D.I., Jaworsky, M.S., Scheffler, M.A., Thomas, S.D. & Laskin, O.L. (**2004**). Clinical pharmacokinetics of thalidomide. Clin. Pharmacokinet.*43*, 311-327.

5. Ariëns, E.J., Soudijn, W. & Timmermans, P.B. Stereochemistry and biological activity of drugs. Blackwell Scientific Publishers: Oxford, **1983**.

6. Ariëns, E.J. (**1984**). Stereochemistry, a basis for sophisticated nonsense in pharmacokinetics and clinical pharmacology. Eur. J. Clin. Pharmacol. *26*, 663-668.

7. FDA (**1992**). FDA's policy statement for the development of new stereoisomeric drugs. Chirality *4*, 338.

8. Ströng, M. (**1999**). FDA policy and regulation of stereoisomers: paradigm shift and the future of safer, more effective drugs. Food Drug Law J. *54*, 463.

9. Noorduin, W.L., Kaptein, B., Meekes, H., van Enckevort, W.J.P., Kellogg, R.M. & Vlieg, E. (**2009**). Fast attrition-enhanced deracemization of naproxen by a gradual in situ feed. Angew. Chem. Int. Ed. *48*, 4581-4583.

10. Faber, K. Biotransformations in Organic Chemistry. Springer Verlag: Berlin, **2004**.

11. Fernández-Álvaro, E., Kourist, R., Winter, J., Böttcher, D., Liebeton, K., Naumer, C., Eck, J., Leggewie, C., Jaeger, K.E. & Streit, W. (**2010**). Enantioselective kinetic resolution of phenylalkyl carboxylic acids using metagenome-derived esterases. Microb. Biotechnol. *3*, 59-64.

12. Hoyos, P., Fernández, M., Sinisterra, J.V. & Alcántara, A.R. (**2006**). Dynamic kinetic resolution of benzoins by lipase- metal combo catalysis. J. Org. Chem. *71*, 7632-7637.

13. Brüsehaber, E., Böttcher, D., Liebeton, K., Eck, J., Naumer, C. & Bornscheuer, U.T. (**2008**). Asymmetric synthesis of cis-3,5-diacetoxycyclopent-1-ene using metagenome-derived hydrolases. Tetrahedron: Asymmetry *19*, 730-732.

14. Domínguez de Maria, P., Kossmann, B., Potgrave, N., Buchholz, S., Trauthwein, H., May, O. & Groger, H. (**2005**). Improved process for the enantioselective hydrolysis of prochiral diethyl malonates catalyzed by pig liver esterase. Synlett, 1746-1748.

15. Sun, X.F., Zhou, L., Wang, C.J. & Zhang, X.M. (**2007**). Rh-catalyzed highly enantioselective synthesis of 3-arylbutanoic acids. Angew. Chem. Int. Ed. *46*, 2623-2626.

16. Nozaki, H., Moriuti, S., Takaya, H. & Noyori, R. (**1966**). Asymmetric induction in carbenoid reaction by means of a dissymmetric copper chelate. Tetrahedron Lett. *7*, 5239-5244.

17. Akutagawa, S. (**1997**). Enantioselective isomerization of allylamine to enamine: practical asymmetric synthesis of (–)-menthol by Rh–BINAP catalysts. Top. Catal. *4*, 271-274.

18. Burgess, K., Lim, H.J., Porte, A.M. & Sulikowski, G.A. (**1996**). New catalysts and conditions for a CH insertion reaction identified by high throughput catalyst screening. Angew. Chem. Int. Ed. *35*, 220-222.

19. Cole, B.M., Shimizu, K.D., Krueger, C.A., Harrity, J.P.A., Snapper, M.L. & Hoveyda, A.H. (**2003**). Discovery of chiral catalysts through ligand diversity: Ti-catalyzed enantioselective addition of TMSCN to meso epoxides. Angew. Chem. Int. Ed. *35*, 1668-1671.

20. Francis, M.B. & Jacobsen, E.N. (**1999**). Discovery of novel catalysts for alkene epoxidation from metal-binding combinatorial libraries. Angew. Chem. Int. Ed. *38*, 937-941.

21. Cole-Hamilton, D.J. (**2003**). Homogeneous catalysis-New approaches to catalyst separation, recovery, and recycling. Science *299*, 1702-1706.

22. Dalko, P.I. & Moisan, L. (**2004**). In the golden age of organocatalysis. Angew. Chem. Int. Ed. *43*, 5138-5175.

23. Westermann, B. (**2003**). Asymmetric catalytic aza-Henry reactions leading to 1, 2-diamines and 1, 2-diaminocarboxylic acids. Angew. Chem. Int. Ed. *42*, 151-153.

24. Eder, U., Sauer, G. & Wiechert, R. (**1971**). New type of asymmetric cyclization to optically active steroid CD partial structures. Angew. Chem. Int. Ed. *10*, 496-497.

25. Hajos, Z.G. & Parrish, D.R. (**1974**). Asymmetric synthesis of bicyclic intermediates of natural product chemistry. J. Org. Chem. *39*, 1615-1621.

26. List, B. (**2000**). The direct catalytic asymmetric three-component Mannich reaction. J. Am. Chem. Soc. *122*, 9336-9337.

27. Notz, W. & List, B. (**2000**). Catalytic asymmetric synthesis of anti-1, 2-diols. J. Am. Chem. Soc. *122*, 7386-7387.

28. Reetz, M.T., List, B., Jaroch, S. & Weinmann, H. Organocatalysis. Springer Verlag: Berlin, **2008**.

29. Bornscheuer, U.T. & Buchholz, K. (**2005**). Highlights in biocatalysis-Historical landmarks and current trends. Eng. Life Sci. *5*, 309-323.

30. Bornscheuer, U.T. Trends and challenges in enzyme technology, in Advances in biochemical engineering/biotechnology, *vol. 100*, 181-203. Springer Verlag: Berlin, **2005**.

31. Patel, R.N. (**2008**). Synthesis of chiral pharmaceutical intermediates by biocatalysis. Coord. Chem. Rev. *252*, 659-701.

32. Schoemaker, H.E., Mink, D. & Wubbolts, M.G. (**2003**). Dispelling the myths-Biocatalysis in industrial synthesis. Science *299*, 1694-1697.

33. Hanson, R.L., Goldberg, S.L., Brzozowski, D.B., Tully, T.P., Cazzulino, D., Parker, W.L., Lyngberg, O.K., Vu, T.C., Wong, M.K. & Patel, R.N. (**2007**). Preparation of an amino acid intermediate for the dipeptidyl peptidase IV inhibitor, saxagliptin, using a modified phenylalanine dehydrogenase. Adv. Synth. Catal. *349*, 1369-1378.

34. Gill, I. & Patel, R. (**2006**). Biocatalytic ammonolysis of (5S)-4, 5-dihydro-1H-pyrrole-1, 5-dicarboxylic acid, 1-(1, 1-dimethylethyl)-5-ethyl ester: preparation of an intermediate to the dipeptidyl peptidase IV inhibitor Saxagliptin. Bioorg. Med. Chem. Lett. *16*, 705-709.

35. Patel, R.N., Chu, L. & Mueller, R. (**2003**). Diastereoselective microbial reduction of (S)-[3-chloro-2-oxo-1-(phenylmethyl) propyl] carbamic acid, 1, 1-dimethylethyl ester. Tetrahedron: Asymmetry *14*, 3105-3109.

36. Mahmoudian, M. & Dawson, M.J. Biotechnology of antibiotics. Marcel Dekker Inc.: New York, **1997**.

37. Münzer, D.F., Meinhold, P., Peters, M.W., Feichtenhofer, S., Griengl, H., Arnold, F.H., Glieder, A. & Raadt, A. (**2005**). Stereoselective hydroxylation of an achiral cyclopentanecarboxylic acid derivative using engineered P450s BM-3. Chem. Commun. 2597-2599.

38. Hanson, R.L., Wasylyk, J.M. & Nanduri, V.B. (**1994**). Site specific enzymatic hydrolysis of taxanes at C-10 and C-13. J. Biol. Chem. *269*, 22145-22149.

39. Nanduri, V.B., Hanson, R.L., LaPorte, T.L., Ko, R.Y., Patel, R.N. & Szarka, L.J. (**2004**). Fermentation and isolation of C10-deacetylase for the production of 10-deacetylbaccatin III from baccatin III. Biotechnol. Bioeng. *48*, 547-550.

40. Patel, R., Banerjee, A., Ko, R., Howell, J., Li, W., Comezoglu, F., Partyka, R. & Szarka, F. (**1994**). Enzymic preparation of (3*R*-cis)-3-(acetyloxy)-4-phenyl-2-azetidinone: a taxol side-chain synthon. Biotechnol. Appl. Biochem. *20*, 23-33.

41. Feske, B.D., Kaluzna, I.A. & Stewart, J.D. (**2005**). Enantiodivergent, biocatalytic routes to both taxol side chain antipodes. J. Org. Chem. *70*, 9654-9657.

42. Phillips, R.S. (**1992**). Temperature effects on stereochemistry of enzymatic reactions. Enzyme Microb. Technol. *14*, 417-419.

43. Ottosson, J., Fransson, L. & Hult, K. (**2002**). Substrate entropy in enzyme enantioselectivity: an experimental and molecular modeling study of a lipase. Protein Sci. *11*, 1462-1471.

44. Kagan, H.B. & Fiaud, J.C. (**1988**). Kinetic resolution. Top. Stereochem. *18*, 249-330.

45. Bornscheuer, U.T. & Kazlauskas, R.J. Hydrolases in Organic Synthesis. Wiley-VCH: Weinheim, **2006**.

46. Chen, C.S., Fujimoto, Y., Girdaukas, G. & Sih, C.J. (**1982**). Quantitative-analyses of biochemical kinetic resolutions of enantiomers. J. Am. Chem. Soc. *104*, 7294-7299.

47. Rakels, J.L.L., Straathof, A.J.J. & Heijnen, J.J. (**1993**). A simple method to determine the enantiomeric ratio in enantioselective biocatalysis. Enzyme Microb. Technol. *15*, 1051-1056.

48. Lu, Y., Zhao, X. & Chen, Z.N. (**1995**). A convenient method for evaluation of the enantiomeric ratio of kinetic resolutions. Tetrahedron: Asymmetry *6*, 1093-1096.

49. Anthonsen, H.W., Hoff, B.H. & Anthonsen, T. (**1995**). A simple method for calculating enantiomer ratio and equilibrium constants in biocatalytic resolutions. Tetrahedron: Asymmetry *6*, 3015-3022.

50. Schmidt, M., Henke, E., Heinze, B., Kourist, R., Hidalgo, A. & Bornscheuer, U.T. (**2006**). A versatile esterase from *Bacillus subtilis*: Cloning, expression and characterization, and its application in biocatalysis. Biotechnol. J. *1*, 1-5.

51. Ollis, D.L., Cheah, E., Cygler, M., Eckstein, E., Dijkstra, B., Frolow, F., Franken, S.M., Harel, M., Remington, S.J., Silman, I., Schrag, J. & Sussman, S.L. (**1992**). The α/β hydrolase fold. Protein Eng. *5*, 197-211.

52. Dodson, G. & Wlodawer, A. (**1998**). Catalytic triads and their relatives. Trends Biochem. Sci. *23*, 347-352.

53. Zhao, H. (**2007**). Directed evolution of novel protein functions. Biotechnol. Bioeng. *98*, 313-317.

54. Jochens, H., Stiba, K., Savile, C., Fujii, R., Yu, J.G., Gerassenkov, T., Kazlauskas, R.J. & Bornscheuer, U.T. (**2009**). Converting an Esterase into an Epoxide Hydrolase. Angew. Chem. Int. Ed. *48*, 3532-3535.

55. Harford-Cross, C.F., Carmichael, A.B., Allan, F.K., England, P.A., Rouch, D.A. & Wong, L.L. (**2000**). Protein engineering of cytochrome P450cam (CYP101) for the oxidation of polycyclic aromatic hydrocarbons. Protein Eng. Des. Sel. *13*, 121-128.

56. Mouratou, B., Kasper, P., Gehring, H. & Christen, P. (**1999**). Conversion of tyrosine phenol-lyase to dicarboxylic amino acid beta-lyase, an enzyme not found in Nature. J. Biol. Chem. *274*, 1320-1325.

57. Bartsch, S., Kourist, R. & Bornscheuer, U.T. (**2008**). Complete inversion of enantioselectivity towards acetylated tertiary alcohols by a double mutant of a *Bacillus subtilis* esterase. Angew. Chem. Int. Ed. *47*, 1508-1511.

58. Scheib, H., Pleiss, J., Kovac, A., Paltauf, F. & Schmid, R.D. (**1999**). Stereoselectivity of *Mucorales* lipases toward triradylglycerols-A simple solution to a complex problem. Protein Sci. *8*, 215-221.

59. Bornscheuer, U.T. (**1998**). Directed evolution of enzymes. Angew. Chem. Int. Ed. *37*, 3105-3108.

60. Lutz, S. & Patrick, W.M. (**2004**). Novel methods for directed evolution of enzymes: quality, not quantity. Curr. Opin. Biotechnol. *15*, 291-297.

61. Leung, D.W., Chen, E. & Goeddel, D.V. (**1989**). A method for random mutagenesis of a defined DNA segment using a modified polymerase chain reaction. Technique *1*, 11-15.

62. Fujii, R., Kitaoka, M. & Hayashi, K. (**2004**). One-step random mutagenesis by error-prone rolling circle amplification. Nucleic Acids Res. *32*, e145.

63. Borrego, B., Wienecke, A. & Schwienhorst, A. (**1995**). Combinatorial libraries by cassette mutagenesis. Nucleic Acids Res. *23*, 1834.

64. Greener, A., Callahan, M. & Jerpseth, B. (**1997**). An efficient random mutagenesis technique using an *E. coli* mutator strain. Mol. Biotechnol. *7*, 189-195.

65. Ho, S.N., Hunt, H.D., Horton, R.M., Pullen, J.K. & Pease, L.R. (**1989**). Site-directed mutagenesis by overlap extension using the polymerase chain reaction. Gene *77*, 51-59.

66. Gray, K.A., Richardson, T.H., Kretz, K., Short, J.M., Bartnek, F., Knowles, R., Kan, L., Swanson, P.E. & Robertson, D.E. (**2001**). Rapid evolution of reversible denaturation and elevated melting temperature in a microbial haloalkane dehalogenase. Adv. Synth. Catal. *343*, 607-617.

67. Murakami, H., Hohsaka, T. & Sisido, M. (**2002**). Random insertion and deletion of arbitrary number of bases for codon-based random mutation of DNAs. Nat. Biotechnol. *20*, 76-81.

68. Hughes, M.D., Nagel, D.A., Santos, A.F., Sutherland, A.J. & Hine, A.V. (**2003**). Removing the redundancy from randomised gene libraries. J. Mol. Biol. *331*, 973-979.

69. Miyazaki, K. & Takenouchi, M. (**2002**). Creating random mutagenesis libraries using megaprimer PCR of whole plasmid. Biotechniques *33*, 1033-1038.

70. Chopra, S., Ranganathan, A., Chang, H.J., Hsu, H.J., Chang, C.F., Peng, H.P., Sun, Y.K., Yu, H.M., Shih, H.C. & Song, C.Y. (**2003**). Protein Evolution by "Codon Shuffling". Chem. Biol. *10*, 917-926.

71. Osuna, J., Yanez, J., Soberon, X. & Gaytan, P. (**2004**). Protein evolution by codon-based random deletions. Nucleic Acids Res. *32*, e136.

72. Matsuura, T., Miyai, K., Trakulnaleamsai, S., Yomo, T., Shima, Y., Miki, S., Yamamoto, K. & Urabe, I. (**1999**). Evolutionary molecular engineering by random elongation mutagenesis. Nat. Biotechnol. *17*, 58-61.

73. Wong, T.S., Tee, K.L., Hauer, B. & Schwaneberg, U. (**2004**). Sequence saturation mutagenesis (SeSaM): a novel method for directed evolution. Nucleic Acids Res. *32*, e26.

74. Qian, Z. & Lutz, S. (**2005**). Improving the catalytic activity of *Candida antarctica* lipase B by circular permutation. J. Am. Chem. Soc. *127*, 13466-13467.

75. Stemmer, W.P. (**1994**). DNA shuffling by random fragmentation and reassembly: *in vitro* recombination for molecular evolution. Proc. Natl. Acad. Sci. U. S. A. *91*, 10747-10751.

76. Stemmer, W.P.C. (**1994**). Rapid evolution of a protein in vitro by DNA shuffling. Nature *370*, 389-391.

77. Crameri, A., Raillard, S.A., Bermudez, E. & Stemmer, W.P.C. (**1998**). DNA shuffling of a family of genes from diverse species accelerates directed evolution. Nature *391*, 288-291.

78. Zhao, H., Giver, L., Shao, Z., Affholter, J.A. & Arnold, F.H. (**1998**). Molecular evolution by staggered extension process (StEP) *in vitro* recombination. Nat. Biotechnol. *16*, 258-261.

79. Coco, W.M., Levinson, W.E., Crist, M.J., Hektor, H.J., Darzins, A., Pienkos, P.T., Squires, C.H. & Monticello, D.J. (**2001**). DNA shuffling method for generating highly recombined genes and evolved enzymes. Nat. Biotechnol. *19*, 354-359.

80. Gibbs, M.D., Nevalainen, K.M. & Bergquist, P.L. (**2001**). Degenerate oligonucleotide gene shuffling (DOGS): a method for enhancing the frequency of recombination with family shuffling. Gene *271*, 13-20.

81. Song, J.K., Chung, B., Oh, Y.H. & Rhee, J.S. (**2002**). Construction of DNA-shuffled and incrementally truncated libraries by a mutagenic and unidirectional

reassembly method: changing from a substrate specificity of phospholipase to that of lipase. Appl. Environ. Microbiol. *68*, 6146-6151.

82. Coco, W.M., Encell, L.P., Levinson, W.E., Crist, M.J., Loomis, A.K., Licato, L.L., Arensdorf, J.J., Sica, N., Pienkos, P.T. & Monticello, D.J. (**2002**). Growth factor engineering by degenerate homoduplex gene family recombination. Nat. Biotechnol. *20*, 1246-1250.

83. Ness, J.E., Kim, S., Gottman, A., Pak, R., Krebber, A., Borchert, T.V., Govindarajan, S., Mundorff, E.C. & Minshull, J. (**2002**). Synthetic shuffling expands functional protein diversity by allowing amino acids to recombine independently. Nat. Biotechnol. *20*, 1251-1255.

84. Zha, D., Eipper, A. & Reetz, M.T. (**2003**). Assembly of designed oligonucleotides as an efficient method for gene recombination: a new tool in directed evolution. ChemBioChem *4*, 34-39.

85. Lee, S.H., Ryu, E.J., Kang, M.J., Wang, E.S., Piao, Z., Choi, Y.J., Jung, K.H., Jeon, J.Y.J. & Shin, Y.C. (**2003**). A new approach to directed gene evolution by recombined extension on truncated templates (RETT). J. Mol. Catal. B: Enzym. *26*, 119-129.

86. Eggert, T., Funke, S.A., Rao, N.M., Acharya, P., Krumm, H., Reetz, M.T. & Jaeger, K.E. (**2005**). Multiplex-PCR-based recombination as a novel high-fidelity method for directed evolution. ChemBioChem *6*, 1062-1067.

87. Ostermeier, M., Shim, J.H. & Benkovic, S.J. (**1999**). A combinatorial approach to hybrid enzymes independent of DNA homology. Nat. Biotechnol. *17*, 1205–1209.

88. Lutz, S., Ostermeier, M., Moore, G.L., Maranas, C.D. & Benkovic, S.J. (**2001**). Creating multiple-crossover DNA libraries independent of sequence identity. Proc. Natl. Acad. Sci. U. S. A. *98*, 1124811253.

89. Sieber, V., Martinez, C.A. & Arnold, F.H. (**2001**). Libraries of hybrid proteins from distantly related sequences. Nat. Biotechnol. *19*, 456-460.

90. O'Maille, P.E., Bakhtina, M. & Tsai, M.D. (**2002**). Structure-based combinatorial Protein Eng. (SCOPE). J. Mol. Biol. *321*, 677-691.

91. Hiraga, K. & Arnold, F.H. (**2003**). General method for sequence-independent site-directed chimeragenesis. J. Mol. Biol. *330*, 287-296.

92. Bittker, J.A., Le, B.V., Liu, J.M. & Liu, D.R. (**2004**). Directed evolution of protein enzymes using nonhomologous random recombination. Proc. Natl. Acad. Sci. U. S. A. *101*, 7011-7016.

93. Henke, E. & Bornscheuer, U.T. (**1999**). Directed evolution of an esterase from *Pseudomonas fluorescens*. Random mutagenesis by error-prone PCR or a mutator strain and identification of mutants showing enhanced enantioselectivity by a resorufin-based fluorescence assay. Biological Chemistry *380*, 1029-1033.

94. Bornscheuer, U.T., Altenbuchner, J. & Meyer, H.H. (**1999**). Directed evolution of an esterase: screening of enzyme libraries based on pH-indicators and a growth assay. Bioorg. Med. Chem. *7*, 2169-2173.

95. Selifonova, O. & Schellenberger, V. Evolution of microorganisms using mutator plasmids. in Methods in Molecular Biology, ***vol. 231***, 45-52. Humana Press: Totowa, New Jersey, **2003**.

96. Cadwell, R.C. & Joyce, G.F. (**1992**). Randomization of genes by PCR mutagenesis. Genome Res. *2*, 28-33.

97. Arnold, F.H. & Georgiou, G. Directed Evolution: Library Creation- Humana Press: Totowa, New Jersey, **2003**.

98. Zaccolo, M., Williams, D.M., Brown, D.M. & Gherardi, E. (**1996**). An approach to random mutagenesis of DNA using mixtures of triphosphate derivatives of nucleoside analogues. J. Mol. Biol. *255*, 589-603.

99. Neylon, C. (**2004**). Chemical and biochemical strategies for the randomization of protein encoding DNA sequences: library construction methods for directed evolution. Nucleic Acids Res. *32*, 1448-1459.

100. Patel, P.H., Kawate, H., Adman, E., Ashbach, M. & Loeb, L.A. (**2001**). A single highly mutable catalytic site amino acid is critical for DNA polymerase fidelity. J. Biol. Chem. *276*, 5044-5051.

101. Cline, J. & Hogrefe, H. (**2000**). Randomize gene sequences with new PCR mutagenesis kit. Strategies *13*, 157-161.

102. Biles, B.D. & Connolly, B.A. (**2004**). Low-fidelity *Pyrococcus furiosus* DNA polymerase mutants useful in error-prone PCR. Nucleic Acids Res. *32*, e176.

103. Peisajovich, S.G., Rockah, L. & Tawfik, D.S. (**2006**). Evolution of new protein topologies through multistep gene rearrangements. Nat. Genet. *38*, 168-174.

104. Arnold, F.H. (**2006**). Fancy footwork in the sequence space shuffle. Nat. Biotechnol. *24*, 328-330.

105. Crameri, A., Whitehorn, E.A., Tate, E. & Stemmer, W.P.C. (**1996**). Improved green fluorescent protein by molecular evolution using DNA shuffling. Nat. Biotechnol. *14*, 315-319.

106. Coco, W.M. RACHITT: Gene family shuffling by Random Chimeragenesis on Transient Templates. in Methods in Molecular Biology, ***vol. 231***, 111-127. Humana Press: Totowa, New Jersey, **2003**.

107. Lutz, S., Ostermeier, M. & Benkovic, S.J. (**2001**). Rapid generation of incremental truncation libraries for protein engineering using a-phosphothioate nucleotides. Nucleic Acids Res. *29*, e16.

108. Meyer, M.M., Silberg, J.J., Voigt, C.A., Endelman, J.B., Mayo, S.L., Wang, Z.G. & Arnold, F.H. (**2003**). Library analysis of SCHEMA-guided protein recombination. Protein Sci. *12*, 1686-1693.

109. Wong, T.S., Zhurina, D. & Schwaneberg, U. (**2006**). The diversity challenge in directed protein evolution. Comb. Chem. High Throughput Screening *9*, 271-288.

110. Kazlauskas, R.J. & Bornscheuer, U.T. (**2009**). Finding better protein engineering strategies. Nat. Chem. Biol. *5*, 526-529.

111. Chica, R.A., Doucet, N. & Pelletier, J.N. (**2005**). Semi-rational approaches to engineering enzyme activity: combining the benefits of directed evolution and rational design. Curr. Opin. Biotechnol. *16*, 378-384.

112. Cherry, J.R., Lamsa, M.H., Schneider, P., Vind, J., Svendsen, A., Jones, A. & Pedersen, A.H. (**1999**). Directed evolution of a fungal peroxidase. Nat. Biotechnol. *17*, 379-384.

113. Park, H.S., Nam, S.H., Lee, J.K., Yoon, C.N., Mannervik, B., Benkovic, S.J. & Kim, H.S. (**2006**). Design and evolution of new catalytic activity with an existing protein scaffold. Science *311*, 475-476.

114. Cheeseman, J.D., Tocilj, A., Park, S., Schrag, J.D. & Kazlauskas, R.J. (**2004**). Structure of an aryl esterase from *Pseudomonas fluorescens*. Acta Crystallogr., Sect D: Biol. Crystallogr. *60*, 1237-1243.

115. Park, S., Morley, K.L., Horsman, G.P., Holmquist, M., Hult, K. & Kazlauskas, R.J. (**2005**). Focusing mutations into the *P. fluorescens* esterase binding site increases enantioselectivity more effectively than distant mutations. Chem. Biol. *12*, 45-54.

116. Jochens, H. & Bornscheuer, U.T. (**2010**). Natural Diversity to Guide Focused Directed Evolution. CheBioChem *11*, 1861-1866.

117. Reetz, M.T., Kahakeaw, D. & Sanchis, J. (**2009**). Shedding light on the efficacy of laboratory evolution based on iterative saturation mutagenesis. Molecular Biosystems *5*, 115-122.

118. Reetz, M.T. & Carballeira, J.D. (**2007**). Iterative saturation mutagenesis (ISM) for rapid directed evolution of functional enzymes. Nat. Protocols *2*, 891-903.

119. Reetz, M.T., Wang, L.W. & Bocola, M. (**2006**). Directed evolution of enantioselective enzymes: iterative cycles of CASTing for probing protein-sequence space. Angew. Chem. Int. Ed. *45*, 1236-1241.

120. Gupta, R.D. & Tawfik, D.S. (**2008**). Directed enzyme evolution via small and effective neutral drift libraries. Nat. Methods *5*, 939-942.

121. Fox, R.J., Davis, S.C., Mundorff, E.C., Newman, L.M., Gavrilovic, V., Ma, S.K., Chung, L.M., Ching, C., Tam, S. & Muley, S. (**2007**). Improving catalytic function by ProSAR-driven enzyme evolution. Nat. Biotechnol. *25*, 338-344.

122. Boersma, Y.L., Dröge, M.J. & Quax, W.J. (**2007**). Selection strategies for improved biocatalysts. FEBS J. *274*, 2181-2195.

123. Goddard, J.P. & Reymond, J.L. (**2004**). Enzyme assays for high-throughput screening. Curr. Opin. Biotechnol. *15*, 314-322.

124. Schmidt-Dannert, C. & Arnold, F.H. (**1999**). Directed evolution of industrial enzymes. Trends Biotechnol. *17*, 135-136.

125. Aharoni, A., Griffiths, A.D. & Tawfik, D.S. (**2005**). High-throughput screens and selections of enzyme-encoding genes. Curr. Opin. Chem. Biol. *9*, 210-216.

126. Klein, G. & Reymond, J.L. (**1999**). Enantioselective fluorogenic assay of acetate hydrolysis for detecting lipase catalytic antibodies. Helv. Chim. Acta *82*, 400-407.

127. Badalassi, F., Wahler, D., Klein, G., Crotti, P. & Reymond, J.L. (**2000**). A versatile periodate-coupled fluorogenic assay for hydrolytic enzymes. Angew. Chem. Int. Ed. *112*, 4233-4236.

128. Moore, J.C. & Arnold, F.H. (**1996**). Directed evolution of a *para*-nitrobenzyl esterase for aqueous-organic solvents. Nat. Biotechnol. *14*, 432-436.

129. Reetz, M.T., Zonta, A., Schimossek, K., Liebeton, K. & Jaeger, K.E. (**1997**). Creation of enantioselective biocatalysts for organic chemistry by *in vitro* evolution. Angew. Chem. Int. Ed. *36*, 2830-2832.

130. Wu, S.H., Guo, Z.W. & Sih, C.J. (**1990**). Enhancing the enantioselectivity of *Candida* lipase-catalyzed ester hydrolysis via noncovalent enzyme modification. J. Am. Chem. Soc. *112*, 1990-1995.

131. Janes, L.E. & Kazlauskas, R.J. (**1997**). Quick E. A fast spectrophotometric method to measure the enantioselectivity of hydrolases. J. Org. Chem. *62*, 4560-4561.

132. Janes, L.E., Löwendahl, A.C. & Kazlauskas, R.J. (**1998**). Quantitative screening of hydrolase libraries using pH indicators: identifying active and enantioselective hydrolases. Chem. Eur. J. *4*, 2324-2331.

133. Baumann, M., Sturmer, R. & Bornscheuer, U.T. (**2001**). A high-throughput-screening method for the identification of active and enantioselective hydrolases. Angew. Chem. Int. Ed. *40*, 4201-4204.

134. Konarzycka-Bessler, M. & Bornscheuer, U.T. (**2003**). A high-throughput-screening method for determining the synthetic activity of hydrolases. Angew. Chem. Int. Ed. *42*, 1418-1420.

135. Henke, E. & Bornscheuer, U.T. (**2003**). Fluorophoric assay for the high-throughput determination of amidase activity. Anal. Chem. *75*, 255-260.

136. Wahler, D. & Reymond, J.L. (**2002**). The adrenaline test for enzymes. Angew. Chem. Int. Ed. *41*, 1229-1232.

137. Banerjee, A., Sharma, R. & Banerjee, U. (**2003**). A rapid and sensitive fluorometric assay method for the determination of nitrilase activity. Biotechnol. Appl. Biochem. *37*, 289-293.

138. Doderer, K., Lutz-Wahl, S., Hauer, B. & Schmid, R.D. (**2003**). Spectrophotometric assay for epoxide hydrolase activity toward any epoxide. Anal. Biochem. *321*, 131-134.

139. Mateo, C., Archelas, A. & Furstoss, R. (**2003**). A spectrophotometric assay for measuring and detecting an epoxide hydrolase activity. Anal. Biochem. *314*, 135-141.

140. Zocher, F., Enzelberger, M.M., Bornscheuer, U.T., Hauer, B. & D Schmid, R. (**1999**). A colorimetric assay suitable for screening epoxide hydrolase activity. Anal. Chim. Acta *391*, 345-351.

141. Zhao, H. A pH-indicator-based screen for hydrolytic haloalkane dehalogenase. in Methods in Molecular Biology, *vol. 230,* 213-222. Humana Press: Totowa, New Jersey, **2003**.

142. Tanaka, F., Thayumanavan, R. & Barbas, C.F. (**2003**). Fluorescent detection of carbon-carbon bond formation. J. Am. Chem. Soc. *125*, 8523-8528.

143. Copeland, G.T. & Miller, S.J. (**1999**). A chemosensor-based approach to catalyst discovery in solution and on solid support. J. Am. Chem. Soc. *121*, 4306-4307.

144. Reetz, M.T., Becker, M.H., Klein, H.W. & Stöckigt, D. (**1999**). A method for high-throughput screening of enantioselective catalysts. Angew. Chem. Int. Ed. *38*, 1758-1761.

145. DeSantis, G., Wong, K., Farwell, B., Chatman, K., Zhu, Z., Tomlinson, G., Huang, H., Tan, X., Bibbs, L. & Chen, P. (**2003**). Creation of a productive, highly enantioselective nitrilase through gene site saturation mutagenesis (GSSM). J. Am. Chem. Soc. *125*, 11476-11477.

146. Reetz, M.T., Eipper, A., Tielmann, P. & Mynott, R. (**2002**). A practical NMR-based high-throughput assay for screening enantioselective catalysts and biocatalysts. Adv. Synth. Catal. *344*, 1008-1016.

147. Petra, D.G.I., Reek, J.N.H., Kamer, P.C.J., Schoemaker, H.E. & Leeuwen, P. (**2000**). IR spectroscopy as a high-throughput screening-technique for enantioselective hydrogen-transfer catalysts. Chem. Commun. 683-684.

148. Reetz, M.T., Kühling, K.M., Wilensek, S., Husmann, H., Häusig, U.W. & Hermes, M. (**2001**). A GC-based method for high-throughput screening of enantioselective catalysts. Catal. Today *67*, 389-396.

149. Moates, F.C., Somani, M., Annamalai, J., Richardson, J.T., Luss, D. & Willson, R.C. (**1996**). Infrared thermographic screening of combinatorial libraries of heterogeneous catalysts. Ind. Eng. Chem. Res. *35*, 4801-4803.

150. Holzwarth, A., Schmidt, H.W. & Maier, W.F. (**1998**). Detection of catalytic activity in combinatorial libraries of heterogeneous catalysts by IR thermography. Angew. Chem. Int. Ed. *37*, 2644-2647.

151. Reetz, M.T., Becker, M.H., Kühling, K.M. & Holzwarth, A. (**1998**). Time-resolved IR-thermographic detection and screening of enantioselectivity in catalytic reactions. Angew. Chem. Int. Ed. *37*, 2647-2650.

152. Reetz, M.T., Hermes, M. & Becker, M.H. (**2001**). Infrared-thermographic screening of the activity and enantioselectivity of enzymes. Appl. Microbiol. Biotechnol. *55*, 531-536.

153. Berkessel, A., Ashkenazi, E. & Andreae, M.R.M. (**2003**). Discovery of novel homogeneous rare earth catalysts by IR-thermography: epoxide opening with alcohols and Baeyer-Villiger oxidations with hydrogen peroxide. Appl. Catal., A *254*, 27-34.

154. Moore, B.D., Stevenson, L., Watt, A., Flitsch, S., Turner, N.J., Cassidy, C. & Graham, D. (**2004**). Rapid and ultra-sensitive determination of enzyme activities using surface-enhanced resonance Raman scattering. Nat. Biotechnol. *22*, 1133-1138.

155. Bornscheuer, U.T. (**2004**). Finding enzymatic gold on silver surfaces. Nat. Biotechnol. *22*, 1098-1099.

156. Reetz, M.T., Kühling, K.M., Deege, A., Hinrichs, H. & Belder, D. (**2000**). Super-high-throughput screening of enantioselective catalysts by using capillary array electrophoresis. Angew. Chem. Int. Ed. *39*, 3891-3893.

157. Taran, F., Gauchet, C., Mohar, B., Meunier, S., Valleix, A., Renard, P.Y., Créminon, C., Grassi, J., Wagner, A. & Mioskowski, C. (**2002**). High-throughput screening of enantioselective catalysts by immunoassay. Angew. Chem. Int. Ed. *41*, 124-127.

158. Matsushita, M., Yoshida, K., Yamamoto, N., Wirsching, P., Lerner, R.A. & Janda, K.D. (**2003**). High-throughput screening by using a blue-fluorescent antibody sensor. Angew. Chem. Int. Ed. *115*, 6166-6169.

159. Dröge, M.J., Rüggeberg, C.J., van der Sloot, A.M., Schimmel, J., Dijkstra, D.S., Verhaert, R., Reetz, M.T. & Quax, W.J. (**2003**). Binding of phage displayed *Bacillus subtilis* lipase A to a phosphonate suicide inhibitor. J. Biotechnol. *101*, 19-28.

160. Hansson, L.O., Widersten, M. & Mannervik, B. (**1997**). Mechanism-based phage displayselection of active-site mutants of human glutathione transferase A1-1 catalyzing SNAr reactions. Biochemistry *36*, 11252-11260.

161. Dröge, M.J., Boersma, Y.L., Braun, P.G., Buining, R.J., Julsing, M.K., Selles, K.G.A., Van Dijl, J.M. & Quax, W.J. (**2006**). Phage display of an intracellular carboxylesterase of *Bacillus subtilis*: comparison of Sec and Tat pathway export capabilities. Appl. Environ. Microbiol. *72*, 4589-4595.

162. Paschke, M. & Höhne, W. (**2005**). A twin-arginine translocation (Tat)-mediated phage display system. Gene *350*, 79-88.

163. Desvaux, M., Dumas, E., Chafsey, I. & Hébraud, M. (**2006**). Protein cell surface display in Gram-positive bacteria: from single protein to macromolecular protein structure. FEMS Microbiol. Lett. *256*, 1-15.

164. Seelig, B. & Szostak, J.W. (**2007**). Selection and evolution of enzymes from a partially randomized non-catalytic scaffold. Nature *448*, 828-831.

165. Tawfik, D.S. & Griffiths, A.D. (**1998**). Man-made cell-like compartments for molecular evolution. Nat. Biotechnol. *16*, 652-656.

166. Griffiths, A.D. & Tawfik, D.S. (**2006**). Miniaturising the laboratory in emulsion droplets. Trends Biotechnol. *24*, 395-402.

167. Cohen, H.M., Tawfik, D.S. & Griffiths, A.D. (**2004**). Altering the sequence specificity of *Hae*III methyltransferase by directed evolution using *in vitro* compartmentalization. Protein Eng. Des. Sel.*17*, 3-11.

168. Zheng, Y. & Roberts, R.J. (**2007**). Selection of restriction endonucleases using artificial cells. Nucleic Acids Res. *35*, e83.

169. Ghadessy, F.J., Ong, J.L. & Holliger, P. (**2001**). Directed evolution of polymerase function by compartmentalized self-replication. Proc. Natl. Acad. Sci. U. S. A. *98*, 4552-4557.

170. Agresti, J.J., Kelly, B.T., Jäschke, A. & Griffiths, A.D. (**2005**). Selection of ribozymes that catalyse multiple-turnover Diels-Alder cycloadditions by using *in vitro* compartmentalization. Proc. Natl. Acad. Sci. U. S. A. *102*, 16170-16175.

171. Stein, V., Sielaff, I., Johnsson, K. & Hollfelder, F. (**2007**). A covalent chemical genotype-phenotype linkage for *in vitro* protein evolution. ChemBioChem *8*, 2191-2194.

172. Griffiths, A.D. & Tawfik, D.S. (**2000**). Man-made enzymes - from design to *in vitro* compartmentalisation. Curr. Opin. Biotechnol. *11*, 338-353.

173. Heine, A., DeSantis, G., Luz, J.G., Mitchell, M., Wong, C.H. & Wilson, I.A. (**2001**). Observation of covalent intermediates in an enzyme mechanism at atomic resolution. Science *294*, 369-374.

174. DeSantis, G., Liu, J., Clark, D.P., Heine, A., Wilson, I.A. & Wong, C.H. (**2003**). Structure-based mutagenesis approaches toward expanding the substrate specificity of 2-deoxyribose-5-phosphate aldolase. Biorg. Med. Chem. *11*, 43-52.

175. Bornscheuer, U.T. (**2004**). High-throughput-screening systems for hydrolases. Eng. Life Sci. *4*, 539-542.

176. Sneeden, J.L. & Loeb, L.A. Genetic complementation protocols. in Methods in Molecular Biology, *vol. 230*, 3-10. Humana Press: Totowa, New Jersey, **2003**.

177. Reetz, M.T. & Rüggeberg, C.J. (**2002**). A screening system for enantioselective enzymes based on differential cell growth. Chem. Commun., 1428-1429.

178. Hwang, B.Y., Oh, J.M., Kim, J. & Kim, B.G. (**2006**). Pro-antibiotic substrates for the identification of enantioselective hydrolases. Biotechnol. Lett. *28*, 1181-1185.

179. Boersma, Y.L., Dröge, M.J., van der Sloot, A.M., Pijning, T., Cool, R.H., Dijkstra, B.W. & Quax, W.J. (**2008**). A novel genetic selection for improved enantioselectivity of *Bacillus subtilis* lipase A. ChemBioChem *9*, 1110- 1115.

180. Reetz, M.T., Hobenreich, H., Soni, P. & Fernandez, L. (**2008**). A genetic selection system for evolving enantioselectivity of enzymes. Chem. Commun., 5502-5504.

181. Shapiro, H.M. Practical Flow Cytometry. John Willey & Sohns, New York, **2003**.

182. Yang, G. & Withers, S.G. (**2009**). Ultrahigh-throughput FACS-based screening for directed enzyme evolution. ChemBioChem *10*, 2704-2715.

183. Olsen, M.J., Stephens, D., Griffiths, D., Daugherty, P., Georgiou, G. & Iverson, B.L. (**2000**). Function-based isolation of novel enzymes from a large library. Nat. Biotechnol. *18*, 1071-1074.

184. Varadarajan, N., Gam, J., Olsen, M.J., Georgiou, G. & Iverson, B.L. (**2005**). Engineering of protease variants exhibiting high catalytic activity and exquisite substrate selectivity. Proc. Natl. Acad. Sci. U. S. A. *102*, 6855-6860.

185. Varadarajan, N., Rodriguez, S., Hwang, B.Y., Georgiou, G. & Iverson, B.L. (**2008**). Highly active and selective endopeptidases with programmed substrate specificities. Nat. Chem. Biol. *4*, 290-294.

186. Varadarajan, N., Georgiou, G. & Iverson, B.L. (**2008**). An engineered protease that cleaves specifically after sulfated tyrosine. Angew. Chem. Int. Ed. *47*, 7861-7863.

187. Lipovsek, D., Antipov, E., Armstrong, K.A., Olsen, M.J., Klibanov, A.M., Tidor, B. & Wittrup, K.D. (**2007**). Selection of horseradish peroxidase variants with enhanced enantioselectivity by yeast surface display. Chem. Biol. *14*, 1176-1185.

188. Antipov, E., Cho, A.E., Wittrup, K.D. & Klibanov, A.M. (**2008**). Highly L and D enantioselective variants of horseradish peroxidase discovered by an ultrahigh-throughput selection method. Proc. Natl. Acad. Sci. U. S. A. *105*, 17694-17699.

189. Becker, S., Schmoldt, H.U., Adams, T.M., Wilhelm, S. & Kolmar, H. (**2004**). Ultra-high-throughput screening based on cell-surface display and fluorescence-activated cell sorting for the identification of novel biocatalysts. Curr. Opin. Biotechnol. *15*, 323-329.

190. Becker, S., Michalczyk, A., Wilhelm, S., Jaeger, K.E. & Kolmar, H. (**2007**). Ultrahigh-throughput screening to identify *E. coli* cells expressing functionally active enzymes on their surface. ChemBioChem *8*, 943-949.

191. Becker, S., Hobenreich, H., Vogel, A., Knorr, J., Wilhelm, S., Rosenau, F., Jaeger, K.E., Reetz, M.T. & Kolmar, H. (**2008**). Single-cell high-throughput screening to identify enantioselective hydrolytic enzymes. Angew. Chem. Int. Ed. *47*, 5085-5088.

192. Tsien, R.Y. (**1998**). The green fluorescent protein. Annu. Rev. Biochem. *67*, 509-544.

193. Cabantous, S. & Waldo, G.S. (**2006**). *In vivo* and *in vitro* protein solubility assays using split GFP. Nat. Methods *3*, 845-854.

194. Pédelacq, J.D., Cabantous, S., Tran, T., Terwilliger, T.C. & Waldo, G.S. (**2005**). Engineering and characterization of a superfolder green fluorescent protein. Nat. Biotechnol. *24*, 79-88.

195. Santoro, S.W. & Schultz, P.G. (**2002**). Directed evolution of the site specificity of Cre recombinase. Proc. Natl. Acad. Sci. USA *99*, 4185-4190.

196. Santoro, S.W., Wang, L., Herberich, B., King, D.S. & Schultz, P.G. (**2002**). An efficient system for the evolution of aminoacyl-tRNA synthetase specificity. Nat. Biotechnol. *20*, 1044-1048.

197. Olsen, K.N., Budde, B.B., Siegumfeldt, H., Rechinger, K.B., Jakobsen, M. & Ingmer, H. (**2002**). Noninvasive measurement of bacterial intracellular pH on a single-cell level with green fluorescent protein and fluorescence ratio imaging microscopy. Appl. Environ. Microbiol. *68*, 4145-4147.

198. Aharoni, A., Thieme, K., Chiu, C.P.C., Buchini, S., Lairson, L.L., Chen, H., Strynadka, N.C.J., Wakarchuk, W.W. & Withers, S.G. (**2006**). High-throughput screening methodology for the directed evolution of glycosyltransferases. Nat. Methods *3*, 609-614.

199. Eklund, B.I., Edalat, M., Stenberg, G. & Mannervik, B. (**2002**). Screening for recombinant glutathione transferases active with monochlorobimane. Anal. Biochem. *309*, 102-108.

200. Griswold, K.E., Aiyappan, N.S., Iverson, B.L. & Georgiou, G. (**2006**). The evolution of catalytic efficiency and substrate promiscuity in human theta class 1-1 glutathione transferase. J. Mol. Biol. *364*, 400-410.

201. Kwon, S.J. & Petri, R. (**2004**). A high-throughput screen for porphyrin metal chelatases: application to the directed evolution of ferrochelatases for metalloporphyrin biosynthesis. ChemBioChem *5*, 1069-1074.

202. Hasegawa, S., Choi, J.W. & Rao, J. (**2004**). Single-cell detection of trans-splicing ribozyme *in vivo* activity. J. Am. Chem. Soc. *126*, 7158-7159.

203. Griffiths, A.D. & Tawfik, D.S. (**2003**). Directed evolution of an extremely fast phosphotriesterase by *in vitro* compartmentalization. EMBO J. *22*, 24-35.

204. Mastrobattista, E., Taly, V., Chanudet, E., Treacy, P., Kelly, B.T. & Griffiths, A.D. (**2005**). High-throughput screening of enzyme libraries: *In vitro* evolution of a β-galactosidase by fluorescence-activated sorting of double emulsions. Chem. Biol. *12*, 1291-1300.

205. Aharoni, A., Amitai, G., Bernath, K., Magdassi, S. & Tawfik, D.S. (**2005**). High-throughput screening of enzyme libraries: thiolactonases evolved by fluorescence-activated sorting of single cells in emulsion compartments. Chem. Biol. *12*, 1281-1289.

206. Hotta, Y., Ezaki, S., Atomi, H. & Imanaka, T. (**2002**). Extremely stable and versatile carboxylesterase from a hyperthermophilic archaeon. Appl. Environ. Microbiol. *68*, 3925-3931.

207. Böttcher, D. Diploma Thesis, Greifswald University (**2002**).

208. Becker, H.G.O., Berger, W. & Domschke, G. Organikum. Wiley-VCH: Weinheim, **2004**.

209. Wisseman Jr, C.L., Smadel, J.E., Hahn, F.E. & Hopps, H.E. (**1954**). Mode of action of chloramphenicol I.: Action of chloramphenicol on assimilation of ammonia and on synthesis of proteins and nucleic acids in *Escherichia coli*. J. Bacteriol. *67*, 662-673.

210. Vollhardt, K.P.C. & Schore, N.E. Química Orgánica - Estructura y función. Omega: Barcelona, **2000**.

211. Pelletier, I. & Altenbuchner, J. (**1995**). A bacterial esterase is homologous with nonheme haloperoxidases and displays brominating activity. Microbiology *141*, 459-468.

212. Krebsfänger, N., Zocher, F., Altenbuchner, J. & Bornscheuer, U.T. (**1998**). Characterization and enantioselectivity of a recombinant esterase from *Pseudomonas fluorescens*. Enzyme Microb. Technol. *22*, 641-646.

213. Schmidt, M., Hasenpusch, D., Kähler, M., Kirchner, U., Wiggenhorn, K., Lange, W. & Bornscheuer, U.T. (**2006**). Directed evolution of an esterase from *Pseudomonas fluorescens* yields a mutant with excellent enantioselectivity and activity for the kinetic resolution of a chiral building block. ChemBioChem *7*, 805-809.

214. Hidalgo, A., Schliessmann, A., Molina, R., Hermoso, J. & Bornscheuer, U.T. (**2008**). A one-pot, simple methodology for cassette randomisation and recombination for focused directed evolution. Protein Eng. Des. Sel. *21*, 567-576.

215. Schliessmann, A., Hidalgo, A., Berenguer, J. & Bornscheuer, U.T. (**2009**). Increased enantioselectivity by engineering bottleneck mutants in an esterase from *Pseudomonas fluorescens*. ChemBioChem *10*, 2920-2923.

216. Brock, T.D. (**1961**). Chloramphenicol. Bacteriol. Rev. *25*, 32-48.

217. Varadharaj, G., Hazell, K. & Reeve, C.D. (**1998**). An efficient preparative scale resolution of 3-phenylbutyric acid by lipase from *Burkholderia cepacia* (Chirazyme L1). Tetrahedron: Asymmetry *9*, 1191-1195.

218. Kamal, A., Malik, M.S., Shaik, A.A. & Azeeza, S. (**2007**). Enantioselective synthesis of (*R*)- and (*S*)-curcumene and curcuphenol: an efficient chemoenzymatic route. Tetrahedron: Asymmetry *18*, 2547-2553.

219. Panke, S., Held, M. & Wubbolts, M. (**2004**). Trends and innovations in industrial biocatalysis for the production of fine chemicals. Curr. Opin. Biotechnol. *15*, 272-279.

220. Baumann, M., Hauer, B.H. & Bornscheuer, U.T. (**2000**). Rapid screening of hydrolases for the enantioselective conversion of 'difficult-to-resolve' substrates. Tetrahedron: Asymmetry *11*, 4781-4790.

221. Schmeisser, C., Stockigt, C., Raasch, C., Wingender, J., Timmis, K.N., Wenderoth, D.F., Flemming, H.C., Liesegang, H., Schmitz, R.A., Jaeger, K.E. & Streit, W.R. (**2003**). Metagenome survey of biofilms in drinking-water networks. Appl. Environ. Microbiol. *69*, 7298-7309.

222. Elend, C., Schmeisser, C., Leggewie, C., Babiak, P., Carballeira, J.D., Steele, H.L., Reymond, J.L., Jaeger, K.E. & Streit, W.R. (**2006**). Isolation and biochemical characterization of two novel metagenome-derived esterases. Appl. Environ. Microbiol. *72*, 3637-3645.

223. Rotticci, D., Orrenius, C., Hult, K. & Norin, T. (**1997**). Enantiomerically enriched bifunctional *sec*-alcohols prepared by *Candida antarctica* lipase B catalysis. Evidence of non-steric interactions. Tetrahedron: Asymmetry *8*, 359-362.

224. Norin, M., Hult, K., Mattson, A. & Norin, T. (**1993**). Molecular modelling of chymotrypsin-substrate interactions: calculation of enantioselectivity. Biocatal. Biotransform. *7*, 131-147.

225. Simoni, S., Klinke, S., Zipper, C., Angst, W. & Kohler, H.P.E. (**1996**). Enantioselective metabolism of chiral 3-phenylbutyric acid, an intermediate of linear alkylbenzene degradation, by *Rhodococcus rhodochrous* PB1. Appl. Environ. Microbiol. *62*, 749-755.

226. Diaz, E., Ferrandez, A., Prieto, M.A. & Garcia, J.L. (**2001**). Biodegradation of aromatic compounds by *Escherichia coli*. Microbiol. Mol. Biol. Rev. *65*, 523-569.

227. Lehtinen, J., Nuutila, J. & Lilius, E.M. (**2004**). Green fluorescent protein-propidium iodide (GFP-PI) based assay for flow cytometric measurement of bacterial viability. Cytometry A *60*, 165-172.

228. Stocks, S.M., Plant, N.F.P. & Bagsværd, D. (**2004**). Mechanism and use of the commercially available viability stain, BacLight. Cytometry A *61*, 189-195.

229. López-Amorós, R., Comas, J. & Vives-Rego, J. (**1995**). Flow cytometric assessment of *Escherichia coli* and *Salmonella typhimurium* starvation-survival in seawater using rhodamine 123, propidium iodide, and oxonol. Appl. Environ. Microbiol. *61*, 2521-2526.

230. Hawley, T.S. & Hawley, R.G. Methods in Molecular Biology: Flow Cytometry Protocols. Humana Press Inc.: Totowa, New Jersey.

231. Kubitschek, H.E. (**1990**). Cell volume increase in *Escherichia coli* after shifts to richer media. J. Bacteriol. *172*, 94-101.

232. Ferrari, B.C., Oregaard, G. & Sorensen, S.J. (**2004**). Recovery of GFP-labeled bacteria for culturing and molecular analysis after cell sorting using a benchtop flow cytometer. Microb. Ecol. *48*, 239-245.

233. Matin, A., Auger, E.A., Blum, P.H. & Schultz, J.E. (**1989**). Genetic basis of starvation survival in nondifferentiating bacteria. Annu. Rev. Microbiol. *43*, 293-314.

234. Ortyn, W.E., Hall, B.E., George, T.C., Frost, K., Basiji, D.A., Perry, D.J., Zimmerman, C.A., Coder, D. & Morrissey, P.J. (**2006**). Sensitivity measurement and compensation in spectral imaging. Cytometry A *69*, 852-862.

235. Hult, K. & Berglund, P. (**2007**). Enzyme promiscuity: mechanism and applications. Trends Biotechnol. *25*, 231-238.

236. Bornscheuer, U.T. & Kazlauskas, R.J. (**2004**). Catalytic promiscuity in biocatalysis: using old enzymes to form new bonds and follow new pathways. Angew. Chem. Int. Ed. *43*, 6032-6040.

237. Kourist, R., Bartsch, S., Fransson, L., Hult, K. & Bornscheuer, U.T. (**2008**). Understanding promiscuous amidase activity of an esterase from *Bacillus subtilis*. ChemBioChem *9*, 67-69.

238. Kuchner, O. & Arnold, F.H. (**1997**). Directed evolution of enzyme catalysts. Trends Biotechnol. *15*, 523-530.

239. Wyatt, M.D. & Pittman, D.L. (**2006**). Methylating agents and DNA repair responses: methylated bases and sources of strand breaks. Chem. Res. Toxicol. *19*, 1580-1594.

240. Sczodrok, J. Diploma Thesis, University of Greifswald (**2009**).

241. Kourist, R., Nguyen, G.S., Strübing, D., Böttcher, D., Liebeton, K., Naumer, C., Eck, J. & Bornscheuer, U.T. (**2008**). Hydrolase-catalyzed stereoselective preparation of protected α,α-dialkyl-α-hydroxycarboxylic acids. Tetrahedron: Asymmetry *19*, 1839-1943.

242. Krishna, S.H., Persson, M. & Bornscheuer, U.T. (**2002**). Enantioselective transesterification of a tertiary alcohol by lipase A from *Candida antarctica*. Tetrahedron: Asymmetry *13*, 2693-2696.

243. The PyMOL Molecular Graphics System. DeLano Scientific LLC. DeLano, W.L. Palo Alto, CA, USA: **2008**.

244. Byun, J.S., Rhee, J.K., Kim, N.D., Yoon, J.H., Kim, D.U., Koh, E., Oh, J.W. & Cho, H.S. (**2007**). Crystal structure of hyperthermophilic esterase EstE 1 and the relationship between its dimerization and thermostability properties. BMC Struct. Biol. *7*, 47-57.

245. Wei, Y., Contreras, J.A., Sheffield, P., Osterlund, T., Derewenda, U., Kneusel, R.E., Matern, U., Holm, C. & Derewenda, Z.S. (**1999**). Crystal structure of brefeldin A esterase, a bacterial homolog of the mammalian hormone-sensitive lipase. Nat. Struct. Mol. Biol. *6*, 340-345.

246. Zhu, X., Larsen, N.A., Basran, A., Bruce, N.C. & Wilson, I.A. (**2003**). Observation of an arsenic adduct in an acetyl esterase crystal structure. J. Biol. Chem. *278*, 2008-2014.

247. Nam, K.H., Kim, M.Y., Kim, S.J., Priyadarshi, A., Kwon, S.T., Koo, B.S., Yoon, S.H. & Hwang, K.Y. (**2009**). Structural and functional analysis of a novel hormone-sensitive lipase from a metagenome library. Proteins *74*, 1036-1040.

248. De Simone, G., Menchise, V., Manco, G., Mandrich, L., Sorrentino, N., Lang, D., Rossi, M. & Pedone, C. (**2001**). The crystal structure of a hyper-thermophilic carboxylesterase from the archaeon *Archaeoglobus fulgidus*. J. Mol. Biol. *314*, 507-518.

249. Nam, K.H., Kim, M.Y., Kim, S.J., Priyadarshi, A., Lee, W.H. & Hwang, K.Y. (**2009**). Structural and functional analysis of a novel EstE5 belonging to the

subfamily of hormone-sensitive lipase. Biochem. Biophys. Res. Commun. *379*, 553-556.

250. Khalameyzer, V., Fischer, I., Bornscheuer, U.T. & Altenbuchner, J. (**1999**). Screening, nucleotide sequence, and biochemical characterization of an esterase from *Pseudomonas fluorescens* with high activity towards lactones. Appl. Environ. Microbiol. *65*, 477-482.

251. Henke, E. PhD Thesis, University of Stuttgart (**2001**).

252. Brakmann, S. & Grzeszik, S. (**2001**). An error-prone T7 RNA polymerase mutant generated by directed evolution. ChemBioChem *2*, 212-219.

253. Sambrook, J. & Russell, D.W. Molecular cloning: a laboratory manual. Cold Spring Harbour Laboratory Press: New York, **2001**.

254. Berney, M., Hammes, F., Bosshard, F., Weilenmann, H.U. & Egli, T. (**2007**). Assessment and interpretation of bacterial viability by using the LIVE/DEAD BacLight kit in combination with flow cytometry. Appl. Environ. Microbiol. *73*, 3283-3290.

255. Hanahan, D. (**1983**). Studies on transformation of *Escherichia coli* with plasmids. J. Mol. Biol. *166*, 557-580.

256. Laemmli, U.K. (**1970**). Cleavage of structural proteins during the assembly of the head of bacteriophage T4. Nature *227*, 680-685.

257. Bornscheuer, U., Reif, O.W., Lausch, R., Freitag, R., Scheper, T., Kolisis, F.N. & Menge, U. (**1994**). Lipase of *Pseudomonas cepacia* for biotechnological purposes: purification, crystallization and characterization. Biochim. Biophys. Acta *1201*, 55-60.

258. Hashimoto, N., Aoyama, T. & Shioiri, T. (**1981**). New methods and reagents in organic synthesis. A simple efficient preparation of methyl esters with trimethylsilyldiazomethane (TMSCHN2) and its application to gas chromatographic analysis of fatty acids. Chem. Pharm. Bull. *29*, 1475-1478.

259. Yang, H., Henke, E. & Bornscheuer, U.T. (**1999**). The use of vinyl esters significantly enhanced enantioselectivities and reaction rates in lipase-catalyzed resolutions of arylaliphatic carboxylic acids. J. Org. Chem. *64*, 1709-1712.

260. Kocienski, P.J. Protecting groups. Georg Thieme Verlag: Stuttgart, Germany, **2005**.

261. Yadav, J.S. & Sasmal, P.K. (**1999**). Diels-Alder approach towards the stereocontrolled construction of a taxol® C ring fragment. Tetrahedron *55*, 5185-5194.

Hiermit erkläre ich, dass diese Arbeit bisher von mir weder an der Mathematisch-Naturwissenschaftlichen Fakultät der Ernst-Moritz-Arndt-Universität Greifswald noch einer anderen wissenschaftlichen Einrichtung zum Zwecke der Promotion eingereicht wurde.

Ferner erkläre ich, dass ich diese Arbeit selbständig verfasst und keine anderen als die darin angegebenen Hilfsmittel benutzt habe.

_____

Unterschrift

Acknowledgements

I am deeply thankful to Prof. Dr. Uwe T. Bornscheuer for giving me the opportunity of being part of his team and for giving me liberty to orientate my research during my PhD thesis. His ideas and suggestions have been very helpful and encouraging in the difficult moments and his perspective of scientific work and team building has meant a lot to me.

I wish to thank Dr. Dominique Böttcher for her close and enthusiastic supervision of my work (experimental part and writing) and for invaluable help in scientific and non-scientific issues.

I am indebted to Dr. Radka Snajdrova for her contribution on this work. It has been a great pleasure to share the days in the laboratory and very nice evenings with her. I appreciate a lot her constructive critics to this manuscript.

I thank all members of Prof. Bornscheuer´s working group for the nice time in and out of the lab. I specially thank Konni, Anna, Martin and Sebastian Bartsch for the time they dedicated to help me. I am grateful to Anita Gollin, Anne and Julia for her support in organic synthesis, and to all the students who contributed to this work.

I thank Prof. Dr. Winfried Hinrich´s working group for their help in the crystallization of PestE and for elucidating the enzyme structure.

I owe Prof. Dr. Atomi for providing the gene coding for esterase PestE to our laboratory.

BRAIN AG (Zwingenberg) is gratefully acknowledged for providing the metagenome-derived esterases and the gene coding for esterase CL1.

I would like to thank the Deutsche Bundesstiftung Umwelt (Grant AZ 13198-32) for financial support.

I want to express my appreciation for Dr. Aurelio Hidalgo and Dr. Pablo Domínguez de María for fruitful discussions and tips during my PhD thesis. I warmly thank Dr. Aurelio Hidalgo for his comments to this manuscript.

My gratitude goes to my friends from Greifswald: Melanie, Fabian, Elisabeth, Gabi, Víctor, Oli, Ronni and Thomas; for all the nice moments. I am also very grateful to my friends in Spain for their support during the writing time.

I can't be thankful enough to my family, for being always with me during the good and the bad moments. I sincerely thank my parents and my abuela Espe because they are always there to help me with anything. I thank Martin and Pablo for being the best part of my life.